AD NUMBER

AD001246

NEW LIMITATION CHANGE

TO

Approved for public release, distribution unlimited

FROM

Distribution authorized to DoD only; Administrative/Operational Use; 01 DEC 1952. Other requests shall be referred to Wright Air Development Center, Wright-Patterson AFB, OH 45433. Pre-dates formal DoD distribution statements. Treat as DoD only.

AUTHORITY

SEG ltr dtd 22 Nov 1965

AD-

1246

UNCLASSIFIED

The
Antenna
Laboratory

Department of Electrical Engineering

The Normal Modes of Cavity Antennas

Contract No. AF 18(600)85
E. O. Nos.: 112-110 SR-6f2
112-105 SA-9B

486-7

1 December 1952

The Ohio State University
Research Foundation
Columbus, Ohio

PROJECT REPORT 486-7

REPORT

by

THE OHIO STATE UNIVERSITY RESEARCH FOUNDATION

COLUMBUS 10, OHIO

Cooperator	Air Research and Development Command Wright Air Development Center Wright-Patterson Air Force Base Ohio
Investigation of	Flush Mounted Antennas For Direction-Finding and ECM
Contract	AF 18(600)85 E.O. Nos: 112-110 SR-6f2 112-105 SA-9B
Subject of Report	The Normal Modes of Cavity Antennas
Submitted by	Marshall H. Cohen Antenna Laboratory Department of Electrical Engineering
Date	1 December 1952

CONTENTS

THE NORMAL MODES OF CAVITY ANTENNAS

ABSTRACT

This dissertation is primarily an attempt at arriving at an understanding of the resonance properties of small cavity antennas by studying their normal modes. These modes are similar to the free oscillations of other oscillatory systems. Each one has a characteristic configuration and a complex exponential time dependence. It is assumed that there is an infinite, discrete set of them. There is one fundamental distinction between them and others more commonly investigated; namely, that they occupy an infinite volume and that the damping is a result of radiation. One result of this is that the customary statements of existence, orthogonality, and completeness cannot be applied. These questions are not considered in the present work. The concept of Q is discussed and it is defined in terms of the complex frequency.

The normal modes are actually transient oscillations, and one section is employed for the development and discussion of some pertinent time-dependent electromagnetic theory. An equivalence theorem is first developed. This states that the field in a source-free region is equivalent

to that produced by a double layer of surface currents, electric currents $\underline{J} = \underline{H} \times \underline{n}$, and magnetic currents $\underline{K} = \underline{n} \times \underline{E}$, where $\underline{n}$ is the outward normal. This much of the theorem is identical with the customary forms. In addition to the boundary values it is necessary to include initial values if the boundary values are not known for all past times. Thus, if initial values of the fields are known at $t = t_a$, and boundary values for $t \geq t_a$, then the surface currents plus volume impulse currents which "fire" at $t = t_a$ generate an equivalent field. These volume impulse currents are of two kinds, electric and magnetic, and these have strengths $\underline{D}$ and $\underline{B}$, respectively. The termination properties of the equivalent currents are also discussed.

The behavior of waves with a complex exponential time dependence is the second topic of section II. The envelope of such a wave is an exponential curve which increases in the direction of propagation. In a waveguide the phase velocity is greater than the envelope velocity, so that individual waves advance with respect to the envelope and hence the waves themselves increase as they propagate. An example is given to show that this does not lead to paradoxical situations. It is further shown that these fields in a waveguide have quasi-steady-state characteristics with respect to cutoff phenomena.

The third section of the dissertation contains a theoretical treatment of the normal modes of radiating cavities. An arbitrary cavity opening into a half-space is considered, and by a variational method a

stationary formula for the complex frequencies (eigenvalues) is obtained.

In the cavity region the field is expanded as a sum of cavity modes. This expansion is discussed in detail in an appendix, because most previous discussions of this are incorrect in that the expansions used are not *complete.*

The theory greatly simplifies when the cavity is restricted to be a section of waveguide, since ordinary waveguide theory can then be used. Further simplifications are possible when it is assumed that the aperture field is just the lowest order waveguide mode, and that the cavity has a high Q. Several interesting analogies to circuits appear when these assumptions are made.

A series of calculations was made for the first normal mode of a square waveguide cavity. The cavity has a side dimension a, depth ℓ, and is filled with a medium of dielectric constant ϵ_r. It is specified by the four parameters $\frac{\ell}{a}$, ϵ_r, $\frac{a}{\lambda}$, and Q, where λ is the free-space wavelength at resonance. Curves of $\frac{\ell}{a}$ and Q vs. $\frac{a}{\lambda}$, for various values of ϵ_r, are shown. It is shown that there is a minimum value of Q associated with every value of $\frac{a}{\lambda}$ and that specific values of $\frac{\ell}{a}$ and ϵ_r are necessary to obtain it. The minimum Q was computed and is shown in a graph as a function of $\frac{a}{\lambda}$. The accompanying parameters $\frac{\ell}{a}$ and ϵ_r are also shown. It turns out that the minimum Q graph is a straight line on log-log paper; the following formula closely represents it for

$\frac{a}{\lambda} < 0.35$:

$$Q_{min} = 0.424\left(\frac{a}{\lambda}\right)^{-3}.$$

The effect of a lossy dielectric may be found by using a complex dielectric constant. The relation of the dielectric loss factor to the Q and radiation efficiency is discussed.

The last section of this work deals with some experiments that were made to check the theory. A brief review of the methods of correlating measured and calculated resonance frequency and Q is first made. Then the results of measurements on three square waveguide cavity antennas are given. The antennas had $\frac{\ell}{a}$ values of 7.7, 2.0, and 0.4, with corresponding ϵ_r values of 3.80, 3.88, and 8.41. The first six modes of the first one were measured, four modes of the second were measured, and only the first mode of the last one was measured. The measured resonance frequencies agreed very well with the calculated ones; i. e., within a few per cent. The values of Q did not agree so closely, but the agreement was generally within 30%, which is reasonable. Various factors which might affect these results are discussed.

THE NORMAL MODES OF CAVITY ANTENNAS

I. INTRODUCTION

In recent years small cavity antennas have become important for a variety of purposes. A typical antenna is shown in Fig. 1. It consists of a deformation in a conducting screen, together with some exciting mechanism. The aperture is on the order of a quarter of a wavelength in its greatest dimension. These antennas always have marked resonance properties, which are undesirable, since an antenna is more useful when it can be operated over a broad band of frequencies. The resonance properties are therefore of considerable interest, and it is the purpose of this dissertation to discuss them.

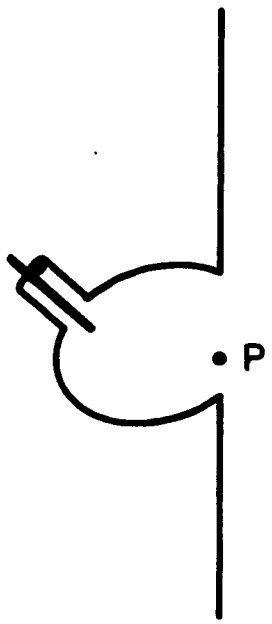

Fig. 1. Cavity antenna.

The antenna characteristics which are of interest are the resonance frequency and the Q. The Q, or quality factor, is a measure of the sharpness of resonance, and it can be directly connected to the operating range of the antenna in terms of the standing wave ratio on the input transmission line. (See section IV below.)

The general definition of Q is as follows:

$$Q = 2\pi \frac{\text{Average energy stored}}{\text{Energy dissipated per cycle, at resonance}} . \qquad (1.1)$$

If the system has more than one degree of freedom there is a Q defined for each mode, and this holds for a system with an infinite number of degree of freedom, as, for example, a closed cavity. However, when the concept is extended to antennas a serious difficulty appears. The energy in an electromagnetic field is defined in terms of volume integrals, and they are infinite for an antenna because E^2 decreases as $1/r^2$, but the volume increases as r^3. Hence Q as defined by eq. (1.1) is infinite for an antenna.

This difficulty is in principle resolved by stating that by stored energy we do not mean the total field energy, but only that part of it in the "local" field, as opposed to the radiation field. But this statement does not clear up the trouble — we must now decide what we mean by local field. This must be done very carefully; since, in general, superposition does not apply to energy, and it cannot be arbitrarily broken down into components. In the case of a waveguide there are well-defined orthogonal modes, and superposition may be applied to the mode energies. Schwinger[1] has used this property to show that in the neighborhood of a discontinuity in a waveguide the total field energy is the sum of two parts — that in the propagating mode, and that stored in the higher modes. He showed that the latter component by itself has all the

properties which are associated with stored energy of circuits.

Chu[2] examined the antenna problem by means of orthogonal modes. He considered an omnidirectional antenna and expanded the field outside a sphere surrounding the antenna in spherical waves. Each wave could be replaced by an equivalent circuit which had a well-defined Q. In this way Chu obtained relations between the antenna size, Q, and gain. He assumed very idealized conditions between the antenna and the surrounding sphere, so that the theory gives limits of performance of actual antennas.

Counter[3] defined stored energy as the difference between the total energy and a "flow" energy, which he defined as the energy in that plane wave which has the same Poynting vector as the field under consideration. This gives a basis for calculating a finite Q for an antenna from eq. (1.1). However, it can be shown that this definition does not agree with Schwinger's in the waveguide case.

In this paper a different method of attack is adopted; Q will be calculated by finding the normal modes of oscillation of the antenna. It is, of course, well-known that the transients give an indication of the Q. For example, if a system "rings" for a long time after the source is removed, then it has a high Q. A more precise statement of this is now made by a brief discussion of a simple RLC circuit.

Consider a series RLC circuit, as in Fig. 2. The energy definition (1.1) leads directly to the value,

$$Q = \frac{\omega_r L}{R} , \tag{1.2}$$

where

$$\omega_r = \frac{1}{\sqrt{LC}} = \text{resonance frequency.} \tag{1.3}$$

If the terminals in Fig. 2 are connected the resulting circuit will have one normal mode of oscillation. In this mode the voltage and current have a time dependence of the form $e^{jp_n t}$,* where p_n is a complex number:

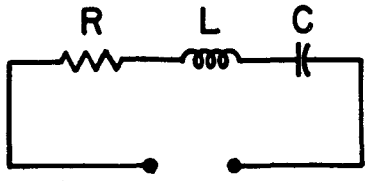

Fig. 2. Elementary series circuit.

$$p_n = \omega_n + j\xi_n . \tag{1.4}$$

The real and imaginary portions of the complex frequency p_n can be found in terms of the circuit constants; one way to do this is as follows. The assumed exponential time dependence allows us to keep the concept of impedance; the transient (normal-mode) impedance is identical to the steady-state impedance, with ω replaced by p_n. Now consider terminals across the capacitor, as in Fig. 3. A consideration of the

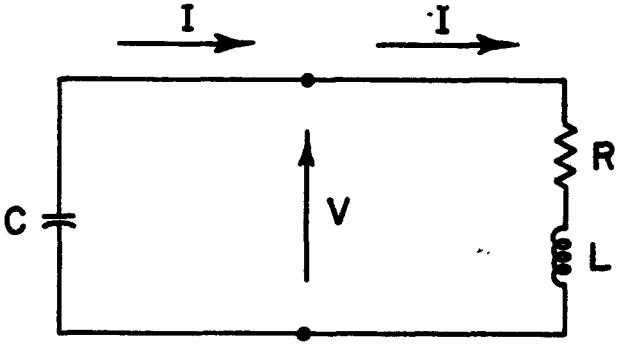

Fig. 3. Series circuit oscillating in the normal mode.

* In this paper the symbol $j = \sqrt{-1}$ is used exclusively.

voltages and currents shows that the impedance looking to the left at the terminals must be the negative of that looking to the right. Thus

$$\frac{1}{j p_n C} = -(R + j p_n L). \tag{1.5}$$

When (1.4) is inserted and real and imaginary parts separated, one obtains

$$\xi_n = \frac{R}{2L} \tag{1.6}$$

$$\omega_n^2 = \omega_r^2 - \xi_n^2. \tag{1.7}$$

Now define the normal mode Q:

$$Q_n = \frac{\omega_n}{2\xi_n} . \tag{1.8}$$

It is evident that this is approximately equal to the steady-state Q (eq. (1.2)). It is only approximate because the resonance and normal-mode frequencies are slightly different, but the difference is less than 1% for $Q > 3.5$.

The normal mode Q may be directly connected with the stored energy. When Q is high the field decays very slowly, and we may reasonably speak of an average stored energy that dies out as $e^{-2\xi_n t}$. Call this average energy $\bar{U}$. Then

$$\bar{U} \sim e^{-2\xi_n t} \tag{1.9}$$

$$\frac{\partial \bar{U}}{\partial t} = -2\xi_n \bar{U} \tag{1.10}$$

$$Q_n = \frac{\omega_n}{2\zeta_n} = \omega_n \frac{\bar{U}}{-\frac{\partial \bar{U}}{\partial t}} \tag{1.11}$$

$$Q_n = 2\pi \frac{\text{Average stored energy}}{\text{Energy dissipated per transient cycle}} \tag{1.12}$$

This compares with eq. (1.1) for the steady-state Q.

We shall subsequently assume that the radiating cavity has normal modes which have a similarly defined Q. The subject of normal modes in open regions is not altogether new; in particular, oscillations about a sphere and a spheroid have been discussed for a long time. These bodies were examined first because their surfaces coincided with separable coordinate surfaces. The sphere problem is treated in detail by Stratton,[4] who finds expressions for the fields as well as the first few eigenvalues. Schelkunoff[5] gives a summary of the results obtained by several writers on the prolate spheroid. This problem is of considerable interest because a wire is the limiting case of a prolate spheroid.

Oscillations on other shapes have apparently been considered only to a very minor extent. Schelkunoff also discusses modes on a very thin wire bent to an arbitrary curve, and makes some calculations for a straight wire. Apart from this discussion, the author can find no reference to normal modes of more complex antenna structures.

The present investigation uses a variational method to obtain the solution. This is a powerful technique which quickly yields a good

approximation. It is an outgrowth of the work done by Schwinger[6] on discontinuities in waveguides. It consists essentially of obtaining an integral equation for an aperture field (or obstacle current) and then properly manipulating the equation to obtain a stationary formula for some parameter of interest. The techniques have been applied to a wide variety of field theory problems, such as impedance calculations, scattering and diffraction problems, and propagation problems. Some typical references to this work are listed in the references.[6, 7, 8] The present application is similar in some ways to the theory used to compute the propagation constant for a slotted waveguide.[9]

II. ELECTROMAGNETIC TRANSIENTS

In this section we discuss several aspects of time-dependent electromagnetic field theory which are interesting and useful in connection with the normal mode theory in the next section. First the time dependent equivalence theorem is established. Then the behavior of fields with a time dependence $e^{j\omega t} e^{-\xi t}$ is discussed.

1. EQUIVALENCE THEOREM

The equivalence theorem is a frequently used theorem for scalar and vector fields. It states that the field interior to some surface S is equivalent to that produced by certain source distributions on S. The theorem is intimately connected with uniqueness theorems which state that functions which satisfy appropriate equations are uniquely specified inside S if their values on S are given. For steady-state electromagnetic fields the equivalent sources are electric and magnetic currents, with strengths $\underline{H} \times \underline{n}$ and $\underline{n} \times \underline{E}$.[10] The uniqueness theorem states that either tangential $\underline{E}$ or $\underline{H}$ specifies the interior field, so that with appropriate boundary conditions either set of currents can be made sufficient by itself. Most classical statements of this result include surface charges as well as currents.[11] This is a redundant formulation, since the surface charges and currents are connected by the continuity equation.

The time dependent theorem follows from the steady-state case by the use of Fourier integrals. However, this method obscures some points, and it is of interest to examine this case independently. The

general uniqueness theorem for a time-dependent electromagnetic field[12] states that the distribution of $\underline{E}$ and $\underline{H}$ throughout V at the initial time t_a plus either tangential $\underline{E}$ or $\underline{H}$ on the bounding surface for $t \geq t_a$ specifies the field in V for $t \geq t_a$. An equivalence theorem will now be set up in which the field is produced by electric and (or) magnetic currents on S plus a volume distribution of impulse currents which "fire" at $t = t_a$. The standard statements of this theorem (Larmor-Tedone formulas)[13] use surface charges as well as surface currents, and they go back in time to $t = -\infty$. There is no provision for initial values. The method of proof used here is substantially the same as that used by Professor V. H. Rumsey to prove the theorem for the case of sinusoidal time dependence.*

Let there be given a region V bounded by S containing a linear isotropic medium (Fig. 4). The medium constants $\mu \epsilon \sigma$ are continuous functions of position; it is assumed that any sharp boundaries are replaced by thin layers where the constants vary rapidly but continuously. Inside V is an electromagnetic field generated by sources $\underline{J}$. The fields satisfy the Maxwell equations:

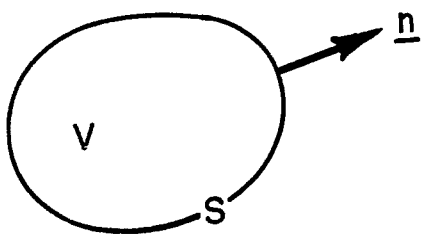

Fig. 4.

* Classroom presentation.

$$\nabla \times \underline{E} = -\mu \frac{\partial \underline{H}}{\partial t} \quad * \tag{2.1}$$

$$\nabla \times \underline{H} = \epsilon \frac{\partial \underline{E}}{\partial t} + \sigma \underline{E} + \underline{J}. \tag{2.2}$$

For a Green's function we use the field due to an impulse current $\underline{J}_o$. This current is an impulse in both space and time; it is defined as

$$\underline{J}_o = \underline{q}\, \delta (P - Q) \delta (t - t_o). \tag{2.3}$$

The δ-function is the unit impulse function, defined by

$$\int_a^b f(t) \delta (t - t_o)\, dt = \begin{cases} f(t_o) & \text{if } a < t_o < b \\ 0 & \text{otherwise.} \end{cases} \tag{2.4}$$

The symbol $\delta (P - Q)$ stands for the triple product,

$$\delta (P - Q) = \delta (x_P - x_Q)\ \delta (y_P - y_Q)\, \delta (z_P - z_Q). \tag{2.5}$$

The impulse current and the fields it would produce are discussed in Appendix I.

Let $\underline{G}_o (P t_o, Q t, \underline{q})$ and $\underline{F}_o (P t_o, Q t, \underline{q})$ be the electric and magnetic fields, respectively, at point P at time t_o due to an impulse current $\underline{J}_o$ at point Q at time t. By the law of superposition, the electric field of an arbitrary current distribution $\underline{J}$ can be written as[14]

$$\underline{E} (P t_o) = \int_V \int_t J (Q t)\, \underline{G}_o (P t_o, Q t, \underline{1})\, dv_Q\, dt, \tag{2.6}$$

where $\underline{1}$ is a unit impulse current parallel to $\underline{J}$, and J is the magnitude

* Rationalized MKS units are used throughout this paper.

of $\underline{J}$. This may also be written as

$$\underline{E}(Pt_o) = \int_V dv_Q \int_{-\infty}^{\infty} \underline{G}_o (Pt_o, Qt, \underline{J})\, dt. \tag{2.7}$$

Because of the finite velocity of propagation, the upper limit on the time integral can be reduced from $+\infty$ to $(t_o - (r/c))$, where r is the distance from P to Q.

The fields $\underline{G}_o$ and $\underline{F}_o$* are the response of the system (i. e., the region V) to the elementary source $\underline{J}_o$. They satisfy the equations

$$\nabla \times \underline{G}_o = -\mu \frac{\partial \underline{F}_o}{\partial t_o} \tag{2.8}$$

$$\nabla \times \underline{F}_o = \epsilon \frac{\partial \underline{G}_o}{\partial t_o} + \sigma \underline{G}_o + \underline{q}\, \delta (P - Q)\, \delta (t - t_o). \tag{2.9}$$

Inside V the constants $\mu\, \epsilon\, \sigma$ are the same for the Green's function as for the fields $(\underline{E},\underline{H})$; outside V they are as yet arbitrary.

Now form the volume integral of $\nabla \cdot (\underline{E} \times \underline{F}_o - \underline{G}_o \times \underline{H})$.

$$\int_V \nabla \cdot (\underline{E} \times \underline{F}_o)\, dv = \int_V (\underline{F}_o \cdot \nabla \times \underline{E} - \underline{E} \cdot \nabla \times \underline{F}_o)\, dv_P \tag{2.10}$$

$$= \int_V \left\{ -\underline{F}_o \cdot \mu \frac{\partial \underline{H}}{\partial t} - \underline{E} \cdot \left[\epsilon \frac{\partial \underline{G}_o}{\partial t_o} + \sigma \underline{G}_o + \underline{q}\, \delta (P - Q)\, \delta (t - t_o) \right] \right\} dv_P$$

$$\int_V \nabla \cdot (\underline{G}_o \times \underline{H})\, dv = \int_V \left\{ -\underline{H} \cdot \mu \frac{\partial \underline{F}_o}{\partial t_o} - \underline{G}_o \cdot \left[\epsilon \frac{\partial \underline{E}}{\partial t} + \sigma \underline{E} + \underline{J} \right] \right\} dv_P. \tag{2.11}$$

* The arguments of these and similar functions are sometimes omitted for convenience. In any such case it will be clear what the argument is.

The integrations are performed over points P. When they are subtracted and the divergence theorem is used on the left-hand side, one obtains

$$\int_S (\underline{E} \times \underline{F}_o - \underline{G}_o \times \underline{H}) \cdot \underline{n}\, ds = \int_V \mu \left(\underline{H} \frac{\partial \underline{F}_o}{\partial t_o} - \underline{F}_o \frac{\partial \underline{H}}{\partial t}\right) dv$$

$$+ \int_V \epsilon \left(\underline{G}_o \frac{\partial \underline{E}}{\partial t} - \underline{E} \frac{\partial \underline{G}_o}{\partial t_o}\right) dv + \int_V \underline{G}_o \cdot \underline{J}\, dv - \underline{q} \cdot \underline{E}(Q t) \delta (t - t_o). \tag{2.12}$$

Now integrate over time, from $t = t_a$ to $t = \infty$. The time t_a is the initial time, while t_o is a variable time. In the final result (e.g., eq. (2.30)), t_o is the observer's time.

$$\int_{t_a}^{\infty} dt \int_S (\underline{E} \times \underline{F}_o - \underline{G}_o \times \underline{H}) \cdot \underline{n}\, ds = \int_{t_a}^{\infty} dt \int_V \mu \left(\underline{H} \frac{\partial \underline{F}_o}{\partial t_o} - \underline{F}_o \frac{\partial \underline{H}}{\partial t}\right) dv$$

$$+ \int_{t_a}^{\infty} dt \int_V \epsilon \left(\underline{G}_o \frac{\partial \underline{E}}{\partial t} - \underline{E} \frac{\partial \underline{G}_o}{\partial t_o}\right) dv + \int_{t_a}^{\infty} dt \int_V \underline{G}_o \cdot \underline{J}\, dv - \underline{q} \cdot \underline{E}(Q t_o). \tag{2.13}$$

The time dependence of $\underline{G}_o$ and $\underline{F}_o$ can occur only as $(t - t_o)$, hence

$$\frac{\partial \underline{F}_o}{\partial t_o} = -\frac{\partial \underline{F}_o}{\partial t}$$

and (2.14)

$$\frac{\partial \underline{G}_o}{\partial t_o} = -\frac{\partial \underline{G}_o}{\partial t}.$$

Interchange the order of integration in the first two volume integrals and use (2.14). The result is

$$\underline{q} \cdot \underline{E}(Q t_o) = \int_V -\mu \underline{H} \cdot \underline{F}_o \Big|_{t = t_a}^{\infty} dv + \int_V \epsilon \underline{E} \cdot \underline{G}_o \Big|_{t_a}^{\infty} dv + \int_{t_a}^{\infty} dt \int_V \underline{G}_o \cdot \underline{J}\, dv$$

$$- \int_{t_a}^{\infty} dt \int_S (\underline{E} \times \underline{F}_o - \underline{G}_o \times \underline{H}) \cdot \underline{n}\, ds. \tag{2.15}$$

At the upper limit, $t = \infty$, $\underline{F}_o$ and $\underline{G}_o$ are zero, since

$$\underline{F}_o(Pt_o, Qt, \underline{q}) \equiv \underline{G}_o(Pt_o, Qt, \underline{q}) \equiv 0 \qquad \text{for } t_o < (t + \tfrac{r}{c}). \tag{2.16}$$

Hence

$$\begin{aligned}
\underline{q} \cdot \underline{E}(Qt_o) = &\int_V - \underline{B}(Pt_a) \cdot \underline{F}_o(Pt_o, Qt_a, \underline{q})\, dv_P \\
&+ \int_V \underline{D}(Pt_a) \cdot \underline{G}_o(Pt_o, Qt_a, \underline{q})\, dv_P \\
&+ \int_{t_a}^{\infty} dt \int_V \underline{G}_o(Pt_o, Qt, \underline{q}) \cdot \underline{J}(Pt)\, dv_P \\
&- \int_{t_a}^{\infty} dt \int_S \underline{E}(Pt) \times \underline{F}_o(Pt_o, Qt, \underline{q}) \cdot \underline{n}\, ds_P \\
&+ \int_{t_a}^{\infty} dt \int_S \underline{G}_o(Pt_o, Qt, \underline{q}) \times \underline{H}(Pt) \cdot \underline{n}\, ds_P.
\end{aligned} \tag{2.17}$$

To interpret these integrals we need the reciprocity theorem. The mathematical statement can be quickly obtained from eq. (2.15), if we let the time interval be $(-\infty, +\infty)$ instead of (t_a, ∞), and if we let $(\underline{E}, \underline{H})$ be the fields at (Pt) due to an impulse current $\underline{m}$ at (Mt_1):

$$\underline{E}(Pt) = \underline{G}_o(Pt, Mt_1, \underline{m}) \tag{2.18}$$

$$\underline{H}(Pt) = \underline{F}_o(Pt, Mt_1, \underline{m}). \tag{2.19}$$

Then, we obtain from (2.15),

$$\begin{aligned}
&\underline{q} \cdot \underline{G}_o(Qt_o, Mt_1, \underline{m}) - \int_{-\infty}^{\infty} dt \int_V \underline{G}_o(Pt_o, Qt, \underline{q}) \cdot \underline{m}\, \delta(P - M)\, \delta(t - t_1)\, dv_P \\
&= \int_V -\mu\, \underline{F}_o(Pt, Mt_1, \underline{m}) \cdot \underline{F}_o(Pt_o, Qt, \underline{q}) \Big|_{t = -\infty}^{\infty} dv_P
\end{aligned}$$

(Equation continued on next page.)

$$+ \int_V \epsilon \, \underline{G}_o(Pt, Mt_1, \underline{m}) \cdot \underline{G}_o(Pt_o, Qt, \underline{q}) \Big|_{t=-\infty}^{\infty} dv_P$$

$$- \int_{-\infty}^{\infty} dt \int_S \Big[\underline{G}_o(Pt, Mt_1, \underline{m}) \times \underline{F}_o(Pt_o, Qt, \underline{q})$$

$$- \underline{G}_o(Pt_o, Qt, \underline{q}) \times \underline{F}_o(Pt, Mt_1, \underline{m}) \Big] \cdot \underline{n} \, ds_P. \qquad (2.20)$$

The second factor in each of the two volume integrals on the right-hand side is zero at the upper limit by eq. (2.16), and because the first factors have the source and observer times interchanged, they are zero at $t = -\infty$. The surface integral must be a constant because the left-hand side is independent of S. To show that the constant is zero, let S recede to infinity.

By eq. (2.16) the zero intervals of $\underline{G}_o(Pt, Mt_1, \underline{m})$ and $\underline{F}_o(Pt_o, Qt, \underline{q})$ overlap, because the distances from P to points M and Q are infinite. It follows that the surface integral is identically zero for all t.* The final result, the reciprocity theorem, is

$$\underline{q} \cdot \underline{G}_o(Qt_o, Mt_1, \underline{m}) = \underline{m} \cdot \underline{G}_o(Mt_o, Qt_1, \underline{q}). \qquad (2.21)$$

The method used to establish this theorem is an extension to the time-dependent case of the method used by Schelkunoff.

An alternative form of the theorem is obtained as follows. Let $\underline{G}_1(Pt_o, Qt, \underline{q})$ and $\underline{F}_1(Pt_o, Qt, \underline{q})$ be the electric and magnetic fields of an impulse *magnetic* current of strength $\underline{q}$. These fields satisfy

* This result is a special case of a more general theorem: the surface integral $\int_S \underline{E}_1 \times \underline{H}_2 - \underline{E}_2 \times \underline{H}_1) \cdot \underline{n} \, ds$ is zero when all sources of both fields are on the same side of S.

$$\nabla \times \underline{G}_1 = -\mu \frac{\partial \underline{F}_1}{\partial t_o} - \underline{q}\, \delta (P - Q)\, \delta (t - t_o) \tag{2.22}$$

$$\nabla \times \underline{F}_1 = \epsilon \frac{\partial \underline{G}_1}{\partial t_o} + \sigma\, \underline{G}_1. \tag{2.23}$$

Now form $\nabla \cdot \{\underline{G}_o(Pt, Mt_1, \underline{m}) \times \underline{F}_1(Pt_o, Qt, \underline{q})$

$$- \underline{G}_1(Pt_o, Qt, \underline{q}) \times \underline{F}_o(Pt, Mt_1, \underline{m})\}$$

and integrate. After manipulations identical to those above, one obtains

$$-\underline{q} \cdot \underline{F}_o(Qt_o, Mt_1, \underline{m}) = \underline{m} \cdot \underline{G}_1(Mt_o, Qt_1, \underline{q}). \tag{2.24}$$

The integrals on the right-hand side of (2.17) are now examined separately. With the help of eq. (2.24) the first term becomes

$$\int_V -\underline{B}(Pt_a) \cdot \underline{F}_o(Pt_o, Qt_a, \underline{q})\, dv_P = \underline{q} \cdot \int_V \underline{G}_1(Qt_o, Pt_a, \underline{B})\, dv_P. \tag{2.25}$$

This is just the electric field at (Qt_o) due to magnetic current impulses which "fire" at $t = t_a$; they are distributed according to the magnetic induction $\underline{B}$ which existed then.

Use eq. (2.21) on the second term of (2.17) to obtain

$$\int_V \underline{D}(Pt_a) \cdot \underline{G}_o(Pt_o, Qt_a, \underline{q})\, dv_P = \underline{q} \cdot \int_V \underline{G}_o(Qt_o, Pt_a, \underline{D})\, dv_P. \tag{2.26}$$

This is the electric field at (Qt_o) due to electric current impulses which "fire" at $t = t_a$; they are distributed according to the electric displacement $\underline{D}$ which existed then.

The surface integrals are similarly transformed:

$$-\int_{t_a}^{\infty} dt \int_S \underline{E}(Pt) \times \underline{F}_o(Pt_o, Qt, \underline{q}) \cdot \underline{n}\, ds_P =$$

$$\underline{q} \cdot \int_{t_a}^{\infty} dt \int_S \underline{G}_1(Qt_o, Pt, (\underline{n} \times \underline{E}))\, ds_P \tag{2.27}$$

$$\int_{t_a}^{\infty} dt \int_S \underline{G}_o(Pt_o, Qt, \underline{q}) \times \underline{H}(Pt) \cdot \underline{n}\, ds_P =$$

$$\underline{q} \cdot \int_{t_a}^{\infty} dt \int_S \underline{G}_o(Qt_o, Pt, (\underline{H} \times \underline{n}))\, ds_P. \tag{2.28}$$

These terms represent the electric field at Qt_o due to magnetic currents $\underline{K} = \underline{n} \times \underline{E}$ and electric currents $\underline{J} = \underline{H} \times \underline{n}$ distributed on S, for $t \geq t_a$.

The last volume integral is

$$\int_{t_a}^{\infty} dt \int_V \underline{G}_o(Pt_o, Qt, \underline{q}) \cdot \underline{J}\, dv_P = \underline{q} \cdot \int_{t_a}^{\infty} dt \int_V \underline{G}_o(Qt_o, Pt, \underline{J})\, dv_P. \tag{2.29}$$

This is the contribution to the field at (Qt_o) from actual currents within V. The first terms, eqs. (2.25) through (2.28), represent contributions from sources outside V and from sources existing at $t < t_a$.

Notice that the source $\underline{q}$ multiplies all the source integrals, as well as the electric field $\underline{E}(Qt_o)$, in (2.17). Since $\underline{q}$ is arbitrary we may drop it and write

$$\underline{E}(Q t_o) = \int_{t_a}^{\infty} dt \int_V \underline{G}_o(Q t_o, P t, \underline{J})\, dv_P + \int_V \underline{G}_1(Q t_o, P t_a, \underline{B})\, dv_P$$

$$+ \int_V \underline{G}_o(Q t_o, P t_a, \underline{D})\, dv_P + \int_{t_a}^{\infty} dt \int_S \underline{G}_o(Q t_o, P t, (\underline{H} \times \underline{n}))\, ds_P$$

$$+ \int_{t_a}^{\infty} dt \int_S \underline{G}_1(Q t_o, P t, (\underline{n} \times \underline{E}))\, ds_P. \qquad (2.30)$$

The equivalence theorem symbolized in eq. (2.30) may be stated as follows. If a source-free linear isotropic region V bounded by S is excited by external sources, then the internal fields are reproduced identically by surface electric and magnetic currents distributed on S according to $\underline{H} \times \underline{n}$ and $\underline{n} \times \underline{E}$, respectively. The effect of pre-existing fields may be accounted for by volume electric and magnetic impulse currents distributed according to $\underline{D}$ and $\underline{B}$, respectively, which occur at the initial time.

If the sources $\underline{J}$ are outside V, the first term of (2.30) is zero. If $\underline{J}$ exists only inside V, then the first three terms alone must give the field inside V, and the surface currents therefore give zero to interior points. Since the inside and outside may be interchanged, we may infer that the surface currents give zero on the source side of S. This can also be seen from the fact that the surface currents have precisely the values needed to terminate the field. (At a surface current layer, tangential $\underline{E}$ is discontinuous by an amount $\underline{K}$ and tangential

$\underline{H}$, by an amount $\underline{J}$; but $\underline{K} = \underline{n} \times \underline{E}$ and $\underline{J} = \underline{H} \times \underline{n}$, so these terminate the field.)*

Another interesting condition arises when there are no sources after $t = t_a$; there is only a transient field existing, which must get weaker in time. We may remove the surface S to infinity. In such a case the sources on S cannot contribute to any finite point within a finite time, so the volume impulse currents generate the complete field. Consider the field immediately after $t = t_a$. The currents have disappeared, and the field essentially has the prescribed initial value. Since the impulse currents give zero for $t < t_a$, we have a field which at all points of space jumps from zero to $\underline{D}$, $\underline{B}$ at time t_a, when there are impulse electric and magnetic currents of strength $\underline{D}$, $\underline{B}$. Hence we postulate that volume impulse electric currents of strength $\underline{J}$ produce a discontinuity (in time) in $\underline{D}$ equal to $\underline{J}$, at the time the impulse currents occur. Similarly, volume impulse magnetic currents of strength $\underline{K}$ produce a discontinuity in $\underline{B}$ equal to $\underline{K}$. These postulates are analogous to those concerning the discontinuities in space produced by a surface distribution of current.

We now can make a more general statement concerning termination of the field. The equivalent surface and volume currents may be regarded as surface currents on the hyper-surface bounding the (xyzt)

* This termination property may be used to set up the equivalence theorem. See Baker and Copson,[13] also Schelkunoff, S. A., *Some Equivalence Theorems of Electromagnetics and Their Application to Radiation Problems*, B.S.T.J., Vol. XV, January 1936. p. 92.

volume of interest. These currents generate a unique field in the four-dimensional region, and terminate it at the surface. We may make this volume finite by closing it with the hyper-plane $t = t_b$. The appropriate currents to put on this plane are the volume impulse currents $\underline{J}_o = -\underline{D}$, $\underline{K}_o = -\underline{B}$. This leaves us with a set of surface currents which produce a field inside some volume in (xyzt) space. Outside this hyper-volume the fields are zero.

This result is a generalization of the three-dimensional picture obtained by Larmor and Tedone.[13] Undoubtedly it could have been obtained more compactly and more elegantly by starting with the four-dimensional formulation of Maxwell's equations.

So far, the external boundary conditions on the equivalent currents have not been specified. It is evident that they are arbitrary because the currents give zero outside S and any boundaries may be assumed there without affecting the internal fields. If we choose a short circuit on S ($\underline{n} \times \underline{G} = 0$ on S) for the boundary condition, then the surface electric currents will be "shorted out" and only the magnetic currents will be left, radiating against an electric conductor. This may also be seen by examining eq. (2.17). In the last term, $\underline{G}_o \times \underline{n}$ will be zero on S, and thus there is no contribution from the electric currents. Similarly, open-circuit boundary conditions ($\underline{n} \times \underline{F} = 0$ on S) leave only electric currents radiating against a "magnetic conductor." These ideas suffice to prove the uniqueness theorem mentioned above——

that either tangential $\underline{E}$ or $\underline{H}$ on S plus initial values of $\underline{E}$ and $\underline{H}$ throughout V uniquely specify the field.*

As an example of the use of equivalent currents, consider a cavity antenna radiating through an infinite conducting ground plane, as in Fig. 5. Suppose that the field varies sinusoidally with time until $t = t_1$, at which time the aperture is suddenly shorted with an electric conductor. What will happen to the fields in the half-space?

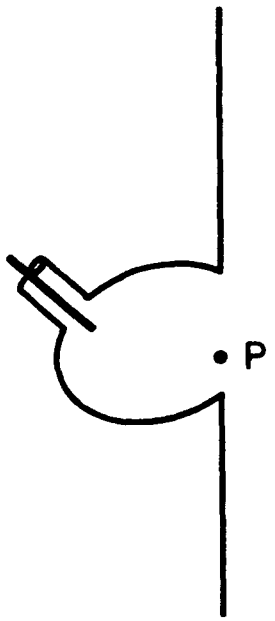

Fig. 5. Cavity antenna.

To answer this question, use the equivalence theorem. The volume V is the half-space, bounded by the plane of the ground plane. It is assumed that the initial time t_a is back far enough so that the contributions from the volume impulse currents have become insignificant. Hence the field at Q is equivalent to that produced by electric currents $\underline{J} = \underline{H} \times \underline{n}$ and magnetic currents $\underline{K} = \underline{n} \times \underline{E}$ on the plane $z = 0$. The unit vector $\underline{n}$ points into the cavity. The magnetic currents $\underline{K}$ are zero except over that portion of the plane where the aperture is, because $\underline{n} \times \underline{E} = 0$ on the ground

* There is no assurance that an arbitrarily specified $\underline{E}$ or $\underline{H}$ will produce a physically possible field. The question of existence is a perplexing one and becomes important when the boundaries of the region include sharp edges.

plane. The picture is greatly simplified when a short circuit boundary condition is adopted. For now, as shown above, we are left with $\underline{K} = \underline{n} \times \underline{E}$ in the aperture, radiating against an infinite conducting plane screen. But now ordinary image theory can be used and it follows that, in the half-space, the fields produced by $\underline{K}$ on the conducting screen are identical to the fields produced by $2\underline{K}$ radiating in free space.*

The time dependence of $\underline{K}$ is of the form

$$\underline{K} \sim \cos \omega t \; U(t_1 - t), \tag{2.31}$$

where $U(t_1 - t)$ is the unit step function,

$$U(t_1 - t) = \begin{cases} 0 \text{ if } t > t_1 \\ 1 \text{ if } t < t_1. \end{cases} \tag{2.32}$$

To obtain the field at Q we can find the field due to an infinitesimal source at P with the above time dependence, and integrate over the aperture. The fields due to this elementary source are discussed in Appendix I. It is shown there that the field at Q will vary sinusoidally with time until $t = t_1 + \frac{r}{c}$, at which time it will abruptly cease, possibly with a spike, depending upon the phase of E when the shutter is closed. The total field at Q is the sum of contributions from all points in the aperture. Since the shutter is closed instantaneously, t_1 is the same

* For an alternative treatment of plane boundaries, leading to the same result, see Smythe, W. R., *The Double Current Sheet in Diffraction*, Phys. Rev., 72, December, 1947. p. 1066.

for all points. Hence in a time $\tau = \frac{s}{c}$ (Fig. 6) the field at Q will change from a steady-state condition to zero.

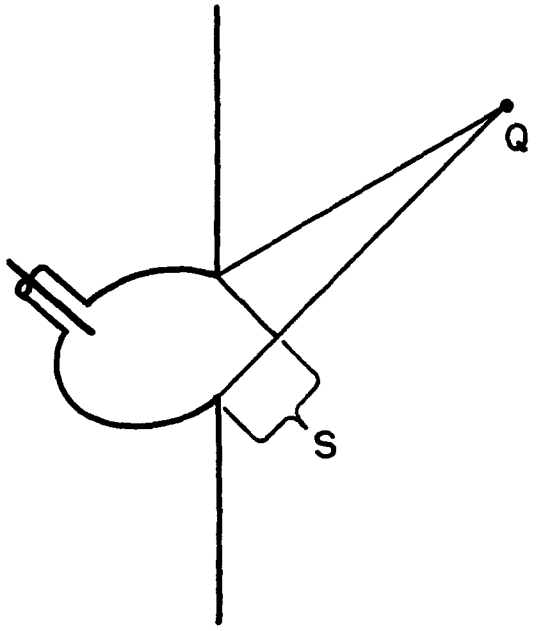

Fig. 6.

The interval τ will be zero for infinitesimal apertures and will be large for large apertures; moreover, it is different for different locations of the point Q. Its behavior is opposite to that of the time constant sought in connection with the bandwidth. Thus τ can give us very little information regarding the bandwidth of the antenna.

There is no characteristic exponential time decay in the above problem because it is a very special case. The equivalent currents were on a plane and they were all stopped instantaneously. On a more general body one would get the exponential time dependence. For example, if the terminals at the base of the feed probe were suddenly shorted, the energy in the cavity would be expected to reverberate and gradually leak out the aperture. The time decay in this case would be connected with the bandwidth.

2. FIELDS WITH AN EXPONENTIAL TIME DEPENDENCE

An oscillating field which is dying out in time may have a time dependence of the form $e^{(j\omega - \xi)t}$. Normal modes of a lossy network

and normal modes in a closed cavity with a lossy dielectric have this time dependence. In the next chapter it is assumed that the normal modes of a radiating cavity also have this time dependence. The radiating cavity differs from the first cases because there is propagation. We now examine this effect.

The one-dimensional wave equation for a field component is

$$\frac{\partial^2 E}{\partial z^2} - \frac{1}{c^2} \frac{\partial^2 E}{\partial t^2} = 0. \tag{2.33}$$

If the time dependence is e^{jpt}, where $p = \omega + j\xi$, then the solution to this is the sum of two waves, traveling in the positive and negative z-directions:

$$E = A\, e^{j\omega\left(t - \frac{z}{c}\right)}\, e^{-\xi\left(t - \frac{z}{c}\right)} + B\, e^{j\omega\left(t + \frac{z}{c}\right)}\, e^{-\xi\left(t + \frac{z}{c}\right)}. \tag{2.34}$$

Consider the first term. The first exponential factor represents a wave traveling in the positive z-direction. The second factor represents an exponential decay; for any value of z, E dies out as $e^{-\xi t}$. However, at a given value of t, E builds up in the positive z-direction, according to $e^{+\frac{\xi}{c} z}$. The field therefore appears as a sine wave which builds up exponentially in the direction of propagation. The complete wave, including the envelope, moves with a phase velocity c. The second term in (2.34) gives a similar wave traveling in the negative z-direction. These are exactly the type of waves that would be obtained on an infinite string which is excited by a source which gets weaker in time exponentially.

These fields become infinite for large values of z, and difficulties with respect to surface integrals at infinity might be expected. It is safest to say that the transient started at some finite time in the past, and because of the finite velocity of propagation, it must be zero for $z > Z$. The maximum value of the transient will be determined by the initial conditions. If it is a spherical wave then it is zero for $r > R$, and the maximum value will decrease as $1/R$.

a. TRANSIENTS IN WAVEGUIDES

The fields in a lossless waveguide are much more complicated than the simple plane wave described above. A waveguide is a dispersive region, because the phase velocity depends on the frequency. Hence, one would expect distortion of, say, a transient pulse, as it traveled down the waveguide. However, normal modes exist in waveguide regions. For example, there would be normal modes in the region shown in Fig. 7. The load may consist of a sheet of lossy

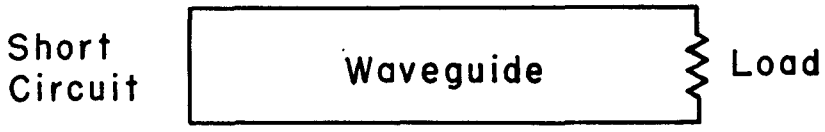

Fig. 7. Waveguide region.

material, or it may be an aperture in an infinite screen. The only case for which there are no normal modes is when the load is matched; i. e., produces no reflections.

The steady-state solutions for waves in the guide are formally correct for the normal modes, but the frequency ω must be replaced

by the complex frequency p, and some new interpretations will be necessary. For convenience the steady-state waveguide theory is now briefly summarized.[15] If $\underline{E}(xyz)$, and $\underline{H}(xyz)$ are fields in the waveguide then the transverse components may be expressed as a sum of waveguide modes:

$$\underline{E}_t(xyz) = \sum_\nu V_\nu(z)\,\underline{e}_\nu(xy) = \sum_\nu (a^+_\nu e^{-\gamma_\nu z} + a^-_\nu e^{+\gamma_\nu z})\,\underline{e}_\nu(xy) \quad (2.35)$$

$$\underline{H}_t(xyz) = \sum_\nu I_\nu(z)\,\underline{h}_\nu(xy) = \sum_\nu (b^+_\nu e^{-\gamma_\nu z} + b^-_\nu e^{+\gamma_\nu z})\,\underline{h}_\nu(xy). \quad (2.36)$$

The vector functions $\underline{e}_\nu$ and $\underline{h}_\nu$ have x- and y-components only; they consist of two separate sets apiece, those going with waveguide modes which have no E_z (TE), and those which have no H_z (TM). The mode functions satisfy the two-dimensional equation

$$\nabla^2 \underline{e}_\nu(xy) + \kappa_\nu^2\,\underline{e}_\nu(xy) = 0 \quad (2.37)$$

with

$$\underline{e}_\nu \times \underline{n} = 0 \quad (2.38)$$

on the waveguide walls. This equation with boundary condition has solutions only for values of κ_ν^2 which are discrete, real, and positive. These eigenvalues are the cutoff wave numbers for the various modes. The frequency and waveguide propagation constant are related by

$$\kappa_\nu^2 = k^2 + \gamma_\nu^2, \quad (2.39)$$

where

$$k^2 = \omega^2 \mu \epsilon \quad . \quad (2.40)$$

The propagation constant is a complex number:

$$\gamma_\nu = \alpha_\nu + j\beta_\nu , \tag{2.41}$$

where

$$\alpha_\nu = \text{attenuation constant for the } \nu^{\text{th}} \text{ mode} \tag{2.42}$$

$$\beta_\nu = \frac{2\pi}{\lambda_g} = \text{phase constant for the } \nu^{\text{th}} \text{ mode.} \tag{2.43}$$

The magnetic modes are similarly defined, with an appropriate boundary condition.

The modes are orthogonal, and may be normalized to unity:

$$\int_S \underline{e}_\nu \cdot \underline{e}_\mu \, ds = \int_S \underline{h}_\nu \cdot \underline{h}_\mu \, ds = \delta_{\nu\mu} \tag{2.44}$$

$$\int_S \underline{e}_\nu \cdot \underline{h}_\mu \, ds = 0. \tag{2.45}$$

The integration is over the waveguide cross section. The following relations may be shown.

$$\underline{e}_\nu (xy) = \underline{h}_\nu (xy) \times \underline{z} \tag{2.46}$$

$$\frac{\overset{+}{a}_\nu}{\overset{+}{b}_\nu} = \begin{cases} \dfrac{j\omega\mu}{\gamma_\nu} = z_\nu^{TE} = \text{transverse wave impedance, for TE modes} \\ \dfrac{\gamma_\nu}{j\omega\epsilon} = z_\nu^{TM} = \text{transverse wave impedance, for TM modes} \end{cases} \tag{2.47}$$

$$\frac{\overset{+}{a}_\nu}{\overset{+}{b}_\nu} = -\frac{\overset{-}{a}_\nu}{\overset{-}{b}_\nu} . \tag{2.48}$$

If the load is at $z = 0$, the load impedance, for the ν^{th} mode, is defined as $\frac{V_\nu(0)}{I_\nu(0)}$. The functions $V_\nu(z)$ and $I_\nu(z)$ obey transmission line equations and are identical to voltage and current on a transmission line of characteristic impedance z_ν and propagation constant γ_ν.

Now, if $\underline{E}(xyz)$ and $\underline{H}(xyz)$ are normal-mode fields, we use the same theory, replacing ω by the complex frequency, $p = \omega + j\xi$. It is of interest to examine the propagation constants γ_ν. From eq. (2.39),

$$\gamma_\nu^2 = \kappa_\nu^2 - k^2 . \tag{2.49}$$

Substitute for γ_ν and k:

$$\alpha^2 - \beta^2 + j2\alpha\beta = \kappa^2 - (\omega^2 - \xi^2 + j2\xi\omega)\mu\epsilon , \tag{2.50}$$

where, for convenience, the subscripts have been omitted. Upon separating real and imaginary quantities, one obtains

$$\alpha\beta = -\xi\omega\mu\epsilon \tag{2.51}$$

$$\alpha^2 - \beta^2 = \kappa^2 - (\omega^2 - \xi^2)\mu\epsilon = (\omega_c^2 - \omega^2 + \xi^2)\mu\epsilon , \tag{2.52}$$

where ω_c = cutoff frequency of ν^{th} mode. This last substitution for κ is not valid unless μ and ϵ are real. Eqs. (2.51) and (2.52) may be solved for α and β; the results are

$$\alpha = \pm \frac{\xi\sqrt{\mu\epsilon}}{g} \tag{2.53}$$

$$\beta = \mp \omega\sqrt{\mu\epsilon}\, g, \tag{2.54}$$

where

$$g = \frac{1}{\sqrt{2}} \left\{ \left[1 - \left(\frac{\omega_c}{\omega}\right)^2 - \left(\frac{1}{2Q}\right)^2 \right] + \sqrt{\left[1 - \left(\frac{\omega_c}{\omega}\right)^2 - \left(\frac{1}{2Q}\right)^2 \right]^2 + \frac{1}{Q^2}} \right\}^{1/2} , \tag{2.55}$$

and, as before,

$$Q = \frac{\omega}{2\xi} . \tag{2.56}$$

The parameter g may be called the "normal-mode factor" for the waveguide. Some sample curves of g vs. $(\frac{\omega_c}{\omega})$ are shown in Fig. 8. If $\xi \to 0$, then $\alpha \to 0$ and $Q \to \infty$. This is the steady-state case, and g for this case is shown on the graph.

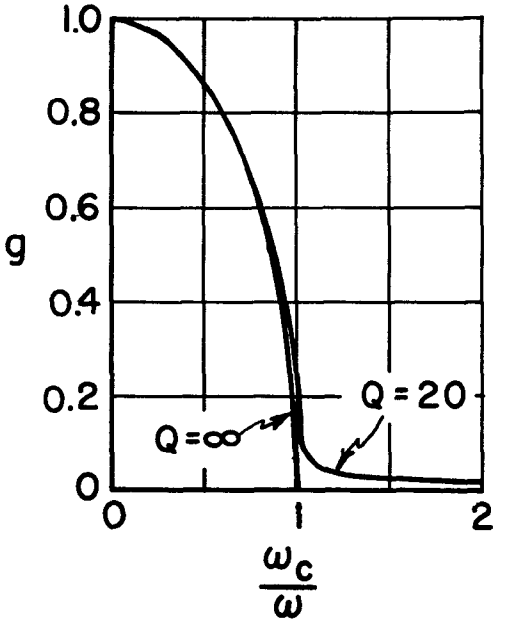

Fig. 8. Normal-mode factor vs. frequency.

When $(\frac{\omega_c}{\omega}) < 1$ the normal mode may be said to be "above cutoff" (of the ν^{th} waveguide mode) and, if Q is high, g essentially coincides with the steady-state curve. The approximation for this case is

$$g \approx \sqrt{1 - \left(\frac{\omega_c}{\omega}\right)^2} , \quad \left(\frac{\omega_c}{\omega}\right) < 1. \tag{2.57}$$

When $(\frac{\omega_c}{\omega}) > 1$ the normal mode is "below cutoff", and, if Q is high, g is approximately given by

$$g \approx \frac{1}{2Q} \frac{1}{\sqrt{\left(\frac{\omega_c}{\omega}\right)^2 - 1}}, \qquad \left(\frac{\omega_c}{\omega}\right) > 1. \tag{2.58}$$

It follows then, from eqs. (2.53) and (2.54), that, for high Q,

$$\left.\begin{aligned} \alpha &\approx \pm \frac{\xi \sqrt{\mu \epsilon}}{\sqrt{1 - \left(\frac{\omega_c}{\omega}\right)^2}} \\ \beta &\approx \mp \omega \sqrt{\mu \epsilon} \sqrt{1 - \left(\frac{\omega_c}{\omega}\right)^2} \end{aligned}\right\} \quad \left(\frac{\omega_c}{\omega}\right) < 1 \qquad (2.59)$$

$$\left.\begin{aligned} \alpha &\approx \pm \omega \sqrt{\mu \epsilon} \sqrt{\left(\frac{\omega_c}{\omega}\right)^2 - 1} \\ \beta &\approx \mp \frac{\xi \sqrt{\mu \epsilon}}{\sqrt{\left(\frac{\omega_c}{\omega}\right)^2 - 1}} \end{aligned}\right\} \quad \left(\frac{\omega_c}{\omega}\right) > 1. \qquad (2.60)$$

When $\left(\frac{\omega_c}{\omega}\right) < 1$ the propagation constant β for a normal-mode wave is essentially the same as that for a steady-state wave above cutoff, at the frequency ω. Below cutoff the attenuation constant α for a normal-mode wave is essentially the same as that for a steady-state wave below cutoff, at the frequency ω. In addition to these "quasi-steady-state" characteristics, the normal-mode wave also has attenuation above cutoff, and propagation below. (Actually, the attenuation is negative, because α and β have opposite signs. This point is discussed below.)

These effects of attenuation and propagation are relatively minor. For example, the wavelength in the waveguide is given by

$$\lambda_g = \frac{2\pi}{\beta} = \frac{\lambda_o}{g}, \qquad (2.61)$$

where λ_o is the wavelength of a plane wave in the medium, at the

frequency ω. Below cutoff g is very small, and λ_g is very large. Over a limited region the wave nature of the disturbance would not be evident. One would observe a field with almost uniform phase, just as for a steady-state wave which is below cutoff.

A wave traveling in the positive z-direction is described by

$$E = e^{j(\omega t - \beta z)} e^{-\xi t - \alpha z}, \tag{2.62}$$

where α is a negative number. This wave increases exponentially in the direction of propagation. Upon using eqs. (2.53) and (2.54), eq. (2.62) becomes

$$E = e^{j\omega(t - \frac{z}{v_1})} e^{-\xi (t - \frac{z}{v_2})}, \tag{2.63}$$

where

$$v_1 = \frac{1}{\sqrt{\mu \epsilon}\ g} \tag{2.64}$$

$$v_2 = \frac{g}{\sqrt{\mu \epsilon}} . \tag{2.65}$$

The phase velocity of the waves is v_1, and we may call v_2 the envelope velocity. For waveguide modes which have $(\frac{\omega c}{\omega}) << 1$ (far above cutoff), v_1 and v_2 approach the velocity of light, and the field becomes a plane wave, as described by eq. (2.34). Below cutoff $g \to 0$ and the phase velocity becomes very large, whereas the envelope velocity becomes small.

In general the envelope velocity v_2 is less than the phase velocity v_1. Hence, if any one particular sinusoid were watched it would appear

to increase as it moved down the waveguide. A similar phenomenon can be observed with water waves; if a group of waves advances into still water, the individual waves will be seen to advance through the group.

The fact that these waves increase in the direction of propagation may appear paradoxical, since it is opposite to the steady-state attenuation effect. To clear this up, it must be remembered that normal modes are characteristic of regions where there are reverberations, and the reflected waves will take care of any apparently paradoxical increases of field strength. A simple example will illustrate this. Let the region be a radiating waveguide, as shown in Fig. 9. Suppose a waveguide mode which is below cutoff is excited at the aperture, and the circumstances are such that the field of that mode is essentially in phase along the length of the guide. The wave will increase toward the rear wall, and the reflected wave will in turn increase toward the aperture. The magnitude of the transverse electric field is illustrated in Fig. 10, and that for the magnetic field, in Fig. 11. The incident and reflected waves are denoted by arrows and are shown dashed. The sum of the two, the total field, is the solid line. The transverse electric field must be zero at the rear wall and hence the reflected electric wave is out of phase with the incident one. The reflected magnetic wave is in phase with the incident one.

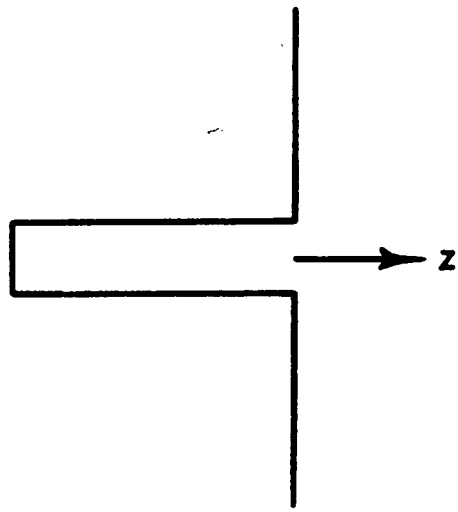

Fig. 9. Radiating waveguide.

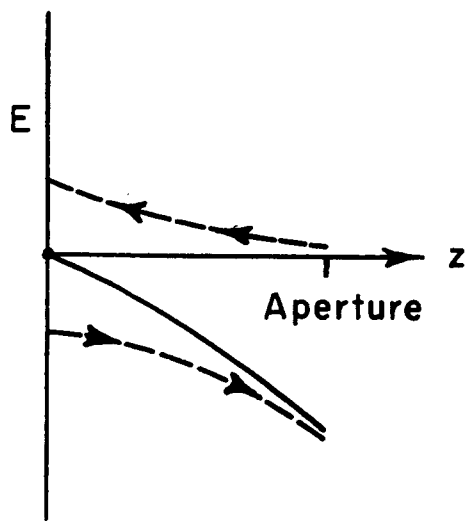

Fig. 10. Transverse electric field

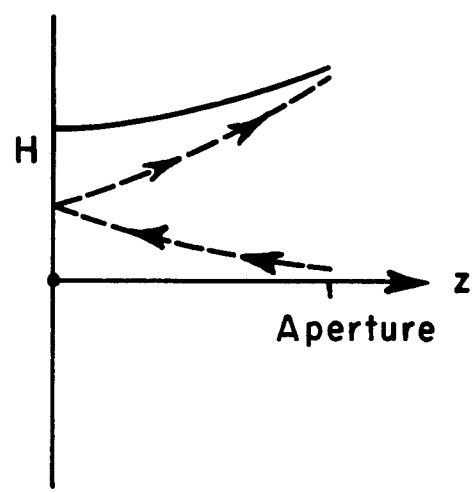

Fig. 11. Transverse magnetic field

The total field in the guide is the same as that of a steady-state waveguide mode which is cut off — it decreases away from the aperture according to a hyperbolic sine or cosine. The ratio of the magnitudes of E and H is controlled by the aperture impedance. One important distinction must be noted between this and the steady-state case — the aperture fields are essentially those *reflected* from the rear wall, rather than incident fields, and this introduces a minus sign into the impedance expressions. This point will be noted again in the next section.

III. NORMAL MODES OF A RADIATING CAVITY

1. GENERAL THEORY

We now consider electromagnetic oscillations in the open region bounded by a cavity and an infinite conducting plane screen, as in Fig. 12. The electric field satisfies the wave equation

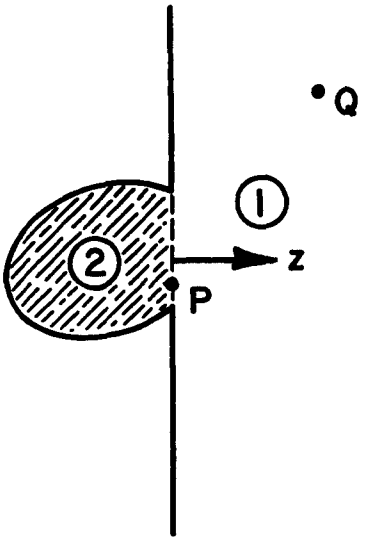

Fig. 12. Source-free radiating cavity.

$$\nabla \times \nabla \times \underline{E} + \mu \epsilon \frac{\partial^2 \underline{E}}{\partial t^2} = 0 \qquad (3.1)$$

and the boundary condition

$$\underline{n} \times \underline{E} = 0 \qquad (3.2)$$

on the ground plane and cavity wall. In addition, the tangential component of the electric field is continuous across the aperture, where there may be a dielectric discontinuity. We also assume that the original source of the field was inside the cavity, so that the energy is propagated outward.

Now assume that there exists a discrete set of solutions which have a time dependence of the form $e^{j p_n t}$, where

$$p_n = \omega_n + j \xi_n. \qquad (3.3)$$

The wave equation then becomes

$$\nabla \times \nabla \times \underline{E}_n - k_n^2 \underline{E}_n = 0,^*$$

* From here on the time dependence $e^{j p_n t}$ will be suppressed.

where

$$k_n^2 = p_n^2 \mu \epsilon \quad . \tag{3.5}$$

The possible electric fields $\underline{E}_n(xyz)$ are eigenfunctions and the propagation constants k_n are eigenvalues. The questions of existence, orthogonality, and completeness of these modes are ignored here. The conventional statements are hard to apply, because of the open region and the fact that the modes increase as $(e^{\alpha r})/r$ as r goes to infinity.

For purposes of computing Q_n only the eigenvalues are necessary, and a variational method will be employed to find them. In the preceding section it was shown how the tangential electric field over a closed surface can be used to generate the fields interior to the surface. This technique is used to set up the variational formulation of the problem. The magnetic field in the the two regions, $\underline{\overset{1}{H}}_n$ in the half-space, and $\underline{\overset{2}{H}}_n$ in the cavity, will be expressed in terms of $\underline{z} \times \underline{E}_n$ in the aperture, and then we will set $\int_A \underline{E}_n \times \underline{\overset{1}{H}}_n \cdot \underline{z}\, ds = \int_A \underline{E}_n \times \underline{\overset{2}{H}}_n \cdot \underline{z}\, ds$. This is obviously true for the correct field $\underline{E}_n$, but its value lies in the fact that values of k_n calculated from this equation are stationary with respect to first-order variations of $\underline{E}_n$ about the true value. (See Appendix III.)

The first step in this procedure is to find the magnetic field in the half-space. In section II it was shown that the fields in the half-space are the same as those produced by magnetic currents $\underline{\overset{1}{K}} = -2\underline{z} \times \underline{E}$ flowing in the aperture, and radiating into free space. They are derivable from an electric vector potential as follows:[16]

$$\underline{\underline{E}} = \nabla \times \underline{\underline{F}} \tag{3.6}$$

where

$$\underline{\underline{F}} = \int_A \underline{\underline{K}} \frac{e^{-jkr}}{4\pi r} ds. \tag{3.7}$$

Then

$$\underline{\underline{H}} = -\frac{1}{jp\mu} [\nabla \nabla \cdot \underline{\underline{F}} + k^2 \underline{\underline{F}}] , \tag{3.8}$$

or

$$\underline{\underline{H}} = \frac{jp\epsilon}{4\pi} \int_A \left[\underline{\underline{K}} \frac{e^{-jkr}}{r} + \frac{1}{k^2} \nabla \nabla \cdot \left(\underline{\underline{K}} \frac{e^{-jkr}}{r} \right) \right] ds. \tag{3.9}$$

The subscript n, referring to the n^{th} normal mode, has been omitted, and it is understood that these remarks apply to any of the modes. In part 3 below the subscript will be used again.

The order of differentiation and integration is immaterial, because the integration is with respect to points P; the differentiation, to points Q. We may now write, in the customary matrix notation:

$$\underline{\underline{H}}(Q,k) = \int_A \underline{\underline{\Gamma}}(Q,P,k) \, K(P) \, ds_P, \tag{3.10}$$

where

$$\underline{K}(P) = \underline{z} \times \underline{E}(P), \tag{3.11}$$

and $\underline{\underline{\Gamma}}$ is a free-space tensor Green's function:*

$$\underline{\underline{\Gamma}}(Q,P,k) = \frac{-jp\epsilon}{2\pi} \left(I + \frac{\nabla\nabla}{k^2} \right) \frac{e^{-jkr}}{r}. \tag{3.12}$$

* For a detailed discussion of tensor Green's functions see reference 31.

I is the unit matrix. The components of $\overset{1}{\Gamma}$ have simple interpretations. For example, $\overset{1}{\Gamma}_{xy}(Q,P)$ is (-2) times the x-component of magnetic field at Q due to a y-oriented unit magnetic current element at P. In common with other Green's functions it has certain symmetry properties; i. e.,

$$\overset{1}{\Gamma}(Q,P) = \overset{\sim}{\overset{1}{\Gamma}}(P,Q). \tag{3.13}$$

The tilde indicates transpose. This follows immediately from the reciprocity theorem, eq. (2.21), which can be rewritten, for this application,* as

$$\tilde{q}\,\Gamma_1(Q,M)\,m = \tilde{m}\,\Gamma_1(M,Q)q. \tag{3.14}$$

If the transpose of the right-hand side is taken, (3.13) follows because q and m are arbitrary. Eq. (3.13) is evident from an examination of the form of the Green's function, in eq. (3.12). However, the symmetry property is much more general than may be deduced in this manner, because (3.12) is valid only for free space.

The magnetic field in the cavity can similarly be written as

$$\overset{2}{\mathbf{H}}(Q,k) = \int_A \overset{2}{\Gamma}(Q,P,k)\,\mathbf{K}(P)\,ds_P. \tag{3.15}$$

The cavity Green's function, $\overset{2}{\Gamma}$, is a separate, extensive topic, and we shall not use it explicitely. The discussion of $\overset{2}{\Gamma}$ is therefore deferred until Appendix II.

* Eq. (2.21) has been derived for the electric field of an electric current element; obviously, a similar statement holds for the magnetic field of a magnetic current.

If we set the tangential magnetic fields equal on the two sides of the aperture, we obtain an integral equation for the electric field:

$$\int_A \overset{1}{\Gamma}(Q,P,k)\mathbb{K}(P)\,ds_P = \int_A \overset{2}{\Gamma}(Q,P,k)\mathbb{K}(P)\,ds_P. \quad (3.16)$$

To get the invariant formula, multiply by $\tilde{\mathbb{K}}$ and integrate again.

$$\int_{A_Q}\int_{A_P} \tilde{\mathbb{K}}(Q)\,\overset{1}{\Gamma}(Q,P,k)\mathbb{K}(P)\,ds_P\,ds_Q = \int_{A_Q}\int_{A_P} \tilde{\mathbb{K}}(Q)\,\overset{2}{\Gamma}(Q,P,k)\mathbb{K}(P)\,ds_P\,ds_Q. \quad (3.17)$$

In Appendix III it is shown that values of k computed from this formula are stationary with respect to first-order variations of $\mathbb{K}$ about the true value.

The stationary property makes this a good approximation method, because, if the first guess to the field is close to the true value, then the calculated k would be expected to be closer to its true value, since the error in it is proportional to the square of the error in $\underline{E}$. This is a very rough statement, but qualitatively it gives the basic reason why the variational method is sometimes superior to other approximation schemes.

The tangential electric field in the aperture can be expanded in the waveguide modes described in section II, and the expansion coefficients and eigenvalues can be found by virtue of the stationary

property (Ritz method).* Then, after these are known, the fields everywhere may be found by eqs. (3.10) and (3.15). Thus, formally, the complete solution of the problem may be found. Practically, of course, the modes are known only for certain simple shapes, and each step in the Ritz procedure involves very laborious calculations. Hence the first step in this procedure, the first-order calculation of k, is as much as is generally done. In this paper we go only a little further, to indicate that one waveguide mode is a good approximation.

Consider the integral in eq. (3.17):

$$\int_{A_Q} \int_{A_P} \tilde{K}(Q)\, \overset{1}{\Gamma}(Q,P,k)\, K(P)\, ds_P\, ds_Q = \int_A \underline{E} \times \underline{\overset{1}{H}} \cdot \underline{z}\, ds. \quad (3.18)$$

This has the dimensions of power, and if we divide it by $\int_A E^2\, ds$ we have an admittance. Actually, a similar aperture admittance has been defined for a waveguide. If an infinite waveguide radiates through an aperture in a ground plane, the aperture admittance, for the propagating waveguide mode, is just

$$Y = \frac{I_1(0)}{V_1(0)}, \quad (3.19)$$

where the symbols are defined in section II. It may be shown[17] that this is equal to

$$Y = \frac{\int_{A_Q} \int_{A_P} \tilde{K}(Q) \left[\overset{3}{\Gamma}(Q,P) - \overset{1}{\Gamma}(Q,P) \right] K(P)\, ds_P\, ds_Q}{\left[\int_A E \cdot e_1\, ds \right]^2}, \quad (3.20)$$

* See any book on quantum mechanics for a discussion of this technique.

where $\underline{e}_1$ = transverse electric field for the propagating mode, and

$$\overset{3}{\Gamma}(Q,P) = - \sum_{\nu=2}^{\infty} y_\nu \, \underline{h}_\nu (Q) \, \underline{h}_\nu (P). \tag{3.21}$$

$\overset{3}{\Gamma}$ is written as a dyadic. y_ν is the characteristic admittance for the ν^{th} waveguide mode ($y_\nu = 1/z_\nu$, eq. (2.47)). This formula for Y is stationary in the sense that its first variation is zero for variations of $\underline{E}$ about the true value. It may be obtained by equating $\int_A \underline{E} \times \underline{H} \cdot \underline{z} \, ds$ across a surface consisting of the aperture and a waveguide cross-section so remote that only the propagating mode exists there.

It is also convenient to define an "interaction admittance":

$$Y_{\nu\mu} = \int_{A_Q} \int_{A_P} \tilde{\mathbf{h}}_\nu (Q) \, \overset{1}{\Gamma}(Q,P) \, \mathbf{h}_\mu (P) \, ds_P \, ds_Q. \tag{3.22}$$

Now the first approximation in solving the problem is to assume that the transverse electric field in the aperture is just the first mode, $\underline{e}_1$. Then we have immediately

$$\int_A \underline{E} \times \underline{H} \cdot \underline{z} \, ds \approx Y \approx Y_{11}. \tag{3.23}$$

For the infinite waveguide case, the correct values for these three quantities are actually very close. Calculations of Y_{11} have been made for a series of rectangular waveguides for the steady-state case, and they agreed with measured values of Y to within experimental accuracy.[17]

For a general cavity we could still assume that the aperture field was the first waveguide mode appropriate to the aperture shape. Values of $\int_A \underline{E} \times \underline{H} \cdot \underline{z}\, ds$ would then be available. For simple geometries Y_{11} may be calculated, or Y may be measured for any shape waveguide. The measurement would, of course, be of a steady-state impedance, but, as shown below, this is all that is needed for one approximation method of actually performing the numerical calculations.

It is to be observed that the general procedures used in setting up this problem are applicable to a much wider variety of normal-mode problems. Suppose it is desired to find the normal modes about an arbitrary finite conducting body. The equivalent currents to be used are electric currents $\underline{J} = \underline{n} \times \underline{H}$ and $\underline{K} = \underline{E} \times \underline{n}$, flowing on the body surface and radiating into free space. These currents produce the correct field exterior to the body. Note though that $\underline{K} = 0$ because the body is a conductor. Hence the currents $\underline{J}$ in free space by themselves produce the fields. (The currents $\underline{J}$ are the *actual* currents flowing on the body.) If $\underline{E}$ is the electric field computed from $\underline{J} = \underline{n} \times \underline{H}$ then the equation

$$\int \underline{E} \times \underline{H} \cdot \underline{n}\, ds = 0 \qquad (3.24)$$

is true for the correct $\underline{H}$, and values of k computed from this formula are stationary with respect to first-order variations of $\underline{H}$ about the true value.

Therefore it is seen that the calculation of Y_{11} for a square aperture is exactly the calculation needed to find the normal modes of a square plate. Also, it is the calculation needed to find the normal modes of a square aperture in an infinite conducting screen, with free space on *both* sides of the screen. These two systems would have a very low Q.

2. WAVEGUIDE CAVITY

Now restrict the cavity to be a section of waveguide, as in Fig. 13.

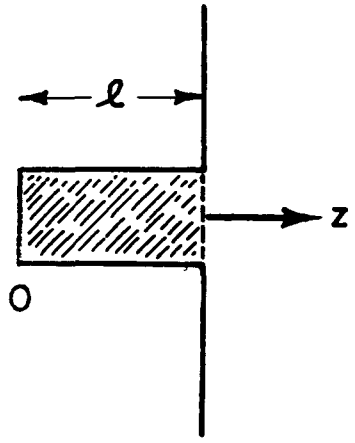

Fig. 13. Waveguide cavity.

The cross section is arbitrary but uniform along the z-axis. The direct connection between the arbitrary cavity expansion and the waveguide case is presented in Appendix II; in this section we shall proceed on the basis of waveguide theory, as outlined in section II.

In the waveguide region, the transverse electric and magnetic fields of the normal mode may be written as a sum of waveguide modes:

$$\underline{\overset{t}{E}}\,(xyz) = \sum_{\nu} V_{\nu}\,(z)\,\underline{e}_{\nu}\,(xy) \qquad (3.25)$$

$$\underline{\overset{t}{H}}\,(xyz) = \sum_{\nu} I_{\nu}\,(z)\,\underline{h}_{\nu}\,(xy). \qquad (3.26)$$

Inasmuch as V and I obey transmission line equations, we have

$$I_{\nu}\,(\ell) = -\,V_{\nu}\,(\ell)\,y_{\nu}\,\coth\gamma_{\nu}\,\ell\ . \qquad (3.27)$$

The minus sign comes from the fact that waves traveling in the positive z-direction are the reflected waves from the short circuit. (See discussion in section II above.) Eq. (3.27) may be derived by combining eqs. (2.35), (2.36), (2.44), (2.47), and (2.48) with the requirement that $\underline{\overset{t}{E}} = 0$ at $z = 0$.

Thus the magnetic field in the aperture becomes

$$\underline{\overset{t}{H}}\,(xy\ell) = \sum_{\nu} - y_{\nu} \coth \gamma_{\nu} \ell \;\; \underline{h}_{\nu}\,(xy) \int_{A} \underline{E} \cdot \underline{e}_{\nu}\, ds, \qquad (3.28)$$

upon substitution of (3.27) and (3.25) into (3.26). This may be written as

$$\overset{t}{\mathbb{H}}\,(Q,k) = \int_{A} \overset{2}{\Gamma}\,(Q,P,k)\, \mathbb{K}\,(P)\, ds_{P}, \qquad (3.29)$$

where $\underline{K} = \underline{z} \times \underline{E}$, and the waveguide-cavity Green's function, $\overset{2}{\Gamma}$, is

$$\overset{2}{\Gamma}\,(Q,P,k) = \sum_{\nu} - y_{\nu} \coth \gamma_{\nu} \ell \;\; \underline{h}_{\nu}\,(Q)\, \underline{h}_{\nu}\,(P). \qquad (3.30)$$

Note that points P and Q are both in the aperture.

To get the variational expression, multiply (3.28) by $\underline{z} \times \underline{E}$, integrate, and set equal to $\int \underline{E} \times \overset{1}{\underline{H}} \cdot \underline{z}\, ds$. This gives

$$\sum_{\nu} - y_{\nu} \coth \gamma_{\nu} \ell \;\; \left(\int_{A} \underline{E} \cdot \underline{e}_{\nu}\, ds\right)^{2} = \int_{A_Q} \int_{A_P} \tilde{\mathbb{K}}\,(Q)\, \overset{1}{\Gamma}\,(Q,P,k)\, \mathbb{K}\,(P)\, ds_{P}\, ds_{Q}. \qquad (3.31)$$

This formula is the invariant expression for the propagation constant k. It is made more concise by inserting the expansion for $\underline{E}$, eq. (3.25), for convenience omitting the argument $z = \ell$. This gives

$$\sum_{\nu} - y_{\nu} \coth \gamma_{\nu} \ell \; V_{\nu}^2 = \sum_{\nu} \sum_{\mu} V_{\nu} \; V_{\mu} \; Y_{\nu \mu} \, . \tag{3.32}$$

As a first approximation, let all the V's be zero except V_1. Physically, this means that the aperture electric field is equal to the lowest waveguide mode configuration. It is known that this cannot be correct, but it is a good approximation, at least for those normal modes which essentially consist of only that one waveguide mode. This approximation leaves

$$- y_1 \coth \gamma_1 \ell = Y_{11}. \tag{3.33}$$

This formula is analogous to the formula used in section I for finding the normal modes of an elementary circuit. If we consider terminals at the aperture for the lowest-order waveguide mode, then

$$Y_{\text{left}} = - Y_{\text{right}}$$

gives eq. (3.33).

Let us examine the situation which results if two modes exist at the aperture. Let

$$\underline{E} = V_1 \, \underline{e}_1 + V_2 \, \underline{e}_2. \tag{3.34}$$

Then eq. (3.32) becomes

$$V_1^2 \, y_1 \coth \gamma_1 \ell + V_2^2 \, y_2 \coth \gamma_2 \ell + V_1^2 \, Y_{11} + V_2^2 \, Y_{22} + 2 V_1 \, V_2 \, Y_{12} = 0. \tag{3.35}$$

* By the reciprocity theorem, $Y_{12} = Y_{21}$.

Call this last expression F. Since we have set it identically equal to zero, it is stationary, and

$$\frac{dF}{dV_1} = 0$$

and (3.36)

$$\frac{dF}{dV_2} = 0.$$

Now

$$\frac{dF}{dV_1} = \frac{\partial F}{\partial V_1} + \frac{\partial F}{\partial k}\,\frac{dk}{dV_1}\,. \tag{3.37}$$

But k is the stationary parameter, and $dk/dV_1 = 0$. Hence

$$\begin{aligned} V_1\,(y_1 \coth \gamma_1 \ell + Y_{11}) + V_2\, Y_{12} &= 0 \\ V_1\, Y_{12} + V_2(y_2 \coth \gamma_2 \ell + Y_{22}) &= 0. \end{aligned} \tag{3.38}$$

This is a pair of simultaneous homogeneous equations; the only way they can be satisfied is for the determinant to be zero.

$$\begin{vmatrix} (y_1 \coth \gamma_1 \ell + Y_{11}) & Y_{12} \\ Y_{12} & (y_2 \coth \gamma_2 \ell + Y_{22}) \end{vmatrix} = 0. \tag{3.39}$$

The expansion of this determinant provides an equation for the eigenvalue k.

Consider the ratio of the amplitudes of the modes. From (3.38),

$$\frac{V_2}{V_1} = \frac{-\,Y_{12}}{y_2 \coth \gamma_2 \ell + Y_{22}}\,. \tag{3.40}$$

Suppose the first waveguide mode is "above cutoff" and the second is not. Then, according to the ideas developed in section II, γ_1 is essentially imaginary and γ_2 is essentially real. The hyperbolic cotangent is large when its argument is small, so $\frac{V_2}{V_1} \to 0$ as $\ell \to 0$. This would be expected from the development in section II. Refer to Fig. 10, which portrays the transverse electric field of a cutoff mode. As ℓ decreases there is less attenuation, and the total aperture field decreases in relation to the "excitation."

The admittances Y_{12} and Y_{22} would have to be calculated to find a more precise effect of the higher mode. It is felt that this slight correction is not worth the labor involved in the additional calculation. All the calculations made on the basis of one waveguide mode agree well enough with experiment to support this view.

3. APPLICATION TO SQUARE WAVEGUIDE

We shall now apply the first approximation of the variational method to a square waveguide, see Fig. 14. It is assumed that only the TE_{10} mode exists in the waveguide. The electric field for this mode has only one component, and is sinusoidally distributed.

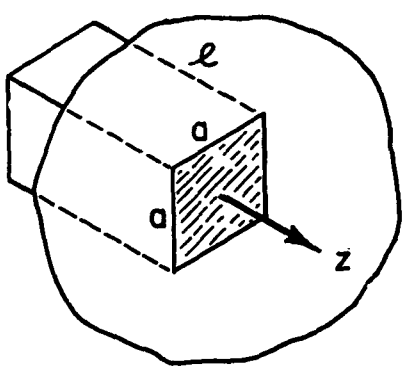

Fig. 14. Square waveguide cavity.

The desired eigenvalues are the roots, p_n, of the equation

$$f(p) = y_1 \coth \gamma_1 \ell + Y_{11} = 0. \tag{3.41}$$

As defined above, p is the complex frequency,

$$p = \omega + j\xi \tag{3.42}$$

and

$$y_1 = \frac{\gamma_1}{jp\mu} \tag{3.43}$$

$$\gamma_1^2 = \kappa_1^2 - k^2 \tag{3.44}$$

$$\kappa_1 = \frac{\pi}{a} \tag{3.45}$$

$$k^2 = p^2 \mu \epsilon . \tag{3.46}$$

The aperture impedance Y_{11} has been computed[17] and is available as a series in $(\frac{ap}{2\pi c})$. When p is real this variable is just (a/λ), and for this case it has been drawn as a graph, in Figs. 15 and 16.

For convenience, let

$$x = \frac{ap}{2\pi c} \tag{3.47}$$

and

$$Y_{11}(x) = G(x) + j\, B(x). \tag{3.48}$$

Suppose $\mu = \mu_o$ and $\epsilon = \epsilon_r \epsilon_o$. Then

$$k^2 = \frac{p^2\, \epsilon_r}{c^2} \tag{3.49}$$

$$\gamma_1^2 = (\frac{\pi}{a})^2 \left[1 - 4\epsilon_r x^2\right] \tag{3.50}$$

$$y_1 = \sqrt{\frac{\epsilon_o}{\mu_o}}\, \frac{\sqrt{4\ \epsilon_r x^2 - 1}}{2x} . \tag{3.51}$$

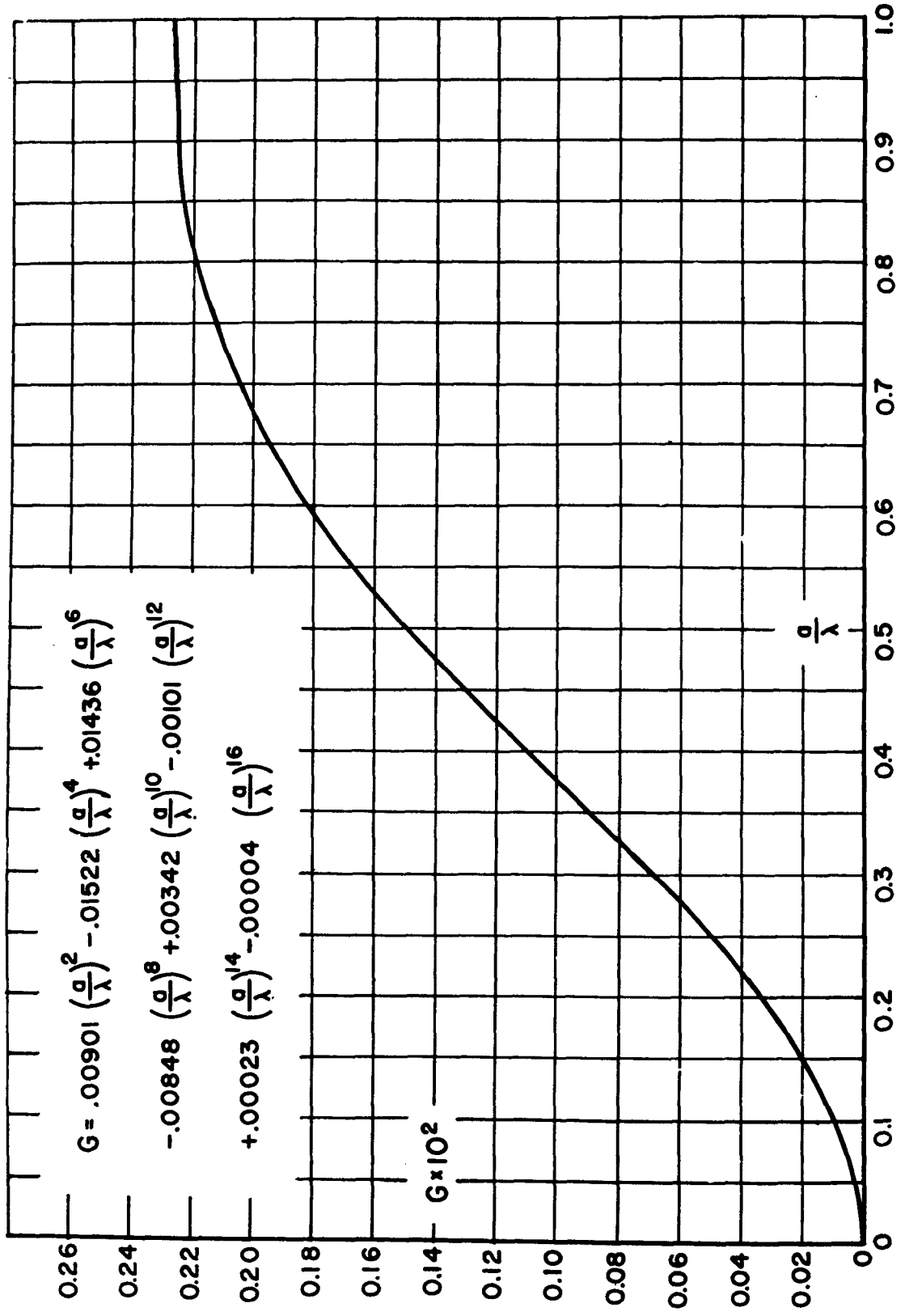

Fig. 15. Aperture conductance for a square waveguide.

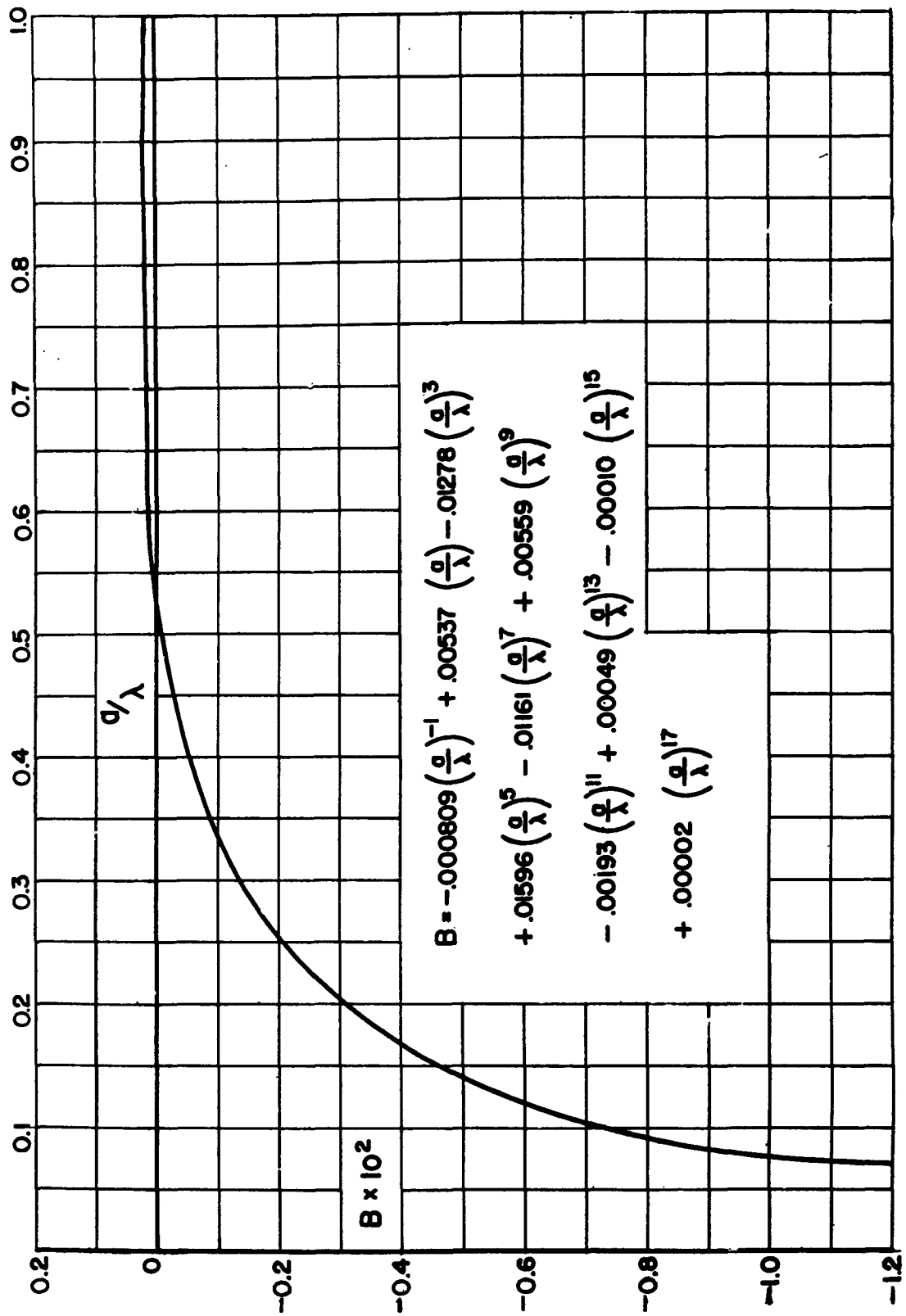

Fig. 16. Aperture susceptance for a square waveguide.

In terms of the dimensionless variables x, ℓ/a, and ϵ_r, the eigenvalue equation becomes

$$f(x, \frac{\ell}{a}, \epsilon_r) = -j\sqrt{\frac{\epsilon_o}{\mu_o}}\frac{\sqrt{4\,\epsilon_r x^2 - 1}}{2x}\cot\left[\pi\frac{\ell}{a}\sqrt{4\,\epsilon_r x^2 - 1}\right] + G(x) + j\,B(x) = 0. \tag{3.52}$$

If real and imaginary parts of (3.52) are separated, there results a pair of simultaneous transcendental equations. Various schemes may be used to find the solutions; we will use one that quickly yields good approximations to them. This problem is almost identical to the problem of finding the normal modes of a transmission line terminated with some load, as in Fig. 17. In such a case, when $Q >> 1$, the voltage is distributed essentially as if G were absent. The major function of G is to contribute to the loss, not to the field distribution. This idea will be carried over to the cavity problem.

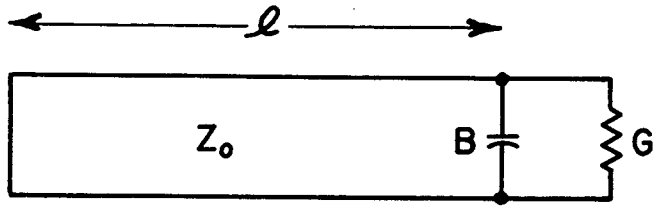

Fig. 17. Transmission line.

Let x_{on} be the roots of

$$-j\sqrt{\frac{\epsilon_o}{\mu_o}}\frac{\sqrt{4\,\epsilon_r x^2 - 1}}{2x}\cot\,\pi\frac{\ell}{a}\sqrt{4\,\epsilon_r x^2 - 1} + j\,B(x) = 0. \tag{3.53}$$

These are real numbers, $x_{on} = (\frac{a}{\lambda})_{on}$. Now assume that the roots, x_n, of eq. (3.52) are close to x_{on}, and expand f(x) in a Taylor's series about the point x_{on}.

$$f(x_n) = f(x_{on}) + \left.\frac{\partial f}{\partial x}\right|_{x_{on}} (x_n - x_{on}) + \frac{1}{2} \left.\frac{\partial^2 f}{\partial x^2}\right|_{x_{on}} (x_n - x_{on})^2 + \ldots = 0. \tag{3.54}$$

If we keep only the linear terms, we obtain, upon substitution of $G(x_{on})$ for $f(x_{on})$,

$$x_n = x_{on} + \frac{-G(x_{on})}{\left.\frac{\partial f}{\partial x}\right|_{x_{on}}} . \tag{3.55}$$

The derivative, evaluated at x_{on}, is

$$\left.\frac{\partial f}{\partial x}\right|_{x_{on}} = -\frac{j}{\left(\frac{a}{\lambda}\right)_{on}} \frac{B\left(\frac{a}{\lambda}\right)_{on}}{\left[4 \epsilon_r \left(\frac{a}{\lambda}\right)^2_{on} - 1\right]}$$

$$+ j2\pi \epsilon_r \sqrt{\frac{\epsilon_o}{\mu_o}} \frac{\ell}{a} \csc^2\left[\pi \frac{\ell}{a} \sqrt{4 \epsilon_r \left(\frac{a}{\lambda}\right)^2_{on} - 1}\right] + \left.\frac{\partial Y_{11}}{\partial x}\right|_{x_{on}} . \tag{3.56}$$

The derivative of Y_{11} is evaluated from the series shown in Figs. 15 and 16. The real and imaginary parts are just $\frac{\partial G}{\partial (a/\lambda)}$ and $\frac{\partial B}{\partial (a/\lambda)}$, and are shown in Fig. 18.

The above equations give the first approximation to the eigenvalues x_n, and from these are obtained Q_n. Since

$$x_n = \frac{a}{2\pi c} (\omega_n + j \xi_n) = \left(\frac{a}{\lambda}\right)_n + j \frac{a \xi_n}{2\pi c} , \tag{3.57}$$

then

$$Q_n = \frac{\omega_n}{2 \xi_n} = \frac{\left(\frac{a}{\lambda}\right)_n}{\frac{a \xi_n}{\pi c}} . \tag{3.58}$$

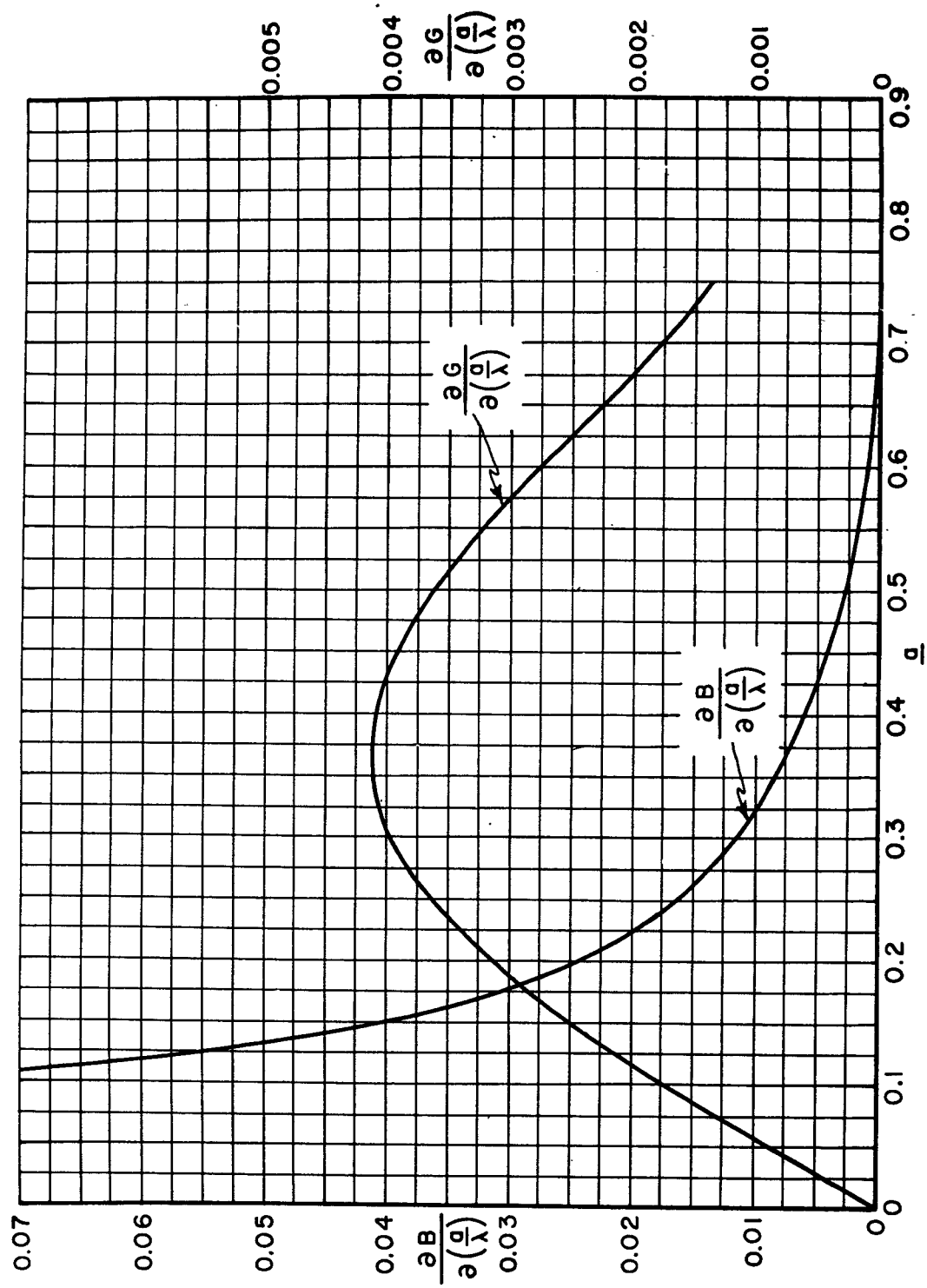

Fig. 18. Derivatives of aperture admittance for square waveguide.

The real part of x_n gives the resonance wavelength, in terms of the aperture, and the imaginary part gives the decay constant in terms of the aperture. Q_n, of course, is a relative measure of how rapidly the n^{th} oscillation dies out.

The validity of keeping only the linear terms was checked by computing the second derivative at one point. The point chosen was $(\frac{a}{\lambda})_{01} = 0.60$, $\epsilon_r = 1$; this is a point of very low Q, and the approximation should be worst here. The inclusion of the second derivative lowered Q by 3% and lowered $(\frac{a}{\lambda})_1$ by 0.7%. This is only a minor change and therefore it is felt that the linear terms alone give sufficiently accurate results.

Another approximation which brings out a close circuit analogy may be made when Q is high. From eq. (3.56) it is seen that $\frac{\partial G}{\partial x}\Big|_{x_{on}}$ is the only term of $\frac{\partial f}{\partial x}\Big|_{x_{on}}$ which is real, and hence it provides the only correction to the real part of x_n; i. e., to the oscillation frequency. The calculations for the first mode indicate that this correction is less than 1% for $Q > 7$. Hence, for a high-Q cavity, we have the approximate formulas,

$$(\frac{a}{\lambda})_n = (\frac{a}{\lambda})_{on} \tag{3.59}$$

$$Q_n = \frac{(\frac{a}{\lambda})_{on}}{2G} \operatorname{Im} \frac{\partial f}{\partial x}\Big|_{x_{on}} = \frac{\omega_n}{2G} \frac{\partial B}{\partial \omega}. \tag{3.60}$$

B is the total admittance at the aperture. Eq. (3.59) states that we may ignore the aperture conductance; i. e., the radiated energy, in computing the oscillation frequency. From (3.60) we see that $\partial G/\partial\omega$ may be ignored in computing Q, but, of course, G itself cannot be ignored. Eq. (3.60) is an approximate circuit equation for Q.[18]

Another problem might be to find what geometry or geometries will resonate at a given $(\frac{a}{\lambda})_n$. To be more general, we may say that, in the n^{th} mode, the cavity is characterized by the four dimensionless parameters, $\frac{\ell}{a}$, ϵ_r, $(\frac{a}{\lambda})_n$, and Q_n. In addition, there is the parameter $(\frac{a}{\lambda})_{on}$ which is an auxiliary quantity used in computing. These parameters are connected by the three equations, (3.53), (3.55), and (3.58). Hence, we might expect that the arbitrary specification of any two of them would fix the values of the others. Actually, this does not happen. Any pair of values of $(\frac{\ell}{a}, \epsilon_r)$ is admissible and leads to unique $(\frac{a}{\lambda})_n$ and Q_n. This is obvious — the geometry must specify the normal modes. But not all of the other pairs of values are realizeable.

a. CALCULATIONS FOR THE FIRST NORMAL MODE

A series of calculations which brings out the relations among the cavity parameters has been made for the first normal mode. The results are displayed in the form of graphs where the independent variables are $\frac{a}{\lambda}$ and ϵ_r. The curves could have been drawn in other ways, but all the information is presented here.

Fig. 19 shows the dependence of $\frac{\ell}{a}$ on $\frac{a}{\lambda}$ for various values of ϵ_r.

The curves asymptotically approach that value of $\frac{a}{\lambda}$ which corresponds to cutoff. It will be observed that very high values of dielectric constant are needed to resonate the cavity when $\frac{a}{\lambda}$ is small.

The values of Q which obtain for the various configurations of Fig. 19 are shown in Fig. 20. One conclusion is evident — various values of ϵ_r may be used to produce the same $\frac{a}{\lambda}$, but one of these values produces a minimum Q. The envelope of the family of curves in Fig. 20 corresponds to the minimum Q. It increases very rapidly as $\frac{a}{\lambda}$ gets smaller.

The minimum Q may be separately evaluated by maximizing the denominator of Q_n (eq. (3.58)) with respect to ϵ_r and $\frac{\ell}{a}$, and at the same time requiring eq. (3.53) to be maintained. This may be done by using a Lagrange multiplier. Let

$$A = \mathrm{Im}\left[\frac{-G}{\frac{\partial f}{\partial x}}\right]_{x_{on}} = \frac{\zeta G}{\eta^2 + \zeta^2} \tag{3.61}$$

$$C = \sqrt{\frac{\epsilon_o}{\mu_o}} \frac{\sqrt{4\epsilon_r \left(\frac{a}{\lambda}\right)^2_{on} - 1}}{2\left(\frac{a}{\lambda}\right)_{on}} \cot\left[\pi \frac{\ell}{a} \sqrt{4\epsilon_r \left(\frac{a}{\lambda}\right)^2_{on} - 1}\right] - B\left(\frac{a}{\lambda}\right)_{on} = 0, \tag{3.62}$$

where

$$\left.\frac{\partial f}{\partial x}\right|_{x_{on}} = \eta + j\zeta \,. \tag{3.63}$$

A is the denominator of Q_n, and is to be maximized. C is the side condition on the variables. Then

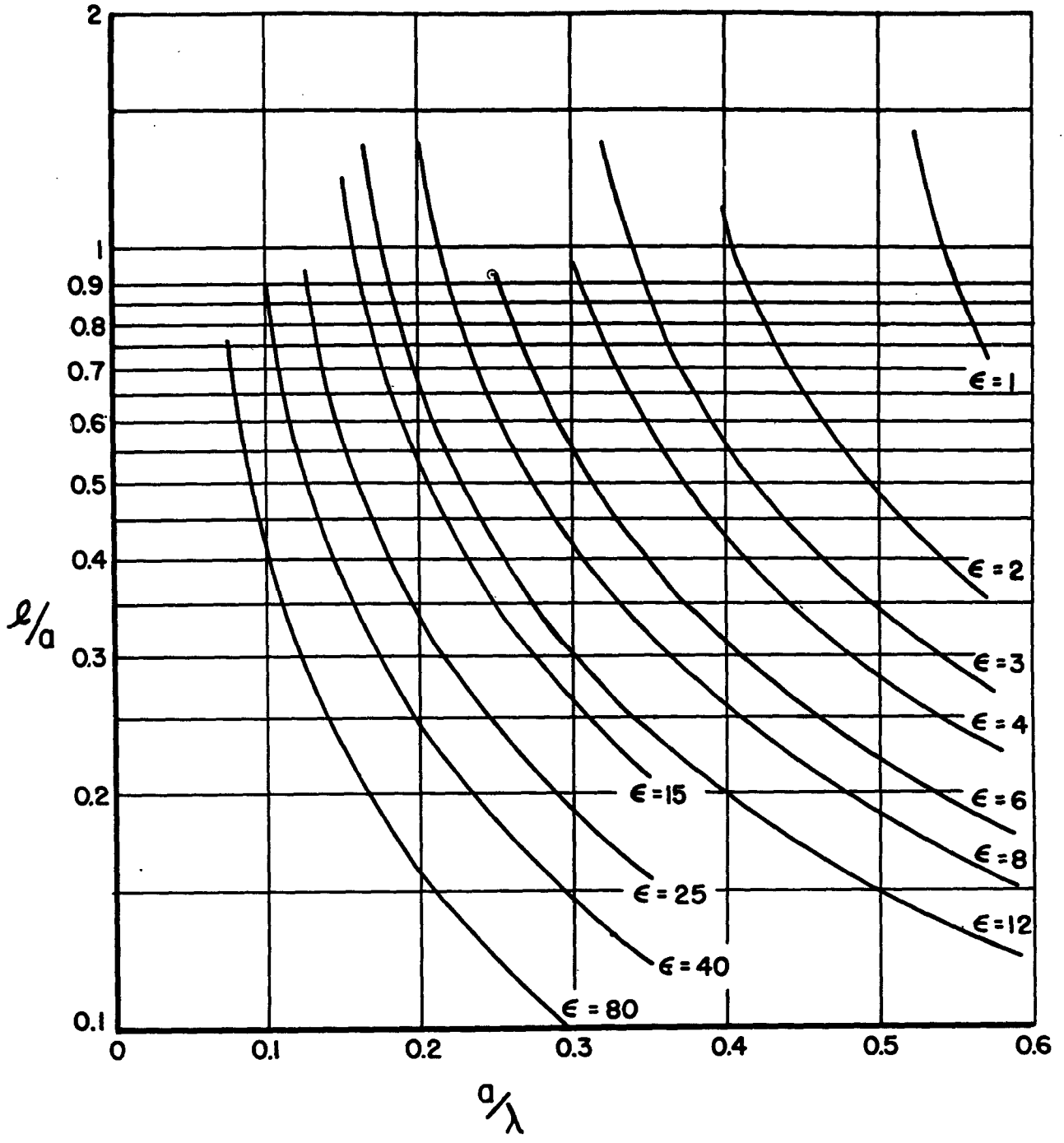

Fig. 19. Relations among cavity parameters for first normal mode of square radiating cavity.

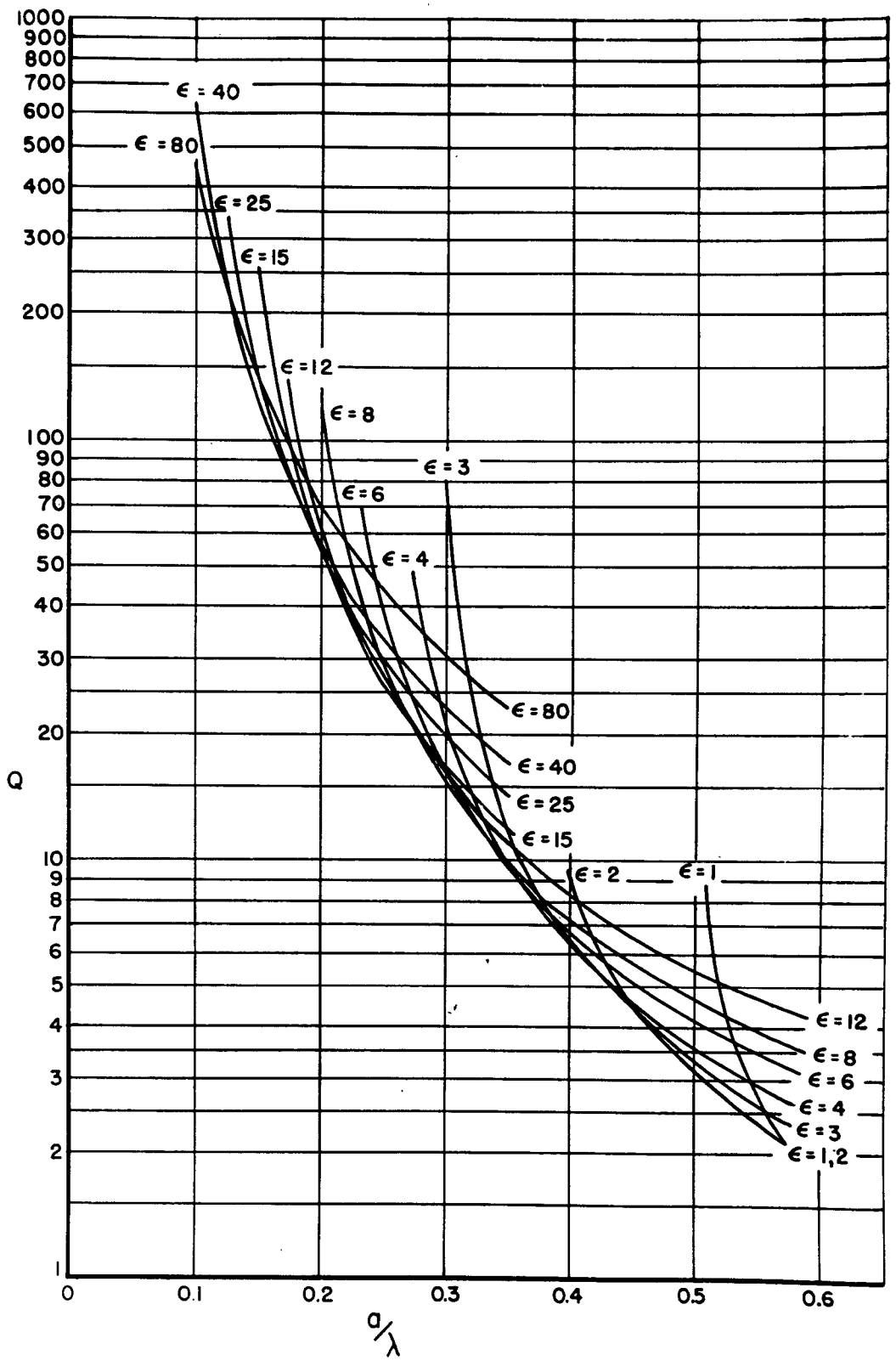

Fig. 20. Resonance characteristics of first normal mode of square radiating cavity.

$$\frac{\partial A}{\partial \epsilon_r} + \lambda \frac{\partial C}{\partial \epsilon_r} = 0$$

$$\frac{\partial A}{\partial \left(\frac{\ell}{a}\right)} + \lambda \frac{\partial C}{\partial \left(\frac{\ell}{a}\right)} = 0. \tag{3.64}$$

A glance at (3.56) reveals that $\frac{\partial \eta}{\partial \epsilon_r} = \frac{\partial \eta}{\partial \left(\frac{\ell}{a}\right)} = 0$, since Y_{11} is a function of $\frac{a}{\lambda}$ only. Hence

$$\frac{\frac{\partial \zeta}{\partial \epsilon_r}}{\frac{\partial \zeta}{\partial \left(\frac{\ell}{a}\right)}} = \frac{\frac{\partial C}{\partial \epsilon_r}}{\frac{\partial C}{\partial \left(\frac{\ell}{a}\right)}} . \tag{3.65}$$

Calculation of the derivatives leads to the condition

$$\frac{\ell}{a}\left[1 - 2\epsilon_r\left(\frac{a}{\lambda}\right)^2_{on}\right] - \frac{2}{\pi}\sqrt{\frac{\mu_o}{\epsilon_o}}\left(\frac{a}{\lambda}\right)_{on} \frac{B \sin^2\left[\pi \frac{\ell}{a}\sqrt{4\epsilon_r\left(\frac{a}{\lambda}\right)^2_{on} - 1}\right]}{\left[4\epsilon_r\left(\frac{a}{\lambda}\right)^2_{on} - 1\right]}$$

$$\left\{1 + 2\epsilon_r\left(\frac{a}{\lambda}\right)^2_{on}\left[1 - 4\pi\sqrt{\frac{\mu_o}{\epsilon_o}}\frac{\ell}{a}\left(\frac{a}{\lambda}\right)_{on} B\right]\right\} = 0. \tag{3.66}$$

The simultaneous solution of (3.66) and (3.62) gives the values of ϵ_r and $\frac{\ell}{a}$ which go with any $\left(\frac{a}{\lambda}\right)_{on}$; and with these $\left(\frac{a}{\lambda}\right)_n$ and the minimum Q may be computed as before, from eqs. (3.55), (3.56), and (3.58).

These calculations were carried out for the first normal mode of the square cavity. The minimum Q is shown in Fig. 21 as a function of $\frac{a}{\lambda}$, and the accompaning parameters $\frac{\ell}{a}$ and ϵ_r are shown as functions of $\frac{a}{\lambda}$ in Figs. 22 and 23. It will be observed that the graph of Q is almost

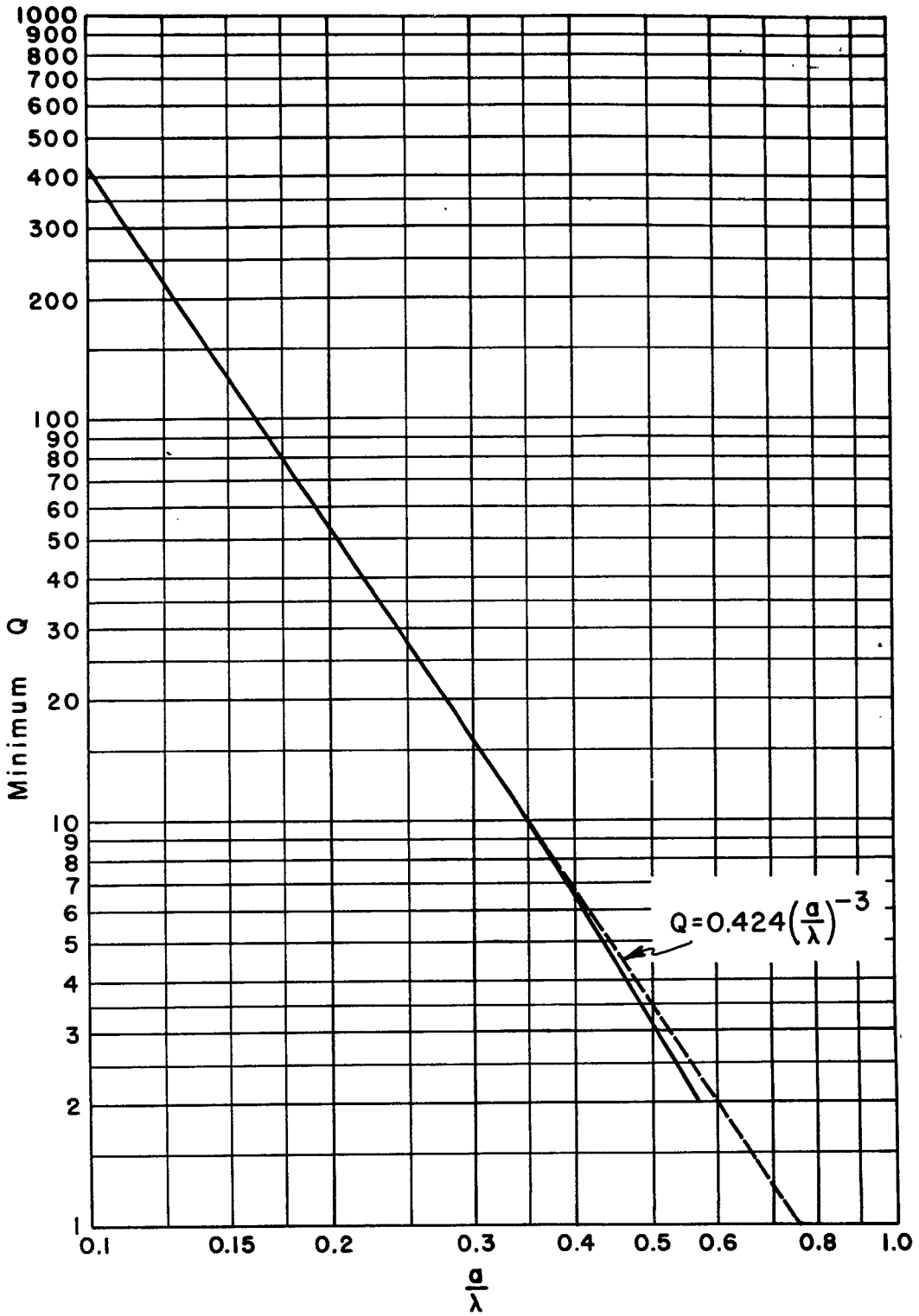

Fig. 21. Minimum Q vs. a/λ for first normal mode of square radiating cavity.

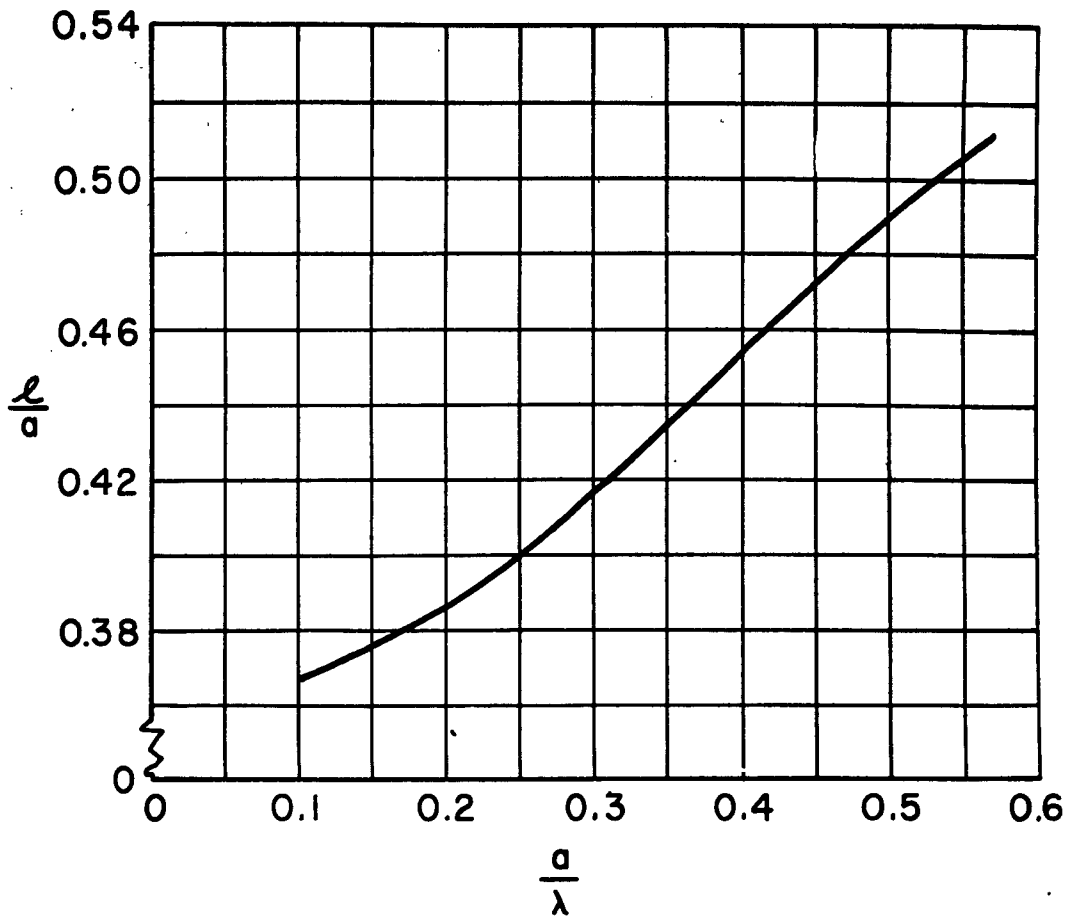

Fig. 22. Geometry necessary to obtain minimum Q.

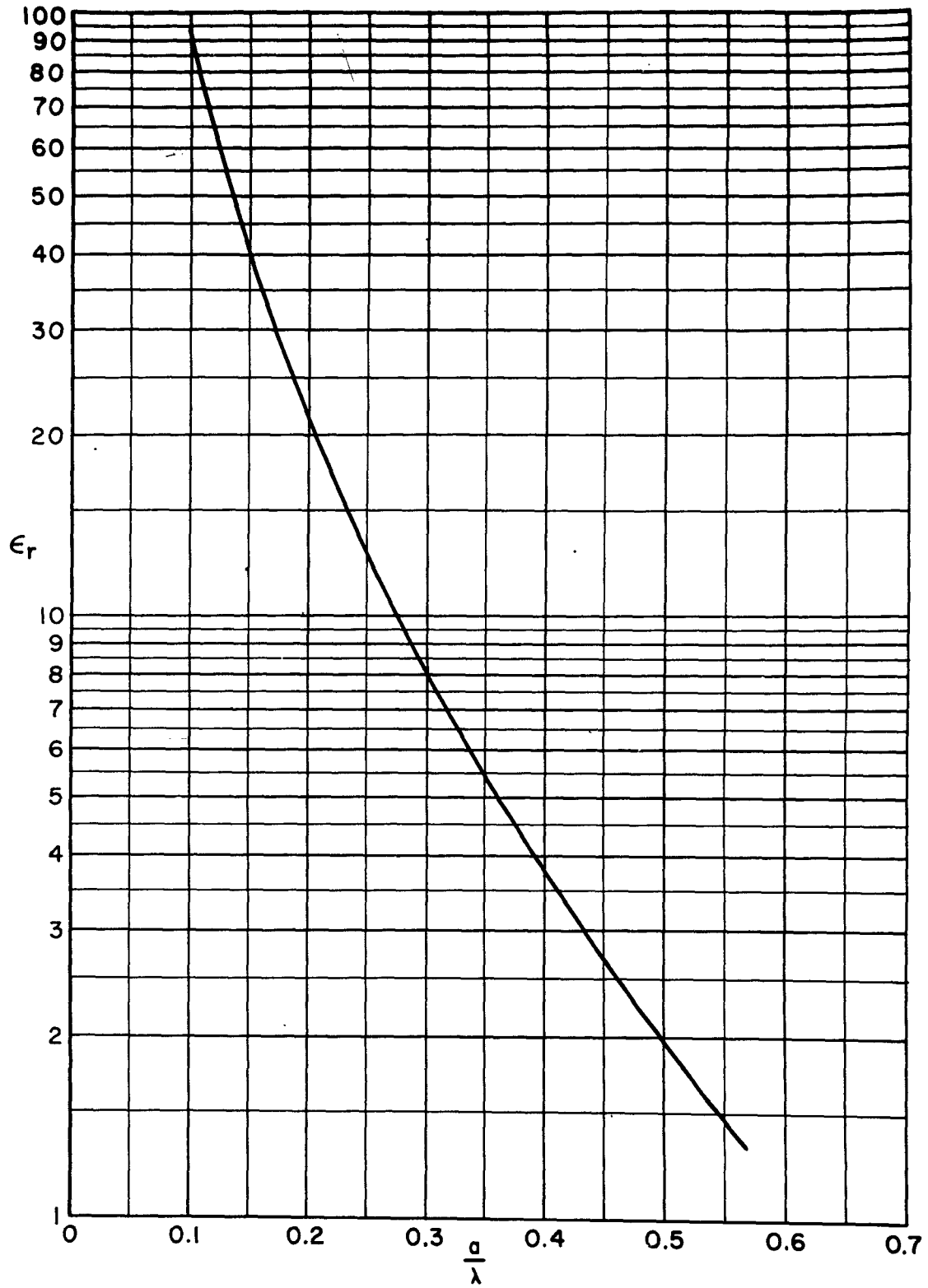

Fig. 23. Dielectric constant to obtain minimum Q.

a straight line. The matching straight line is shown dashed in Fig. 21, and the following formula is very accurate for $\frac{a}{\lambda} < 0.35$:

$$Q_{min} = 0.424 \left(\frac{a}{\lambda}\right)^{-3} . \qquad (3.67)$$

It is not known whether there is any special significance to the cubic dependence on frequency. At any rate, the rapid increase of minimum Q with decreasing $\frac{a}{\lambda}$ is in accord with all experimental evidence.

From Fig. 22 it is seen that relatively shallow cavities are needed to produce the minimum Q, and that $\frac{\ell}{a}$ changes very slowly with frequency. A cavity on the order of one-third to one-half as deep as it is wide will have a low Q.

Fig. 23 gives the value of dielectric constant to be used to obtain the minimum Q at some value of $\frac{a}{\lambda}$. This value is not critical, since Q is a relatively slow function of ϵ_r, near the minimum Q. A typical curve of Q vs. ϵ_r for constant $\frac{a}{\lambda}$ is shown in Fig. 24.

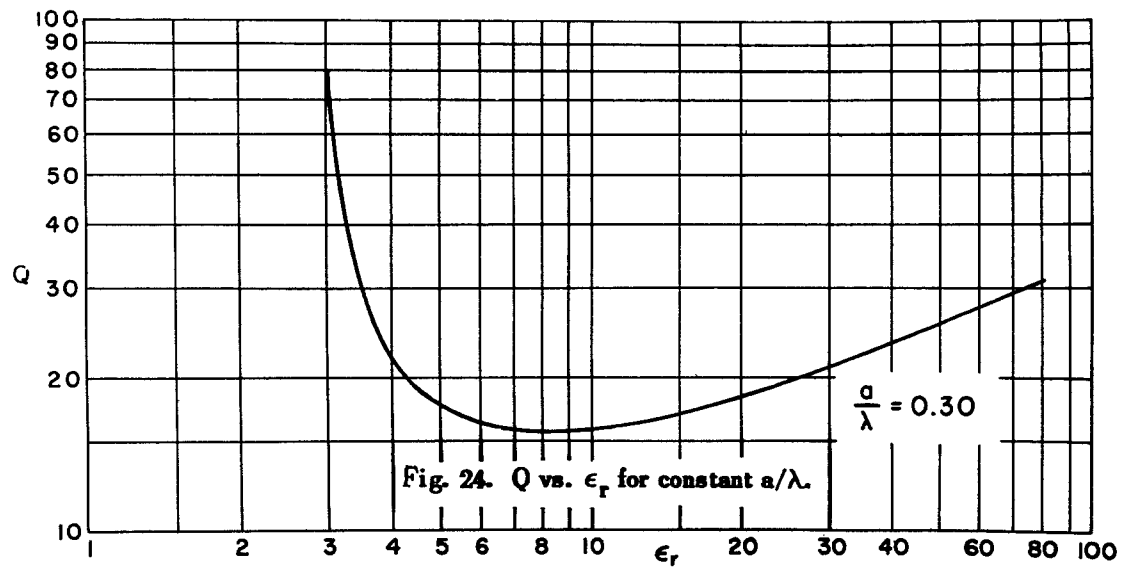

Fig. 24. Q vs. ϵ_r for constant a/λ.

The dielectric constant for minimum Q increases rapidly with decreasing $\frac{a}{\lambda}$, and it quickly attains impractical values. For efficient operation at, say, $\frac{a}{\lambda} = 0.1$, it would be necessary to resort to metal loading of some kind (e.g., longitudinal ridges, etc.). Fundamentally, then, the cavity would have a different shape; it would no longer be a square waveguide cavity, dielectric loaded. The above curves and discussion of minimum Q were derived for a square waveguide cavity, but it is felt that they give at least the order of magnitude of what could be expected from other configurations. On this basis then we would say that the minimum Q obtainable from a dielectric – loaded square waveguide cavity with $\frac{a}{\lambda} = 0.1$, is Q = 424. If by necessity or choice we went to some other configuration, with the same $\frac{a}{\lambda}$, we would not expect to appreciably lower the Q.

b. EFFECT OF DIELECTRIC LOSS

The effect of a finite conductivity of the medium in the cavity may be found by using a complex dielectric constant. To see this, go back to one of Maxwell's curl equations.

$$\nabla \times \underline{H}_n = j p_n \epsilon \, \underline{E}_n + \sigma \, \underline{E}_n = j p_n \epsilon' \, \underline{E}_n, \tag{3.68}$$

where

$$\epsilon' = \epsilon \left(1 + \frac{\sigma}{j p_n \epsilon}\right)$$

$$\approx \epsilon \left(1 + \frac{\sigma}{j \omega_n \epsilon}\right) = \epsilon \left(1 - j \tan \delta\right). \tag{3.69}$$

This approximation is valid when $Q_n >> 1$. The complex relative

dielectric constant may be introduced:

$$\epsilon' = \epsilon_o \epsilon'_r , \tag{3.70}$$

where

$$\epsilon'_r = \epsilon_r (1 - j \tan \delta). \tag{3.71}$$

This complex relative dielectric constant, ϵ'_r, may be inserted into the above equations in place of ϵ_r, and the real and imaginary parts re-evaluated. Rather than do this, it is easier, since $\tan \delta << 1$ for practical dielectrics, to consider f (eq. (3.52)) as a function of two complex variables. Then f may be expanded in a Taylor's series, and only the linear terms need be retained. Thus,

$$f(x_n, \epsilon'_r) = f(x_{on}, \epsilon_r) + \left.\frac{\partial f}{\partial x}\right|_{x_{on}\, \epsilon_r} (x_n - x_{on}) + \left.\frac{\partial f}{\partial \epsilon'_r}\right|_{x_{on},\, \epsilon_r} (\epsilon'_r - \epsilon_r) = 0. \tag{3.72}$$

The second term, $\left.\frac{\partial f}{\partial x}\right|_{x_{on},\, \epsilon_r}$, is given in eq. (3.56). The third term is evaluated from eq. (3.52). The result is (after substitution of (3.53)),

$$\mathcal{G} = \left.\frac{\partial f}{\partial \epsilon'_r}\right|_{x_{on}, \epsilon_r} (\epsilon'_r - \epsilon_r)$$

$$= \left\{ \pi \sqrt{\frac{\epsilon_o}{\mu_o}} \frac{\ell}{a} \left(\frac{a}{\lambda}\right)_{on} \csc^2 \left[\pi \frac{\ell}{a} \sqrt{4 \epsilon_r \left(\frac{a}{\lambda}\right)^2_{on} - 1} \right] - \frac{2\left(\frac{a}{\lambda}\right)^2_{on} B}{\left[4\epsilon_r \left(\frac{a}{\lambda}\right)^2_{on} - 1 \right]} \right\} \epsilon_r \tan \delta . \tag{3.73}$$

From eq. (3.72), the eigenvalues are given by

$$x_n = x_{on} - \frac{G + \mathcal{G}}{\left.\frac{\partial f}{\partial x}\right|_{x_{on}, \epsilon_r}} . \tag{3.74}$$

G is the aperture conductance; we may call G the radiation conductance and $\mathcal{G}$ the dielectric conductance. When the Q is high, $\left.\frac{\partial f}{\partial x}\right|_{x_{on}, \epsilon_r}$ is imaginary, and

$$\left(\frac{a}{\lambda}\right)_n = \left(\frac{a}{\lambda}\right)_{on} \tag{3.75}$$

$$Q_n = \frac{\left(\frac{a}{\lambda}\right)_n \left|\frac{\partial f}{\partial x}\right|_{x_{on}, \epsilon_r}}{2(G + \mathcal{G})}. \tag{3.76}$$

The dielectric loss does not affect the resonance frequency so long as Q remains high, but it may have an appreciable effect on Q.

From eq. (3.76) one may write

$$\frac{1}{Q_T} = \frac{1}{Q_R} + \frac{1}{Q_D}, \tag{3.77}$$

where Q_R is the radiation Q, Q_D is the dielectric Q, and Q_T is the total Q. Then

$$\frac{1}{Q_D} = \frac{2\,\mathcal{G}}{\left(\frac{a}{\lambda}\right)_n \left|\frac{\partial f}{\partial x}\right|_{x_{on}, \epsilon_r}}. \tag{3.78}$$

Now numerical calculations for the first mode reveal that the $\csc^2$ terms in $\mathcal{G}$ and $\frac{\partial f}{\partial x}$ are at least five times as big as the others. If they are dropped, $\frac{1}{Q_D}$ immediately reduces to $\tan \delta$. Thus

$$\frac{1}{Q_T} \approx \frac{1}{Q_R} + \tan \delta. \tag{3.79}$$

A "good" dielectric has $\tan \delta$ on the order of 0.01 or smaller. This

gives an indication of the effect of the dielectric on the total Q.

A few statements about the stored energy associated with the radiating cavity may be made by referring to eq. (1.12), the energy definition of Q. By comparing this definition with eq. (3.76) it is seen that $\left|\frac{\partial f}{\partial x}\right|_{x_{on}, \epsilon_r}$ must be a measure of the stored energy; G, a measure of the radiated energy; and $\mathcal{G}$, a measure of the energy dissipated in the dielectric.

Refer now to eq. (3.56). The individual terms may be ascribed to contributions to stored energy from different regions of the total volume.* Thus, the first two terms are interpreted as a measure of the energy in the waveguide, and $\frac{\partial B}{\partial x}\Big|_{x_{on}}$ is a measure of the energy in the half-space. Now, as noted above, the $\csc^2$ term is much bigger than the others, so we may say that most of the stored energy is in the cavity, and very little is in the half-space.

We can now find a more physical reason why the reciprocal of the dielectric Q equals tan δ. A closed cavity with lossless walls has $\frac{1}{Q_D} = \tan \delta$. If the radiating cavity has a high Q most of the stored energy will be inside the cavity. Also, the fields in the cavity will be close to the configuration existing in a closed cavity. Since the stored energy and losses approximate those in a closed cavity, it is expected that $\frac{1}{Q_D} \approx \tan \delta$.

* For an interesting discussion on location of electromagnetic energy, see Mason and Weaver, *The Electromagnetic Field*, Dover Publishing Company, New York, 1929. p. 266.

The radiation efficiency may be found from these energy considerations. From the statements concerning G and $\mathcal{G}$, it is seen that

$$\text{Efficiency} = \frac{G}{G + \mathcal{G}} \quad , \tag{3.80}$$

which may also be written as

$$\text{Efficiency} = \frac{Q_T}{Q_R} \quad . \tag{3.81}$$

If a substitution is made from eq. (3.79), one has

$$\text{Efficiency} \approx \frac{1}{1 + Q_R \tan \delta} \quad . \tag{3.82}$$

This formula illustrates the principle that a high-Q system fundamentally has a low efficiency. Physically, this is due to the high stored energy; i. e., to high circulating currents and high local field intensities.

IV. CORRELATION OF NORMAL MODES WITH STEADY-STATE BEHAVIOR

1. THEORY

The correlation of normal modes of a linear system with steady-state behavior is a subject which has been widely discussed, particularly in reference to circuits. Foster[19] has shown that any finite lossless network is equivalent to a chain of elementary LC circuits each of which is resonant at one of the normal mode frequencies, and has stored energy corresponding to that in the normal mode. The theorem is readily extended to cover slightly lossy networks by the addition of an R into each LC circuit. This is an approximation which is valid for high-Q networks. Schelkunoff[20] has discussed this, and the extension to a system with an infinite number of modes.

The cavity antennas considered in this paper are in the class of slightly lossy networks with an infinite number of degrees of freedom. Hence, it is assumed that the antenna is representable by a chain of RLC circuits, as in Fig. 25. The antenna is connected to a transmission line of characteristic impedance Z_o.

The application of this equivalent circuit (and the alternate one, a chain of series circuits) to cavity problems has been discussed in the M.I.T. Radiation Laboratory Series,[21,22] and by Slater.[23,24] Some of the results we shall use will be in a slightly different form from those in the references, but the derivations are similar and will not be repeated here.

Any one of the elementary RLC circuits of Fig. 25 has an impedance which changes rapidly near resonance, but is very stable away from resonance. If one of these circuits is resonant at a frequency far from that of any other circuit, then, in the vicinity of its resonance, the rest of the network may be lumped into the series impedance Z_a, which is essentially constant. The resulting equivalent circuit is shown in Fig. 26. It is now assumed that the normal-mode Q is related to the circuit by

$$Q_n = \frac{\omega_n L}{R} \tag{4.1}$$

and that the normal-mode frequency is equal to the resonance frequency, $\omega_n = \frac{1}{\sqrt{LC}}$. In the references cited this Q is spoken of as the unloaded Q, unloaded in the sense that Z_o is not included.

A curve of standing wave ratio (SWR) versus frequency, for this circuit, would have a resonance dip, and the sharpness of it would depend on Q. Typical curves are shown later (see, for example, Fig. 29). This is a measured curve for an antenna, but it is assumed that there is an elementary circuit which matches it. The frequency of minimum SWR is the resonance frequency.

The bandwidth is a term which is often used to describe the operating range of an antenna in terms of some specified SWR limit. However, for simplicity, we shall define bandwidth as the reciprocal of the Q, and the SWR limit will be taken as the variable.

There are two cases to be considered for the equivalent circuit. The simpler one assumes that the effect of Z_a is insignificant and that it can be ignored. In this case the following result can be shown.* Let

$$\sigma_o = \frac{R}{Z_o} = \begin{cases} \text{SWR at resonance, if } \dfrac{R}{Z_o} > 1 \\ \dfrac{1}{\text{SWR}} \text{ at resonance, if } \dfrac{R}{Z_o} < 1. \end{cases} \tag{4.2}$$

Then

$$Q_n = \frac{\omega_n}{\omega_2 - \omega_1} \quad , \tag{4.3}$$

where ω_2 and ω_1 are the frequencies at which the SWR has risen to the value r_1:

$$r_1 = \frac{\sqrt{1 + \frac{1}{2}\sigma_o^2} + \sigma_o + \sqrt{1 + \frac{1}{2}\sigma_o^2} - \sigma_o}{\sqrt{1 + \frac{1}{2}\sigma_o^2} + \sigma_o - \sqrt{1 + \frac{1}{2}\sigma_o^2} - \sigma_o} . \tag{4.4}$$

Experimentally, the correct value for σ_o is obtained by examining the impedance curve, to determine whether R/Z_o is greater or less than one at resonance. See the references for a discussion of this point.

Slater has examined the circuit when Z_a is included. He assumes that Z_a is constant over a wide frequency range and that the SWR far from resonance is what would be obtained at the resonance frequency, if the resonant circuit were removed. Under these conditions it is

* See Slater's article. He finds SWR limits for the loaded Q, but the derivations are similar.

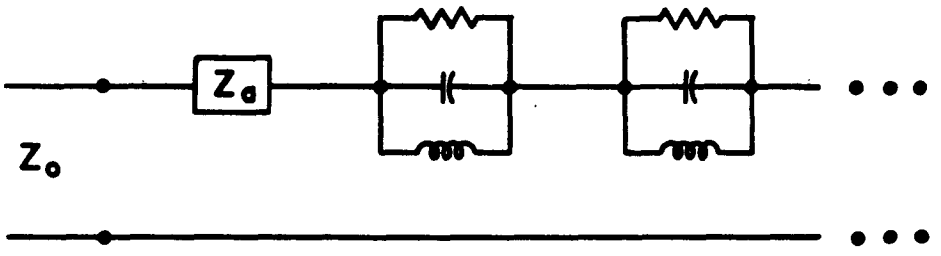

Fig. 25. Equivalent circuit.

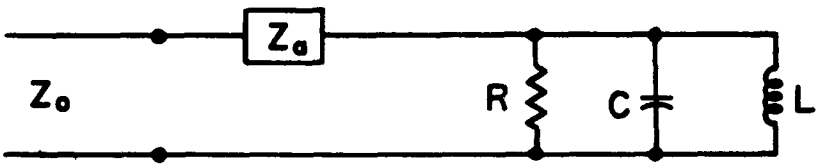

Fig. 26. Equivalent circuit near resonance.

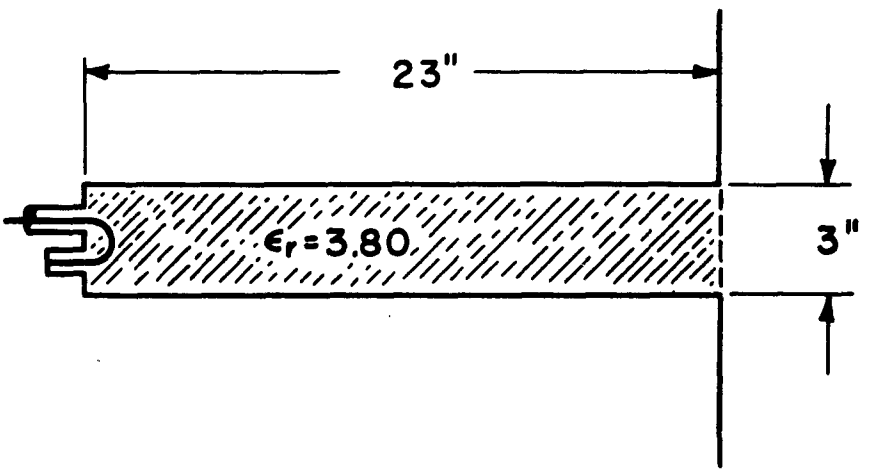

Fig. 27. Deep sulfur-filled antenna.

possible to show that

$$r_2 = \frac{\sqrt{(1+\sigma_o)^2 + (1+\sigma_1)^2} + \sqrt{(1-\sigma_o)^2 + (1-\sigma_1)^2}}{\sqrt{(1+\sigma_o)^2 + (1+\sigma_1)^2} - \sqrt{(1-\sigma_o)^2 + (1-\sigma_1)^2}}, \tag{4.5}$$

where r_2 is the standing wave ratio at ω_1 and ω_2. σ_1 is 1/SWR far from resonance, and σ_o is defined above.

The two formulas, eqs. (4.4) and (4.5), give similar results when $Q \gg 1$. With their aid the Q of an antenna may be computed from an experimental measurement of SWR vs. frequency (plus some phase measurement to eliminate the ambiguity about σ_o). Conversely, if one has a value for Q, the SWR limits on the bandwidth may be computed, after some minimum SWR has been assumed. In the antenna problem it may be assumed that the minimum SWR is one, since the feed geometry is arbitrary and can be changed until this value is obtained. In this case the bandwidth is the percentage frequency range within which the SWR is less than 2.62. This value is obtained from eq. (4.4) when $\sigma_o = 1$, and from eq. (4.5) when $\sigma_o = 1$ and $\sigma_1 = 0$.

It is possible to get lower SWR limits on the bandwidth than the value given above; namely, SWR = 2.62 for minimum SWR = 1. In eq. (4.4), r_1 may be minimized with respect to σ_o; the result is $r_1 = 2.42$, for $\sigma_o = \sqrt{2}$. Hence, if $\sigma_o = \sqrt{2}$, one has the minimum SWR at the ends of the frequency band. This remark is of some interest because the practical problem is to minimize the SWR as much as possible.

2. EXPERIMENTAL

Three experimental models were constructed and tested to check the theory. These were all square waveguide cavities, filled with a dielectric, and flush mounted in a ground plane. These antennas were excited in various ways and the input impedance was measured. From curves of SWR vs. frequency the resonance frequency and Q were obtained, as described above.

The first cavity was 3 by 3 inches in cross section and 23 inches deep. It was filled with a block of cast sulfur and mounted in a 3-foot square ground plane. The dielectric constant of the sulfur was measured by closing the aperture with an aluminum plate and finding the resonance frequencies of the closed cavity. A simple calculation gave the resonance frequencies of the air-filled closed cavity (as a check, these were also measured), and the two sets of frequencies were connected by $\sqrt{\epsilon_r}$. This procedure yielded a value for the dielectric constant, $\epsilon_r = 3.80$, with an average deviation of 0.01 (for the first six resonances).

The antenna was driven by a loop in the rear wall, as shown in Fig. 27. The short-circuited stub in series with the loop was used to help the impedance match. The exact configuration of the loop and stub is unimportant, since we are interested only in the resonance frequency and Q. These characteristics are independent of the

excitation, since it is assumed that, near resonance, the fields are essentially the normal-mode fields. The feed geometry controls the magnitude of the impedance at resonance, and, of course, it does perturb the field and change the resonance properties somewhat. This effect will be noted later.

The antenna was mounted on the side of the building and allowed to radiate into space. The input impedance was measured with a precision slotted line. It is estimated that the measured frequency is accurate to within 2 megacycles, and that small frequency *intervals* (used in measuring bandwidth) are accurate to within 0.2 megacycle. The values of SWR are probably correct to within 5% for SWR < 50. Higher values of SWR are not accurate because of losses in the slotted line.

The SWR of the antenna is shown as a function of frequency in Fig. 28.* The region from 1000 to 1026 megacycles is shown dashed because the theory predicted a resonance dip there. It was missed in the measurement. The structure of the other resonance dips was carefully measured, and a typical one is shown in Fig. 29. The crosses indicate the bandwidth points; the outer ones are at values of r_1 and the inner ones are at r_2. The phase of the impedance was also measured, although it is not shown. It turned out that R/Z_o was less than

* For convenience, all standing wave ratio curves are plotted on a logarithmic scale.

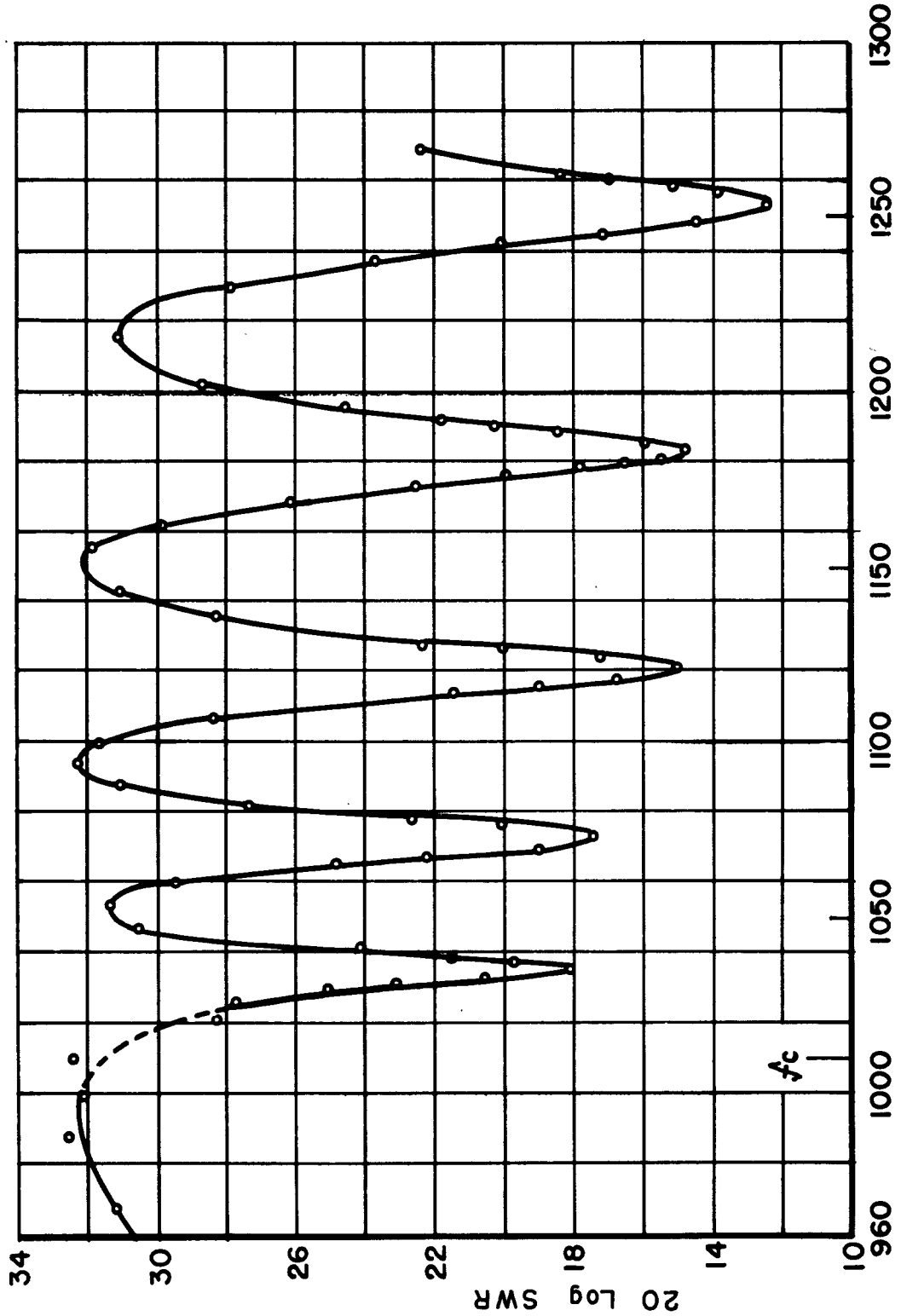

Fig. 28. Standing wave ratio vs. frequency, for deep sulfur-filled antenna.

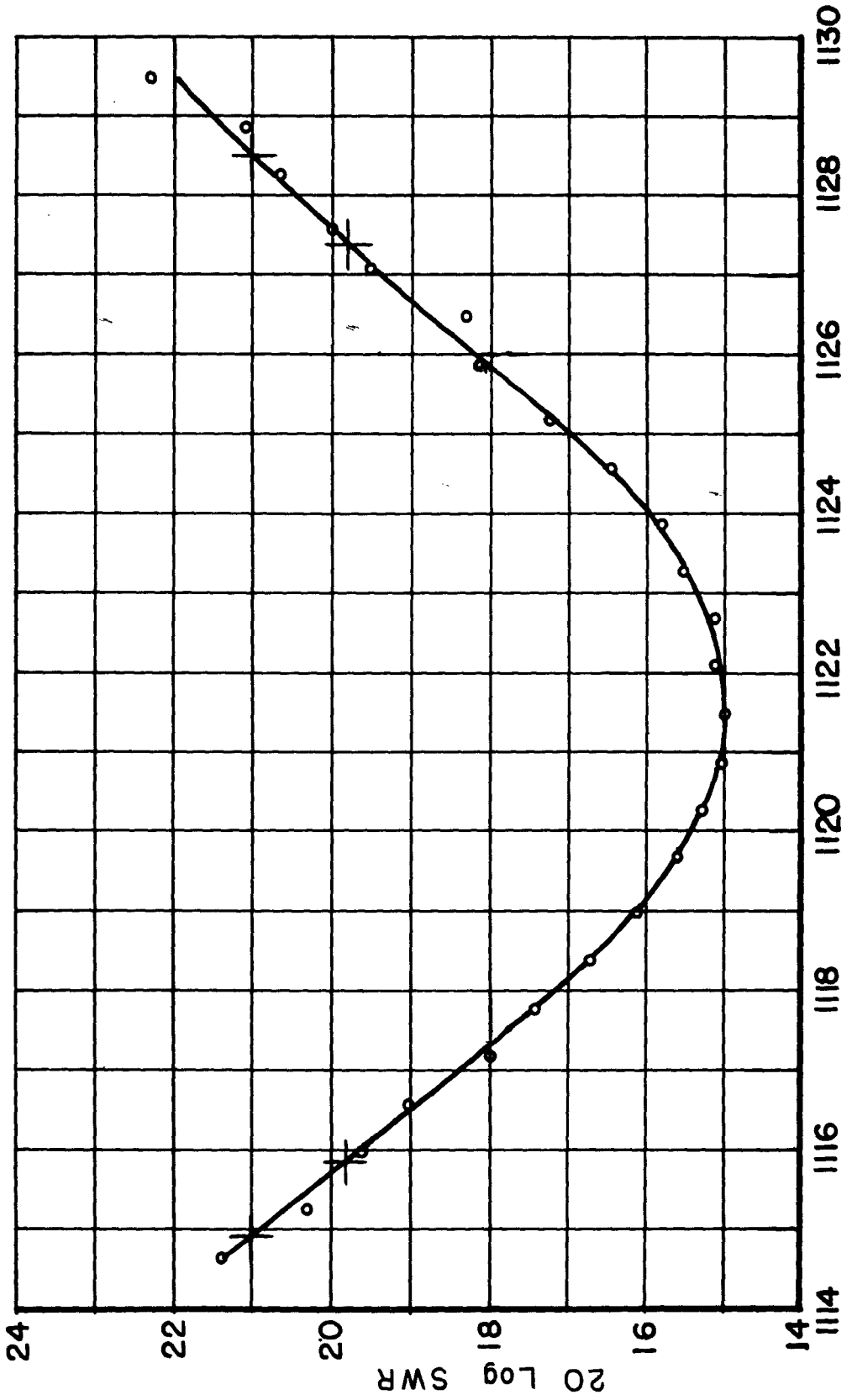

Fig. 29. Resonance curve for fourth mode of deep sulfur-filled antenna.

one, so σ_o = 1/SWR for each mode. This fact indicates that there was weak coupling between the transmission line and the cavity. A better impedance match could have been obtained by using a bigger feed loop.

The antenna has ℓ/a = 7.67, and the first normal mode is very close to cutoff, which occurs at 1009 megacycles. (This frequency is indicated in Fig. 28.) The higher modes come in quick succession because the guide wavelength changes very rapidly with frequency. The first six normal-mode frequencies, and the Q's, were computed according to the above theory. The loss factor ($\tan \delta$) was taken to be the value given by Von Hippel,[25] namely, $\tan \delta = 0.0025$. This changes slightly with frequency.

All of the results are in Table I. The second and third columns give the measured and calculated resonance frequencies for the various modes. The fourth column gives the measured Q assuming only a simple parallel circuit, by eq. (4.4). Column 5 gives the measured Q using the more refined circuit, by eq. (4.5). Column 6 gives the Q calculated from radiation losses only, while column 7 gives the calculated total Q. Column 8 gives the efficiency.

It will be noted that the calculated and measured resonance frequencies agree very closely. In most cases the measured values are a trifle higher than the calculated ones. The Q values, however, are not so close. In the first place, there is a considerable difference between the radiation Q and the total Q. This, of course, is due to the fact

that the cavity is very deep and the dielectric losses are large. This is particularly true for the first modes, near cutoff. Very close to cutoff there are high standing waves in the guide, and these cause the excessive dielectric losses which result in a low Q and a low efficiency.

TABLE I

Results for 3 by 3 by 23-inch sulfur-filled loop-fed cavity antenna.

Mode	Resonance Frequency		Measured Q		Calculated Q		Calculated Efficiency
	Measured	Calculated	Q_1	Q_2	Q_R	Q_T	
1	-	1016	-	-	1470	344	23%
2	1036	1037	104	134	430	220	51%
3	1074	1072	89.6	114	240	156	65%
4	1122	1120	82.5	97.7	172	124	72%
5	1184	1180	76.9	90.4	137	105	77%
6	1254	1251	67.1	75.6	119	93.4	79%

The calculated Q_T is to be compared with the measured Q. The Q_2 values are higher than the Q_1 ones and so are closer to the computed values; they would be expected to be closer because they are derived from a better equivalent circuit. In every case the computed Q_T is higher (in some cases much higher) than Q_2. This also is to be expected, since metal losses were ignored in the calculation. The discrepancy is greatest where Q is very high, because, in general, as noted above, a high-Q system has high losses and a low efficiency.

The second experimental antenna was a 4 by 4 by 8-inch square cavity, also filled with sulfur. The dielectric constant of the sulfur was $\epsilon_r = 3.88$. The difference in ϵ_r for the two sulfur blocks is apparently due to the manner in which it was prepared - the cooling rate of liquid sulfur has a considerable effect on crystal structure and air-bubble formation.

This antenna was excited by a stub close to the aperture, as shown in Fig. 30. This location for the stub was chosen because it is near a voltage maximum for the first two normal modes. Fig. 31 shows the magnitude of the electric field for the TE_{10} waveguide mode for the first two normal modes. These curves were drawn by finding the guide wavelength at the two resonance frequencies.

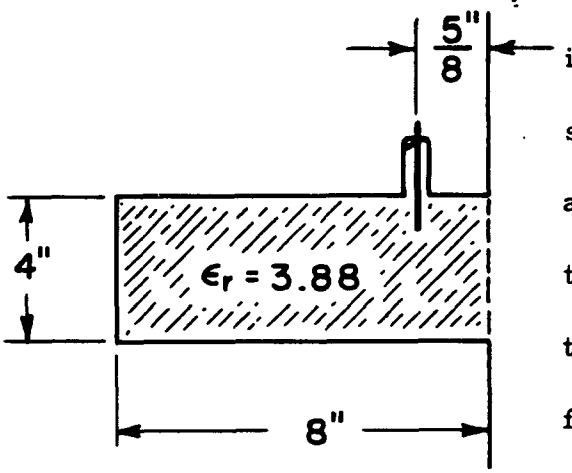

Fig. 30. Second sulfur-filled antenna.

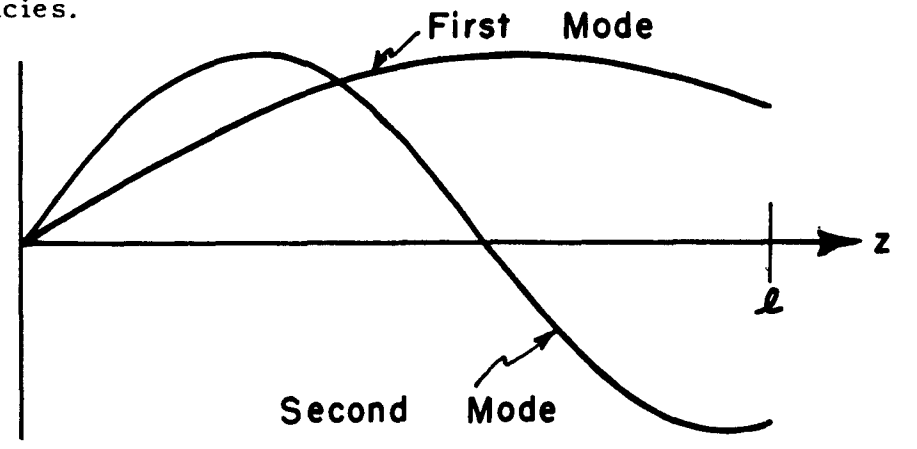

Fig. 31. Transverse electric field for first two normal modes of second sulfur-filled antenna.

A good impedance match to the slotted line was obtained with a stub 1 inch long and 1/8-inch in diameter. This stub screwed on to a modified UG-58U fitting, so that the total protrusion into the cavity was about 3/16-inch longer than the probe. Other length probes were also tried, and they produced different resistance values at resonance. Fig. 32 shows the SWR vs frequency for the 1-inch probe, and Fig. 33 shows the SWR for a 0.3-inch probe. It should be remembered that the data for the 0.3-inch probe are not as accurate as those for the 1-inch one, because of the high SWR's involved.

There are four major resonance dips present on the curves in Figs. 32 and 33. The first two are due to normal modes involving only the TE_{10} waveguide mode. These two are compared with theory in Table II. The TE_{11} mode propagates after the second dip (cutoff frequency of TE_{11} mode is shown on graphs), and the third dip is due to the first resonance of the TE_{11} mode. This portion of the curve is like that obtained from two coupled circuits, and that is exactly the situation here, since there are two propagating modes coupled at the probe. The third resonance of the TE_{10} mode is calculated to be at 1210 megacycles, so this must correspond to the fourth dip of the curves. Again, it is a multiple dip because there are two propagating modes. If the feed were balanced, so that the TE_{11} mode were not excited, then the third dip would be absent, and the fourth would be clean.

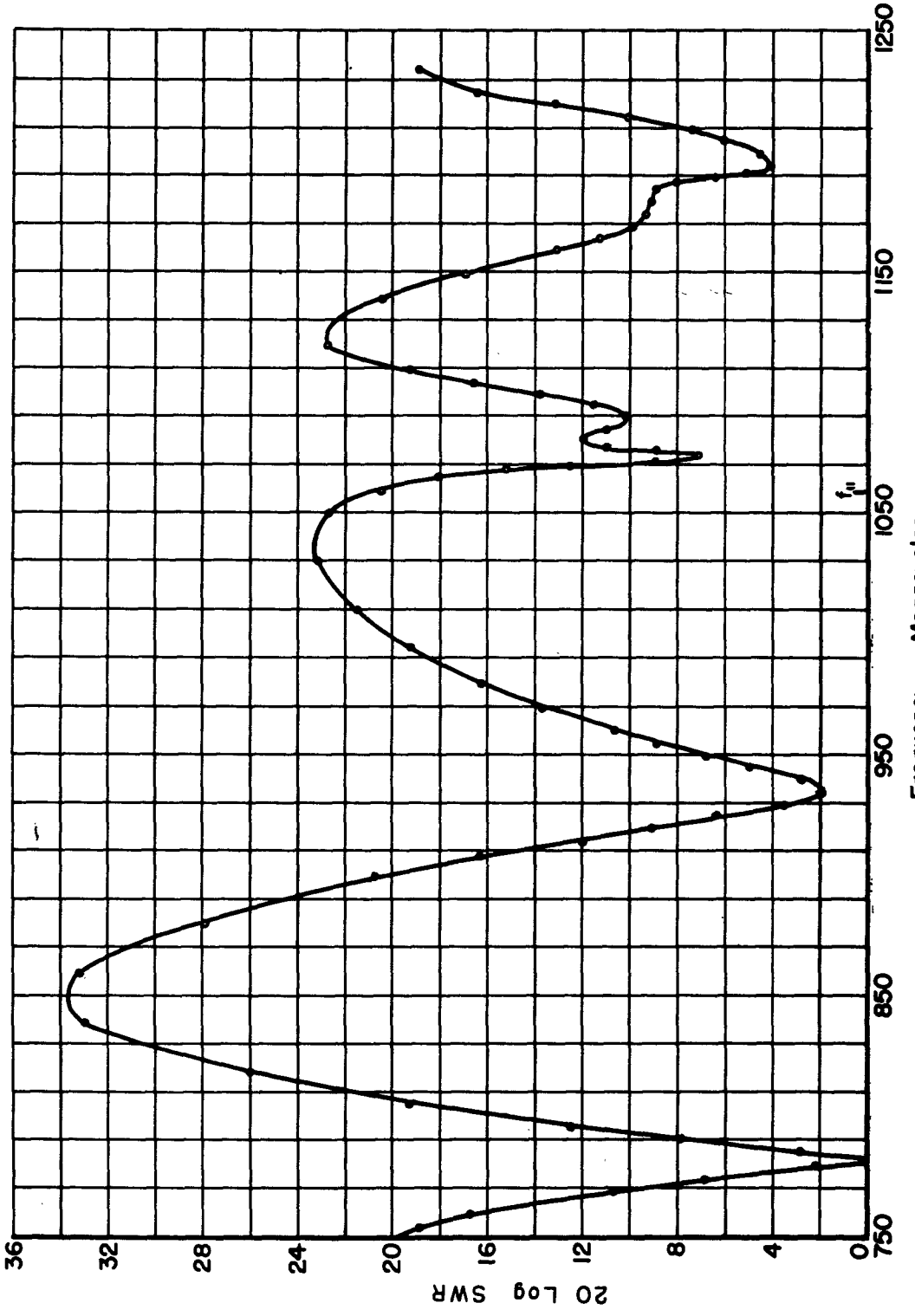

Fig. 32. Standing wave ratio for 4 by 4 by 8-inch sulfur-filled antenna. 1.00-inch probe.

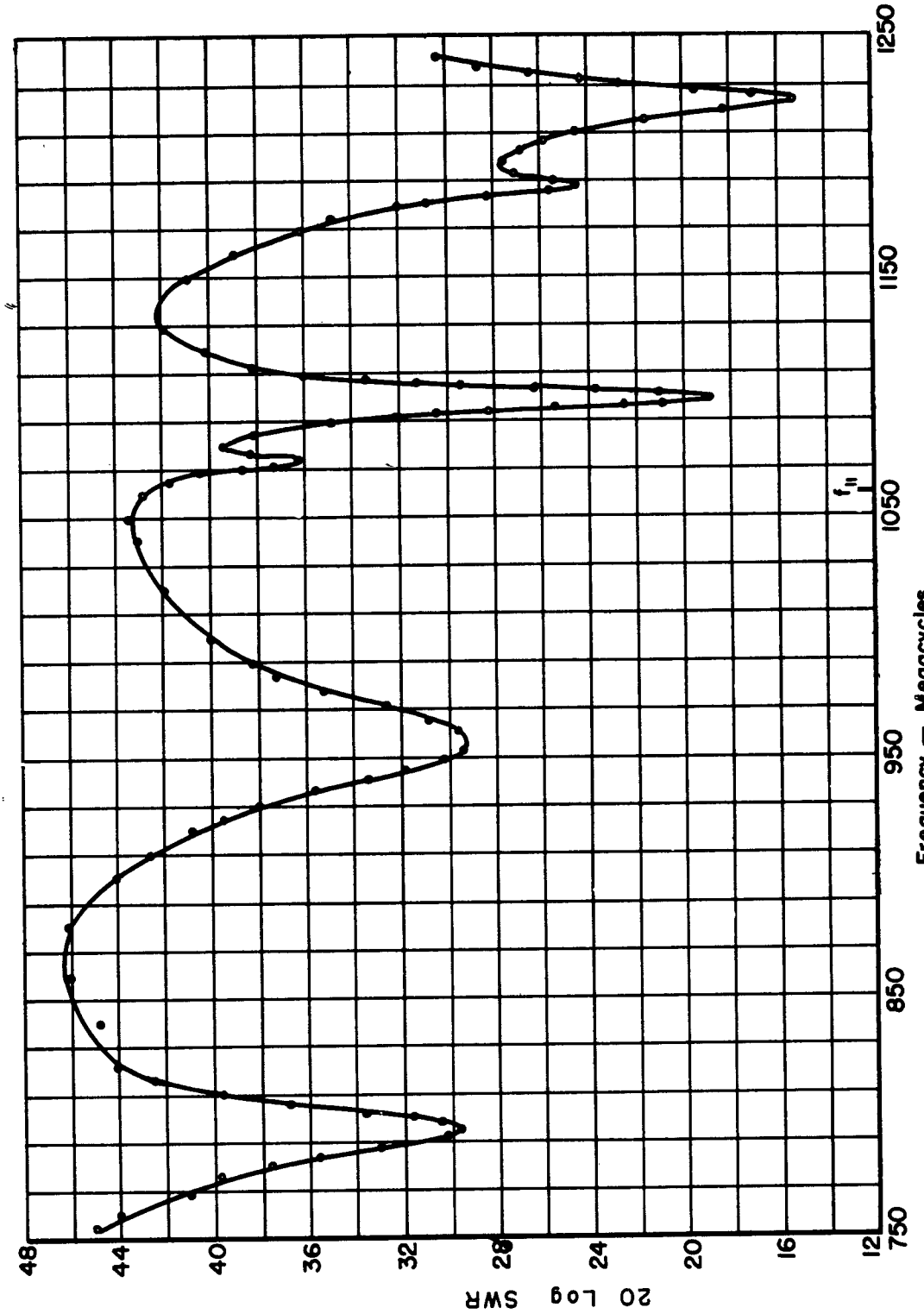

Fig. 33. Standing wave ratio for 4 by 4 by 8-inch sulfur-filled antenna. 0.30-inch probe.

TABLE II.

Results for first two normal modes of 4 by 4 by 8-inch sulfur-filled, probe-fed antenna.

Probe	Mode	Resonance Frequency		Measured Q		Calculated Q		Calculated
		Measured	Calculated	Q_1	Q_2	Q_R	Q_T	Efficiency
1-inch	1	782	799	39.6	41.0	71.9	61.9	86%
	2	936	961	30.7	32.4	32.7	30.4	93%
0.3-inch	1	794	799	35.2	41.8	71.9	61.9	86%
	2	957	961	22.3	26.0	32.7	30.4	93%

The first two resonance dips were measured carefully, and curves similar to that in Fig. 29 were obtained. It will be noted from Table II that the resonance frequencies of the small probe are closer to the computed values than those of the larger probe. The small shifts in resonance frequency are due to a perturbation of the fields by the probe; the smaller probe causes less perturbation and hence less shift. According to general perturbation theory of cavities[28] a metal protrusion in a region of high E and low H should lower the resonance frequency, whereas one is a region of low E and high H should raise it. This general statement correctly predicts the lowering of the resonance frequency in this case. Also, according to this theory, a loop in the rear wall should raise the resonance frequency, and this was observed in the first antenna.

Observe that the measured Q_2 for the 1-inch probe at the second mode is higher than the calculated Q_T. This is the only case in all the measurements where this occurred, and it is not expected because wall losses should lower the measured Q from the computed value. However, this measurement is unique in one other respect — R/Z_o is greater than one, so that the transmission line is strongly coupled to the cavity. This strong coupling implies that there will be high local fields near the probe, and apparently the total stored energy increased by more than enough to offset the wall losses.

It was attempted to make an independent check on the theory by measuring the efficiency of the antenna. This was done on the low-frequency efficiency meter, a special instrument built at this laboratory, which is described in various reports.[27] The measured efficiency for the 1-inch probe at the first resonance was about 80%. This is quite close to the computed value, but it has tentatively been shown that the measured efficiency varies greatly for different probe positions and for slightly different frequencies. This indicates that the efficiency is quite dependent upon the feed perturbation; i.e., upon higher nonpropagating waveguide modes. This has only a minor effect upon the resonance frequency, but the effect on Q may be considerable. Actually, no definite conclusions may be drawn because of possible large inaccuracies in the efficiency measurement.

The third antenna was a shallow one having approximately the geometry necessary for minimum Q. It was basically 3 by 3 by 1.2 inches, but to avoid difficulty with higher modes it was cut in half with an image plane.[17] This automatically balanced the antenna, so that the TE_{11} mode could not be excited. A sketch of the antenna is shown in Fig. 34. The cavity was filled with a mixture of lead-chloride and mineral oil, which had a dielectric constant of 8.41 ± 0.06, measured as described above.

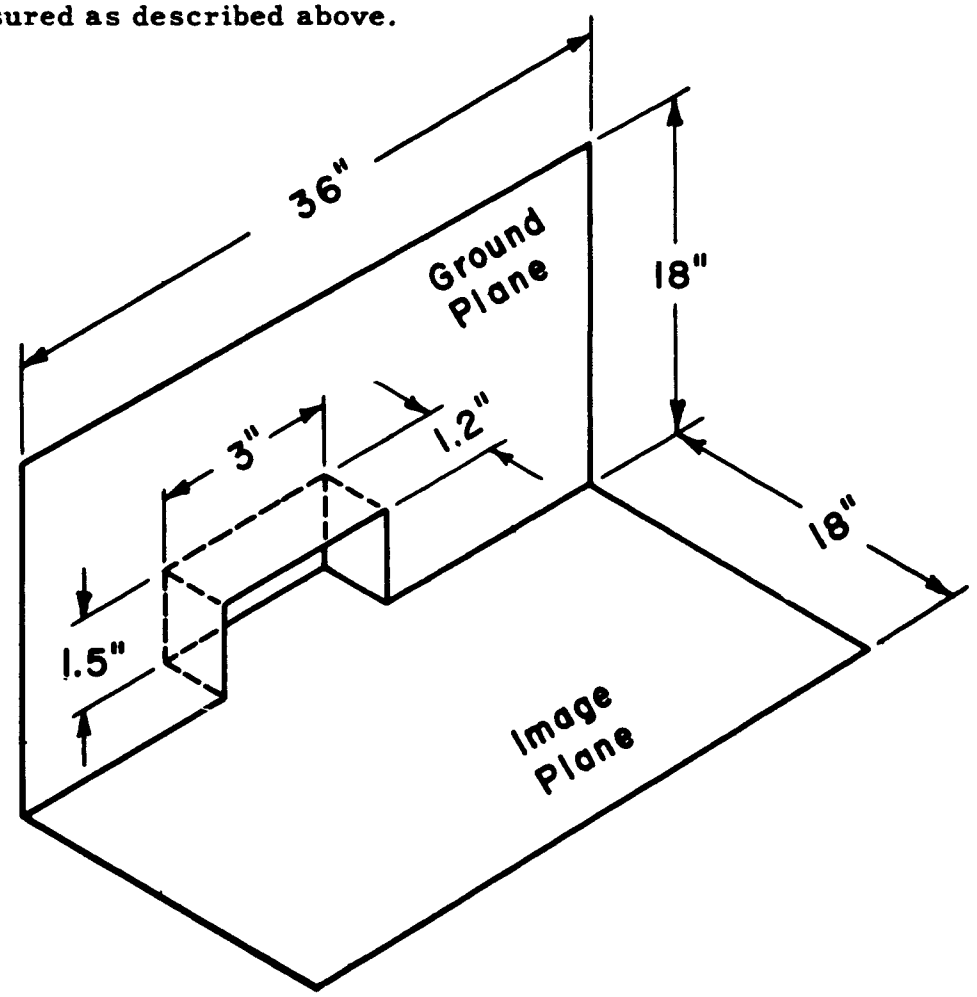

Fig. 34. Shallow half-cavity.

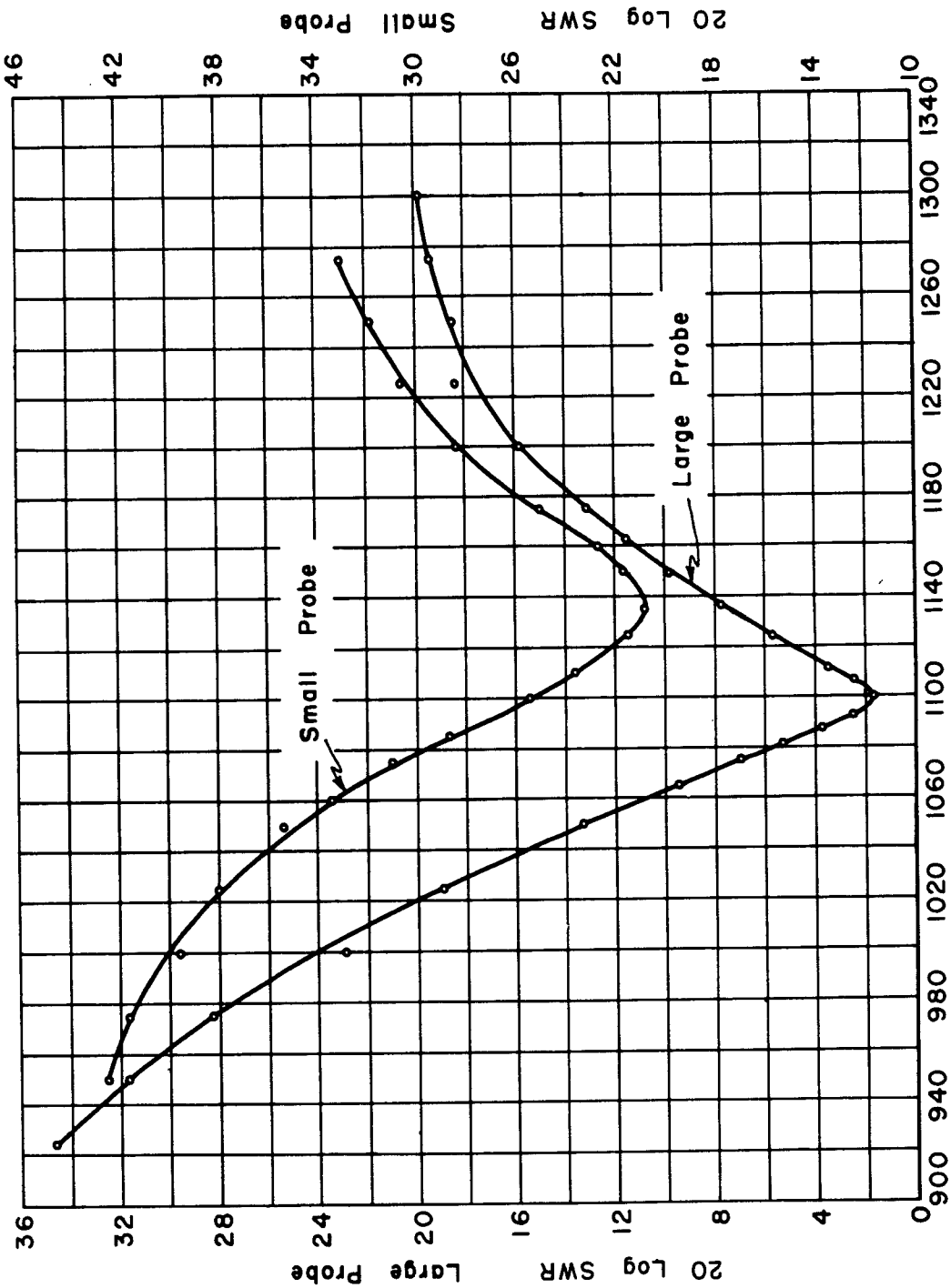

Fig. 35. Standing wave ratio for shallow half-cavity, filled with lead-chloride, mineral-oil mixture.

The cavity was excited with a probe on the center line of the image plane and 1/4-inch from the aperture. A probe 0.240-inch long and 1/8-inch in diameter gave a reasonable impedance match. The SWR on the slotted line was measured as above and it is shown in Fig. 35 as a function of frequency. The antenna impedance was also measured with a much smaller probe, 1/8-inch long and 0.05-inch in diameter. The standing wave ratio with this probe is also shown in Fig. 35.

The calculated resonance frequency for this antenna is 1200 megacycles, so there is a considerable deviation here. According to the above general theory the shift is in the correct direction and is less for the smaller probe, as expected. Apparently for shallow cavities the effect of the feed becomes more important. In this case it presumably shifted the resonance frequency by 8%.

Table III gives the comparison between measured and calculated resonance frequency and Q. The losses in the dielectric were not considered, because the value of $\tan\delta$ for this medium is not known.

TABLE III.

Results for first normal mode of 3 by 1.5 by 1.2-inch cavity with image plane, filled with lead-chloride, mineral oil mixture.

Probe	Resonance Frequency		Measured Q		Calculated Q
	Measured	Calculated	Q_1	Q_2	Q_R
Large	1100	1200	13.7	15.0	15.8
Small	1136	1200	11.8	14.4	15.8

APPENDIX I. FIELDS OF AN IMPULSE CURRENT

We now investigate the fields produced by the impulse current $\underline{J}_o = \underline{q}\,\delta(P - Q)\,\delta(t - t_o)$. The only unusual thing about this current is the δ-function in time. The idea of a current element which is infinitesimal in its spatial extensions has long been a convenient concept. $\underline{J}_o$ may consist simply of a point charge Q moved from A to B at time t_o. Points A and B are very close together, and the motion takes place in a very small time. The current will therefore consist of a pulse at $t = t_o$.

There will be static fields before and after t_o, but they will differ by a static dipole field due to a dipole $Q\vec{AB}$. To see this, use the law of superposition. Fig. 36 (a) shows the configuration for $t > t_o$ and Fig. 36(b) shows the initial configuration, for $t < t_o$. The difference between these is the dipole $Q\vec{AB}$. It is shown below that the dipole moment $Q\vec{AB}$ must equal $\underline{q}$.

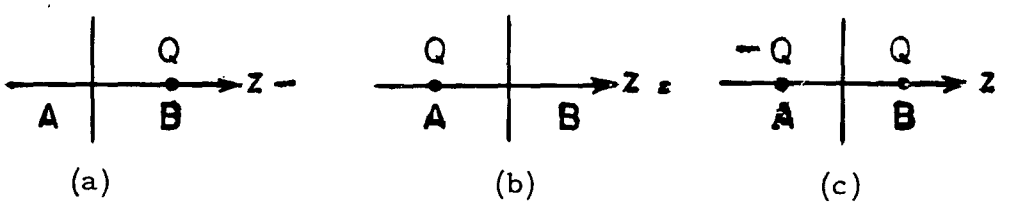

Fig. 36.

Mathematically, the pulse has been represented by a δ-function. It is sufficient for our purposes to define this function by its integral, as was done in section II. For computing the fields we will need the derivative of the current, and thus we need the derivative of the

δ -function. Call this the D-function, and define it by

$$\int_{-\infty}^{t} D(\tau - t_o)\, d\tau = \delta\,(t - t_o). \tag{A.1}$$

If the δ -function is pictorially represented by a steep pulse, then the D-function must be a double pulse, as in Fig. 37. The D-function is sometimes called the "unit doublet impulse" function.[28]

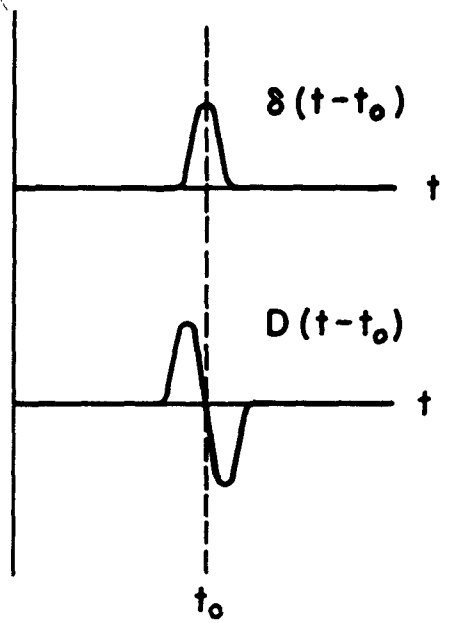

Fig. 37. δ and D functions.

Now consider the equations that the fields satisfy. Maxwell's equations are

$$\nabla \times \underline{H} = \frac{\partial \underline{D}}{\partial t} + \underline{J}_o, \qquad \nabla \cdot \underline{B} = 0 \tag{A.2}$$

$$\nabla \times \underline{E} = -\frac{\partial \underline{B}}{\partial t}, \qquad \nabla \cdot \underline{E} = \rho .$$

Let

$$\underline{B} = \nabla \times \underline{A}, \tag{A.3}$$

then

$$\underline{E} = -\frac{\partial \underline{A}}{\partial t} - \nabla \Phi \tag{A.4}$$

If

$$\nabla \cdot \underline{A} + \mu\epsilon \frac{\partial \Phi}{\partial t} = 0, \tag{A.5}$$

then both $\underline{A}$ and Φ satisfy the wave equation, and $\underline{A}$ is given by[28]

$$\underline{A}(Q) = \mu \int_V \frac{[\underline{J}_o]}{4\pi r}\, dv = \frac{\mu q}{4\pi r}\ \delta\ (t - t_o - \frac{r}{c}). \tag{A.6}$$

By $[\underline{J}_o]$ is meant the retarded value, $\underline{J}_o(t - \frac{r}{c})$, where r is the distance from P to Q. These equations are valid for an isolated source; i. e., one in free space.

Now let $\underline{q}$ be directed along the z-axis, at the origin of coordinates. The coordinate system is shown in Fig. 38. The vector potential $\underline{A}$ has only a z-component and, by symmetry, has no ϕ-dependence; therefore $\underline{H}$ has only a ϕ-component.

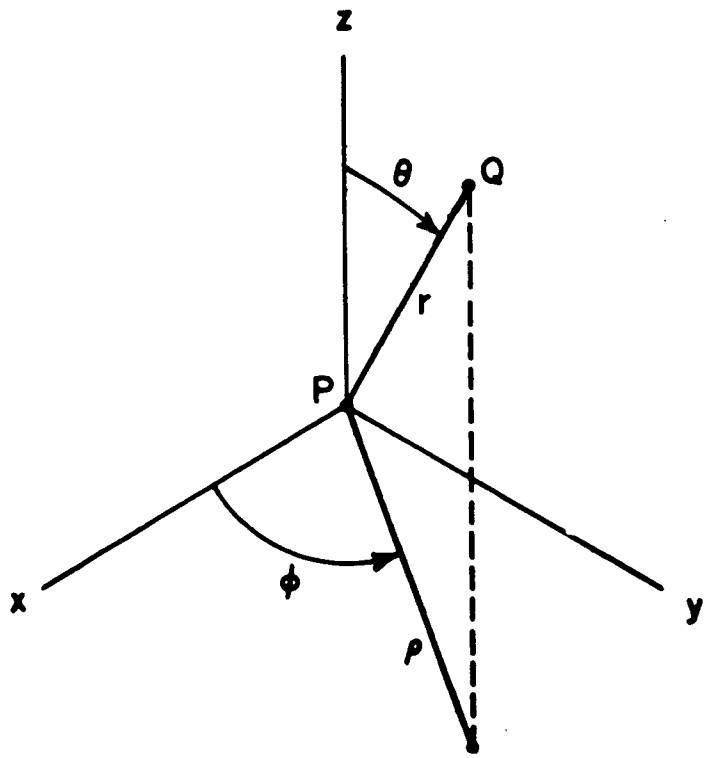

Fig. 38. Spherical polar coordinate system.

$$H_\phi = -\frac{1}{\mu}\frac{\partial A_z}{\partial \rho} = -\frac{1}{\mu}\frac{\partial A_z}{\partial r}\frac{\partial r}{\partial \rho} . \qquad (A.7)$$

Now $\frac{\partial r}{\partial \rho} = \frac{\rho}{r} = \sin\theta$ (the coordinate z is kept constant in this differentiation), and, from (A.6),

$$\frac{\partial A_z}{\partial r} = \frac{\mu q}{4\pi}\left[-\frac{1}{r^2}\ \delta\left(t - t_o - \frac{r}{c}\right) - \frac{1}{rc}\ D\left(t - t_o - \frac{r}{c}\right)\right] . \qquad (A.8)$$

Hence

$$H_\phi = \frac{q \sin\theta}{4\pi}\left[\frac{1}{rc}\ D\left(t - t_o - \frac{r}{c}\right) + \frac{1}{r^2}\ \delta\left(t - t_o - \frac{r}{c}\right)\right] . \qquad (A.9)$$

Now find the potential Φ , from eq. (A.5).

$$\mu\epsilon \frac{\partial \Phi}{\partial t} = -\nabla \cdot A = -\frac{\partial A_z}{\partial z} = -\frac{\partial A_z}{\partial r}\ \frac{\partial r}{\partial z} = -\cos\theta\ \frac{\partial A_z}{\partial r} . \qquad (A.10)$$

Substitute (A.8)

$$\mu\epsilon \frac{\partial \Phi}{\partial t} = \frac{\mu q \cos\theta}{4\pi}\left[\frac{1}{rc}\ D\left(t - t_o - \frac{r}{c}\right) + \frac{1}{r^2}\ \delta\left(t - t_o - \frac{r}{c}\right)\right] . \qquad (A.11)$$

Integrate with respect to t:

$$\epsilon \Phi = \frac{q \cos\theta}{4\pi}\left[\frac{1}{rc}\ \delta\left(t - t_o - \frac{r}{c}\right) + \frac{1}{r^2}\ U\left(t - t_o - \frac{r}{c}\right)\right] . \qquad (A.12)$$

The integral of the δ -function is U, the step function, defined by

$$U(t - t_o) = \begin{cases} 0 & \text{if } t < t_o \\ 1 & \text{if } t > t_o . \end{cases} \qquad (A.13)$$

Note that an arbitrary function which is independent of t may be added to Φ . This corresponds to a residual static field.

The electric field is now found from eq. (A.4). The contribution from the vector potential is

$$\frac{\partial \underline{A}}{\partial t} = \underline{z}\frac{\mu q}{4\pi r}\ D\left(t - t_o - \frac{r}{c}\right) = \frac{\mu q}{4\pi r}\ D\left(t - t_o - \frac{r}{c}\right)(\underline{r}\cos\theta - \underline{\theta}\sin\theta). \qquad (A.14)$$

$\underline{z}$, $\underline{r}$, $\underline{\theta}$, etc. are unit vectors along the respective coordinate lines.

The other part of $\underline{E}$ is

$$\nabla \Phi = \underline{r} \frac{\partial \phi}{\partial r} + \underline{\theta} \frac{1}{r} \frac{\partial \phi}{\partial \theta}$$

$$= \underline{r} \frac{q \cos \theta}{4\pi \epsilon} \left[- \frac{1}{rc^2} D(t - t_o - \frac{r}{c}) - \frac{2}{r^2 c} \delta (t - t_o - \frac{r}{c}) - \frac{2}{r^3} U(t - t_o - \frac{r}{c}) \right]$$

$$- \underline{\theta} \frac{q \sin \theta}{4\pi \epsilon} \left[\frac{1}{r^2 c} \delta (t - t_o - \frac{r}{c}) + \frac{1}{r^3} U(t - t_o - \frac{r}{c}) \right] . \qquad (A.15)$$

Then

$$E_r = \frac{2q \cos \theta}{4\pi} \sqrt{\frac{\mu}{\epsilon}} \left[\frac{1}{r^2} \delta(t - t_o - \frac{r}{c}) + \frac{2c}{r^3} U(t - t_o - \frac{r}{c}) \right] \qquad (A.16)$$

$$E_\theta = \frac{q \sin \theta}{4\pi} \sqrt{\frac{\mu}{\epsilon}} \left[\frac{1}{rc} D(t - t_o - \frac{r}{c}) + \frac{1}{r^2} \delta (t - t_o - \frac{r}{c}) + \frac{c}{r^3} U(t - t_o - \frac{r}{c}) \right] . \qquad (A.17)$$

Equations (A.9), (A.16), and (A.17) give the electric and magnetic fields of the impulse current. In section II these fields are called $\underline{G}_o$ and $\underline{F}_o$.

The $\frac{1}{r}$ terms of $\underline{E}$ and $\underline{H}$ form the customary "far field." When the other terms are ignorable the field becomes transverse, and, as in a plane wave,

$$\frac{E_\theta}{H_\phi} = \sqrt{\frac{\mu}{\epsilon}} . \qquad (A.18)$$

The $\frac{1}{r}$ terms contain the D-function, so the field at a distant point consists of two pulses of opposite sign, one after the other. They arise

from the two accelerations of the charge — one to start it at A and the other to stop it at B. This is analogous to the close waves of compression and rarefaction which propagate after an explosion.

The $\frac{1}{r^3}$ terms of $\underline{E}$ are

$$\underline{E} = \frac{q}{4\pi\epsilon r^3} (\underline{r}\, 2\cos\theta + \underline{\theta} \sin\theta)\ U(t - t_o - \frac{r}{c}), \qquad (A.19)$$

and this is exactly the static field of a dipole $\underline{q}$; the field arises at $t = t_o$ and propagates outward with velocity c. This is the change in the static field due to the current $\underline{J}_o$, as noted above.

The above fields have been derived for an electric current impulse, but if electric and magnetic quantities are properly interchanged they become the fields of a magnetic impulse. Discussions of magnetic sources are found in the literature,* and the application to the impulse current follows exactly the lines indicated above.

As an example of the use of these results, let us find the field of an oscillating dipole which is suddenly shut off at $t = t_1$. We shall confine our remarks to E_θ because that component has all the essential characteristics. The current is represented by

$$\underline{J}(t) = \underline{z}\, q \cos\omega t\ \delta(Q)\ U(t_1 - t). \qquad (A.20)$$

The electric field is given by eq. (2.6) of the text:

* See, for example, Schelkunoff, S. A., *Electromagnetic Waves*, chap. VI.

$$E_\theta(Qt) = \int_V \int_{-\infty}^{\infty} J(Pt_o)\, G_\theta(Qt, Pt_o, \underline{z})\, dt_o\, dv_P. \qquad (A.21)$$

The θ-component of $\underline{G}_o$ is given by eq. (A.17). This gives

$$E_\theta(Qt) = \frac{q \sin\theta}{4\pi} \sqrt{\frac{\mu}{\epsilon}} \int_{-\infty}^{\infty} \cos\omega t_o\, U(t_1 - t_o) \left[\frac{1}{rc} D(t - t_o - \frac{r}{c}) + \frac{1}{r^2}\, \delta(t - t_o - \frac{r}{c}) + \frac{c}{r^3}\, U(t - t_o - \frac{r}{c})\right] dt_o. \qquad (A.22)$$

The first integral on the right-hand side is integrated by parts:

$$\int_{-\infty}^{\infty} [\cos\omega t_o\, U(t_1 - t_o)]\; D(t - t_o - \frac{r}{c})\, dt_o$$

$$= -\cos\omega t_o\, U(t_1 - t_o)\, \delta(t - t_o - \frac{r}{c}) \Big|_{t_o = -\infty}^{\infty}$$

$$- \int_{-\infty}^{\infty} \left[\omega \sin\omega t_o\, U(t_1 - t_o) + \cos\omega t_o\, \delta(t_1 - t_o)\right] \delta(t - t_o - \frac{r}{c})\, dt_o$$

$$= 0 - \omega \sin\omega(t - \frac{r}{c})\, U\left[(t_1 + \frac{r}{c}) - t\right] - \cos\omega t_1\; \delta\left[t - (t_1 + \frac{r}{c})\right]. \qquad (A.23)$$

The first term is zero because the δ-function is zero at $\pm\infty$. The second term is the "radiation" field of the dipole. It is sinusoidal in time and ends abruptly at $(t_1 + \frac{r}{c})$. The third term is a pulse which radiates at the instant the current is stopped. It has a magnitude proportional to $\cos\omega t_1$; i. e., to the instantaneous value of the current when it was stopped. If the current were zero at t_1 there would be no pulse, because no infinite acceleration would be needed to bring the charge to rest.

The second integral in E_θ, eq. (A.22), is integrated directly.

$$\int_{-\infty}^{\infty} \cos \omega t_o \; U(t_1 - t_o) \; \delta\left(t - t_o - \frac{r}{c}\right) dt_o$$

$$= \cos \omega \left(t - \frac{r}{c}\right) U\left[\left(t_1 + \frac{r}{c}\right) - t\right] . \qquad (A.24)$$

This term (when multiplied by its factors) is the $\frac{1}{r^2}$ part, the induction field, of the dipole. It also ceases abruptly, but there is no pulse when it stops.

The third integral in E_θ is integrated by parts.

$$\int_{-\infty}^{\infty} \cos \omega t_o \; U(t_1 - t_o) \; U\left(t - t_o - \frac{r}{c}\right) dt_o$$

$$= \frac{1}{\omega} \sin \omega t_o \; U(t_1 - t_o) \; U\left(t - t_o - \frac{r}{c}\right) \Bigg|_{t_o = -\infty}^{\infty}$$

$$+ \int_{-\infty}^{\infty} \frac{1}{\omega} \sin \omega t_o \left[U(t_1 - t_o) \; \delta\left(t - t_o - \frac{r}{c}\right) + \delta(t_1 - t_o) \; U\left(t - t_o - \frac{r}{c}\right)\right] dt_o$$

$$= \frac{\sin \omega t_o}{\omega} \; U(t_1 - t_o) \; U\left(t - t_o - \frac{r}{c}\right) \Bigg|_{t_o = -\infty}^{\infty} + \frac{1}{\omega} \sin \omega \left(t - \frac{r}{c}\right) U\left[\left(t_1 + \frac{r}{c}\right) - t\right]$$

$$+ \frac{1}{\omega} \sin \omega t_1 \; U\left[t - \left(t_1 + \frac{r}{c}\right)\right] . \qquad (A.25)$$

This second term is the customary $\frac{1}{r^3}$ portion of the field of an oscillating dipole, and it stops at $t = \left(t_1 + \frac{r}{c}\right)$. The last term is the residual static dipole field existing for $t > \left(t_1 + \frac{r}{c}\right)$. It is just a constant extension of the time dependent part; i. e., the second term, which is cut off at $t = \left(t_1 + \frac{r}{c}\right)$. The first term is zero at the upper limit and at the lower

limit may be interpreted as the static dipole field which existed before the current was started. (The transients which occurred when the current was started have been ignored because it may be assumed that they have all died down by time t_1.) Both of these static fields may be ignored, along with the static portion of Φ mentioned above.

Thus we have, for the nonstatic portion of the θ-component of electric field due to an oscillating dipole which cuts off at $t = t_1$:

$$E(\theta) = \frac{q \sin\theta}{4\pi}\sqrt{\frac{\mu}{\epsilon}}\left[-\frac{\omega}{rc}\sin\omega\left(t-\frac{r}{c}\right)+\frac{1}{r^2}\cos\omega\left(t-\frac{r}{c}\right)+\frac{c}{\omega r^3}\sin\omega\left(t-\frac{r}{c}\right)\right]$$

$$\left\{U\left[\left(t_1+\frac{r}{c}\right)-t\right]\right\}-\frac{q\sin\theta}{4\pi}\sqrt{\frac{\mu}{\epsilon}}\frac{1}{rc}\cos\omega t_1\,\delta\left[t-\left(t_1+\frac{r}{c}\right)\right]\ . \qquad \text{(A.26)}$$

APPENDIX II. CAVITY GREEN'S FUNCTIONS

1. INTRODUCTION

This appendix is concerned with the expression of electric and magnetic fields in a closed region in terms of their values on the surface. The fields will be written as a linear combination of normal modes appropriate to the region; these modes satisfy the same differential equation as the field, and certain boundary conditions. The result is a generalized Fourier series, where the function to be expanded is known only on the surface.

This problem has been discussed in the literature, for both scalar and vector fields.[23, 30 to 33] It has been shown[34] that the modes obtained from a cavity with a homogenous "short-circuit" boundary condition (i.e., $\underline{n} \times \underline{E} = 0$ on S) form a complete set for the expansion of vector fields with vanishing tangential component on the surface. The earlier writers on the present subject assumed that these short-circuit modes were complete for the expansion of fields with nonzero tangential component on S, but it turns out that they are not, and additional terms must be introduced. This lack of completeness was first pointed out by Wigner.* It was independently discovered by the author when an attempted expansion failed to yield the correct results.

* Private communication. Professor Wigner and Dr. Teichmann very kindly made some as yet unpublished material available to the author.

The function Teichmann and Wigner use to complete the expansion is different from those used here, although it will be shown that the two methods are equivalent. The complete expansions presented here were originally developed by Schwinger, although the present method of derivation is somewhat different. In the same paper with the complete expansions Schwinger produced an alternative (and apparently simpler) expansion using only the short circuit modes.[31]

2. EXPANSIONS IN EIGENFUNCTIONS

Let V be a homogeneous region bounded by S, with outward normal $\underline{n}$. There is an external source with a time dependence $e^{j\omega t}$ producing a field in V, and the electric and magnetic fields in V satisfy the wave equation

$$\nabla \times \nabla \times \underline{E} - k^2 \underline{E} = 0. \tag{A.27}$$

A knowledge of $\underline{n} \times \underline{E}$ or $\underline{n} \times \underline{H}$ on S determines $\underline{E}$ and $\underline{H}$ in V.

Now define the functions $\underline{E}_a$ as solutions of the equation

$$\nabla \times \nabla \times \underline{E}_a - k_a^2 \underline{E}_a = 0 \tag{A.28}$$

subject to the boundary condition

$$\underline{n} \times \underline{E}_a = 0 \quad \text{on S}. \tag{A.29}$$

To show the orthogonality of these functions, use the vector analogue of Green's theorem:[35]

$$\int_V (\underline{A} \cdot \nabla \times \nabla \times \underline{B} - \underline{B} \cdot \nabla \times \nabla \times \underline{A}) dv$$

$$= \int_S (\underline{B} \times \nabla \times \underline{A} - \underline{A} \times \nabla \times \underline{B}) \cdot \underline{n}\, ds. \tag{A.30}$$

If $\underline{A} = \underline{E}_\alpha$ and $\underline{B} = \underline{E}_\beta$, then from eqs. (A.28) and (A.29),

$$(k_\alpha^2 - k_\beta^2) \int_V \underline{E}_\alpha \cdot \underline{E}_\beta \, dv = 0. \tag{A.31}$$

The functions corresponding to different eigenvalues are therefore orthogonal, and, if there is degeneracy, appropriate linear combinations will yield an orthogonal set of functions going with the same eigenvalue. The functions may also be normalized, by setting

$$\int_V \underline{E}_\alpha \cdot \underline{E}_\beta \, dv = \delta_{\alpha\beta} \, . \tag{A.32}$$

We also need the magnetic-type modes, denoted by $\underline{H}_\alpha$ and defined by

$$k_\alpha \underline{H}_\alpha = \nabla \times \underline{E}_\alpha \, . \tag{A.33}$$

Then, from eq. (A.28),

$$k_\alpha \underline{E}_\alpha = \nabla \times \underline{H}_\alpha \, . \tag{A.34}$$

The functions $\underline{H}_\alpha$ satisfy the wave equation

$$\nabla \times \nabla \times \underline{H}_\alpha - k_\alpha^2 \underline{H}_\alpha = 0 \tag{A.35}$$

with

$$\underline{n} \times \nabla \times \underline{H}_\alpha = 0 \quad \text{on S.} \tag{A.36}$$

To demonstrate their orthogonality use the identity

$$\nabla \cdot (\underline{A} \times \underline{B}) = \underline{B} \cdot \nabla \times \underline{A} - \underline{A} \cdot \nabla \times \underline{B} \, . \tag{A.37}$$

Thus,

$$\int_V \underline{H}_\alpha \cdot \underline{H}_\beta \, dv = \frac{1}{k_\beta} \int_V \underline{H}_\alpha \cdot \nabla \times \underline{E}_\beta \, dv$$

$$= \frac{1}{k_\beta} \left[\int_V \nabla \cdot (\underline{E}_\beta \times \underline{H}_\alpha) dv + \int_V \underline{E}_\beta \cdot \nabla \times \underline{H}_\alpha \, dv. \right] \tag{A.38}$$

Substitute (A. 34) and use the boundary conditions to obtain

$$\int_V \underline{H}_\alpha \cdot \underline{H}_\beta \, dv = \delta_{\alpha\beta} \quad . \tag{A.39}$$

The sets of functions $\underline{E}_\alpha$ and $\underline{H}_\alpha$ are the electric and magnetic fields – the normal modes – which can exist in the closed cavity. Note that, because of the normalization, $\underline{E}_\alpha$ and $\underline{H}_\alpha$ do not form an electromagnetic field; if $\underline{E}_\alpha$ is an electric field then $\left(j\sqrt{\frac{\epsilon}{\mu}}\,\underline{H}_\alpha\right)$ is the associated magnetic field.

Now consider the eigenvalue zero. It must be examined separately because the above definitions are not valid in this case. Let the index ρ denote functions going with this eigenvalue, and from now on reserve α for eigenvalues other than zero. The electric-type functions satisfy

$$\nabla \times \nabla \times \underline{E}_\rho = 0 \tag{A.40}$$

with

$$\underline{n} \times \underline{E}_\rho = 0 \text{ on S.} \tag{A.41}$$

From these two equations it is possible to show that $\underline{E}_\rho$ is irrotational. Thus, set

$$\nabla \times \underline{E}_\rho = \nabla u \tag{A.42}$$

Then

$$\nabla^2 u = 0 \tag{A.43}$$

and, from (A.41),

$$\underline{n} \cdot \nabla \times \underline{E}_\rho = \frac{\partial u}{\partial n} = 0 \quad \text{on S.} \tag{A.44}$$

The only solution to (A.43) and (A.44) is u = constant, and hence

$$\nabla \times \underline{E}_\rho = 0. \tag{A.45}$$

The functions $\underline{E}_\rho$ are irrotational, and all the functions $\underline{E}_\alpha$ are solenoidal. Inasmuch as the fields to be expanded are solenoidal, it might seem reasonable to assume that the functions $\underline{E}_\rho$ are unnecessary here, although they may be useful for the expansion of a static field. However, to obtain a complete set it is necessary to have the eigenfunctions going with *all* eigenvalues; therefore we shall keep the irrotational functions.

There is an infinite number of functions $\underline{E}_\rho$. They may be defined by

$$\underline{E}_\rho = \frac{1}{\lambda_\rho} \nabla \phi_\rho \ , \tag{A.46}$$

where

$$\nabla^2 \phi_\rho + \lambda_\rho{}^2 \phi_\rho = 0 \quad \text{in V} \tag{A.47}$$

and

$$\phi_\rho = 0 \quad \text{on S.} \tag{A.48}$$

By using Green's theorem it is shown that the functions ϕ_ρ form an orthonormal set:

$$\int_V \phi_\rho \, \phi_\nu \, dv = \delta_{\rho\nu} \ , \tag{A.49}$$

and it then follows that

$$\int_V \underline{E}_\rho \cdot \underline{E}_\nu \, dv = \delta_{\rho\nu} \quad . \tag{A.50}$$

The condition $\underline{n} \times \underline{E}_\rho = 0$ on S is also satisfied.

Similarly, the functions $\underline{H}_\rho$ are defined by

$$\underline{H}_\rho = \frac{1}{\lambda_\rho} \nabla\psi_\rho \quad , \tag{A.51}$$

where

$$\nabla^2\psi_\rho + \lambda_\rho{}^2\psi_\rho = 0 \quad \text{in V} \tag{A.52}$$

$$\frac{\partial\psi_\rho}{\partial n} = 0 \quad \text{on S.} \tag{A.53}$$

The ψ_ρ's may be normalized:

$$\int_V \psi_\rho\psi_\nu \, dv = \delta_{\rho\nu} \quad , \tag{A.54}$$

and then

$$\int_V \underline{H}_\rho \cdot \underline{H}_\nu \, dv = \delta_{\rho\nu} \, . \tag{A.55}$$

Also, $\underline{n} \cdot \underline{H} = 0$ on S. This is the appropriate magnetic-type boundary condition to satisfy here, rather than (A.36), because $\nabla \times \underline{H}_\rho$ is identically zero.

The functions ϕ_ρ and ψ_ρ are complete sets for the expansion of scalar functions (which satisfy certain requirements as to continuity, etc). They are the functions used by Sommerfeld in his discussion of the scalar cavity Green's function.[30] From the theory of Laplace's

equation it can be shown that there are no functions going with $\lambda_\rho = 0$, (except ψ = constant). Therefore, none of the functions $\underline{E}_\rho$ and $\underline{H}_\rho$ are possible source-free static fields, because their divergence is not zero.

Now assume that, at every point within the cavity, it is possible to write $\underline{E}$ and $\underline{H}$ as linear combinations of the above functions:

$$\underline{E} = \sum_\alpha a_\alpha \underline{E}_\alpha + \sum_\rho a_\rho \underline{E}_\rho \qquad (A.56)$$

$$\underline{H} = \sum_\alpha b_\alpha \underline{H}_\alpha + \sum_\rho b_\rho \underline{H}_\rho \quad . \qquad (A.57)$$

By the orthogonality relations,

$$a_\alpha = \int_V \underline{E} \cdot \underline{E}_\alpha \, dv$$

$$a_\rho = \int_V \underline{E} \cdot \underline{E}_\rho \, dv, \qquad (A.58)$$

and similarly for the b's. The expansion coefficients are found in terms of $\underline{n} \times \underline{E}$ from Green's theorem. From (A.27) and (A.28),

$$(k_\alpha^2 - k^2)\int_V \underline{E} \cdot \underline{E}_\alpha \, dv = \int_V (\underline{E} \cdot \nabla \times \nabla \times \underline{E}_\alpha - \underline{E}_\alpha \cdot \nabla \times \nabla \times \underline{E}) \, dv$$

$$= \int_S (\underline{E}_\alpha \times \nabla \times \underline{E} - \underline{E} \times \nabla \times \underline{E}_\alpha) \cdot \underline{n} \, ds.$$

(A.59)

Therefore,

$$\int_V \underline{E} \cdot \underline{E}_\alpha \, dv = \frac{k_\alpha}{k^2 - k_\alpha^2} \int_S (\underline{n} \times \underline{E}) \cdot \underline{H}_\alpha \, ds. \qquad (A.60)$$

Similarly

$$\int_V \underline{E} \cdot \underline{E}_\rho \, dv = 0 \tag{A.61}$$

$$\int_V \underline{H} \cdot \underline{H}_\alpha \, dv = \frac{j\omega\epsilon}{k^2 - k_\alpha^2} \int_S (\underline{n} \times \underline{E}) \cdot \underline{H}_\alpha \, ds \tag{A.62}$$

$$\int_V \underline{H} \cdot \underline{H}_\rho \, dv = \frac{j}{\omega\mu} \int_S (\underline{n} \times \underline{E}) \cdot \underline{H}_\rho \, ds. \tag{A.63}$$

Therefore,

$$\underline{E} = \sum_\alpha \frac{k_\alpha}{k^2 - k_\alpha^2} \underline{E}_\alpha \int_S (\underline{n} \times \underline{E}) \cdot \underline{H}_\alpha \, ds \tag{A.64}$$

$$\underline{H} = \sum_\alpha \frac{j\omega\epsilon}{k^2 - k_\alpha^2} \underline{H}_\alpha \int_S (\underline{n} \times \underline{E}) \cdot \underline{H}_\alpha \, ds + \sum_\rho \frac{j}{\omega\mu} \underline{H}_\rho \int_S (\underline{n} \times \underline{E}) \cdot \underline{H}_\rho ds. \tag{A.65}$$

The solenoidal set $\underline{E}_\alpha$ alone is sufficient to represent $\underline{E}$ but both sets, $\underline{H}_\alpha$ and $\underline{H}_\rho$, are needed for $\underline{H}$. This difference is due to the different boundary conditions on the $\underline{E}_\alpha$ and $\underline{H}_\alpha$. The expansion is analogous to a Fourier series over the half-interval $0 < x < \pi$. The sines alone form a complete set, but the cosines must also contain the constant term. The constant term is derived from the eigenvalue zero.

Teichmann and Wigner[32,33] complete the expansion by adding an irrotational vector, as follows:*

$$\underline{E} = \sum_{\alpha} a_{\alpha} \underline{E}_{\alpha} \tag{A.66}$$

$$\underline{H} = \sum_{\alpha} b_{\alpha} \underline{H}_{\alpha} + \nabla u, \tag{A.67}$$

where

$$\nabla^2 u = 0 \quad \text{in } V \tag{A.68}$$

$$\frac{\partial u}{\partial n} = \underline{n} \cdot \underline{H} \quad \text{on } S. \tag{A.69}$$

The function u is defined by eqs. (A.68) and (A.69), in terms of normal $\underline{H}$ on the surface. Now the coefficients a_α and b_α are given in terms of tangential $\underline{E}$, and it would seem advantageous to completely specify the expansion in terms of tangential $\underline{E}$, as was done above, in eqs. (A.64) and (A.65). Actually, of course, tangential $\underline{E}$ specifies normal $\underline{H}$, so there is no essential simplification. The two methods are in fact equivalent, as will now be shown.

The function u may be written as

$$u(Q) = \int_S N(Q,P) \frac{\partial u}{\partial n} \, ds_P , \tag{A.70}$$

where N(Q,P) is the Neumann function (Green's function) for the region. It is given by another boundary-value problem, but may be

* Their functions $\underline{E}_\alpha$ and $\underline{H}_\alpha$ are slightly different from the ones used here, because of different normalization conditions.

written as[30]

$$N(Q,P) = \sum_{\rho} \frac{1}{\lambda_\rho^2} \psi_\rho(Q)\, \psi_\rho(P) . \qquad (A.71)$$

When this expansion for $N(Q,P)$ is substituted into (A.70) the gradient may be taken, and it may then be shown that the result is equal to the second series in eq. (A.65).

The procedure outlined above does not work when $k = k_\alpha$; i.e., when the actual field oscillates at a resonance frequency of the cavity. In such a case, since $\int_V \underline{E} \cdot \underline{E}_\alpha \, dv$ is finite, the surface integral $\int_S \underline{n} \times \underline{E} \cdot \underline{H}_\alpha \, ds$ must be zero. This is the exceptional case when the uniqueness theorem is not valid. A more precise uniqueness theorem would read: values of $\underline{n} \times \underline{E}$ on a closed surface uniquely determine the (source-free) interior field unless the oscillation frequency happens to coincide with a resonance frequency. In this case, since the resonant mode has $\underline{n} \times \underline{E} = 0$ on S, it may be added to the field without changing $\underline{n} \times \underline{E}$ on S.

Since the functions $\underline{E}_\alpha$ correctly represent $\underline{E}$ they must also be adequate to represent $\underline{H}$. We may therefore write

$$\underline{H} = \sum_\alpha c_\alpha \underline{E}_\alpha \ , \qquad (A.72)$$

where

$$c_\alpha = \frac{k_\alpha}{k^2 - k_\alpha^2} \int_S (\underline{n} \times \underline{H}) \cdot \underline{H}_\alpha \, ds. \qquad (A.73)$$

$\underline{H}$ is now expressed as a sum of solenoidal functions, in terms of $\underline{n} \times \underline{H}$ on S. However, if $\underline{n} \times \underline{H}$ (rather than $\underline{n} \times \underline{E}$) is known on S,

the expansion for $\underline{E}$ would use both sets of functions, $\underline{H}_\alpha$ and $\underline{H}_\rho$. In the present case the theory is applied to a radiating cavity where $\underline{n} \times \underline{E}$ is known (or assumed) in the aperture; therefore the first expansions above are used. Other combinations would be possible if we had followed Slater and allowed a piece of the surface to be an open circuit (magnetic conductor).[23] If it covered the entire surface then the $\underline{H}_\alpha$'s would be the $\underline{E}_\alpha$'s of the above discussion, and obviously nothing new would be gained. If mixed boundary conditions were allowed then both sets of functions would be needed, in general.

It is of interest to show that the series (A.64) and (A.65) satisfy the Maxwell equations. However, as pointed out by Slater, the series for $\underline{E}$ and $\underline{H}$ cannot be differentiated term-wise; but it can still be shown, for example, that the expansion for curl $\underline{E}$ agrees with the expansion for $\underline{H}$. Curl $\underline{E}$ may be expanded as a sum of the $\underline{H}_\alpha$ and $\underline{H}_\rho$ functions:

$$\nabla \times \underline{E} = \sum_\alpha \underline{H}_\alpha \int_V \underline{H}_\alpha \cdot \nabla \times \underline{E}\, dv + \sum_\rho \underline{H}_\rho \int_V \underline{H}_\rho \cdot \nabla \times \underline{E}\, dv. \tag{A.74}$$

Use the divergence theorem to obtain

$$\nabla \times \underline{E} = \sum_\alpha \underline{H}_\alpha \left[k_\alpha \int_V \underline{E} \cdot \underline{E}_\alpha\, dv + \int_S (\underline{n} \times \underline{E}) \cdot \underline{H}_\alpha\, ds \right]$$

$$+ \sum_\rho \underline{H}_\rho \int_S (\underline{n} \times \underline{E}) \cdot \underline{H}_\rho\, ds. \tag{A.75}$$

The first part of the first sum in (A.75) is equivalent to what one would obtain by taking the termwise curl of (A.64). Substitution of (A.60) yields

$$\nabla \times \underline{E} = -j\omega\mu \left[\sum_{\alpha} \underline{H}_{\alpha} \frac{j\omega\epsilon}{k^2 - k_{\alpha}^2} \int_S (\underline{n} \times \underline{E}) \cdot \underline{H}_{\alpha} \, ds \right.$$

$$\left. + \sum_{\rho} \underline{H}_{\rho} \frac{j}{\omega\mu} \int_S (\underline{n} \times \underline{E}) \cdot \underline{H}_{\rho} \, ds \right] . \qquad (A.76)$$

The bracketed expression is exactly the expansion for $\underline{H}$, eq. (A.65).

The cavity Green's function, $\overset{2}{\Gamma}(Q,P,k)$ is defined by

$$\mathbf{H}(Q) = \int_A \overset{2}{\Gamma}(Q,P,k) \, \mathbf{K}(P) \, ds. \qquad (A.77)$$

A comparison of this with eq. (A.65) shows that $\overset{2}{\Gamma}$ may be written as

$$\overset{2}{\Gamma}(Q,P,k) = \sum_{\alpha} \frac{j\omega\epsilon}{k^2 - k_{\alpha}^2} \underline{H}_{\alpha}(Q) \underline{H}_{\alpha}(P) + \sum_{\rho} \frac{j}{\omega\mu} H_{\rho}(Q) H_{\rho}(P). \qquad (A.78)$$

This is the tensor (dyadic) cavity Green's function. Note that

$$\overset{2}{\Gamma}_2(Q,P) = \widetilde{\overset{2}{\Gamma}}(P,Q). \qquad (A.79)$$

3. APPLICATION TO WAVEGUIDE CAVITY

These results will now be applied to a cavity in the shape of a waveguide. The cross section is arbitrary but uniform along the z-axis; there is a short circuit at $z = 0$ and the aperture is at $z = \ell$ (Fig. 39).

a. CONSTRUCTION OF EIGENFUNCTIONS

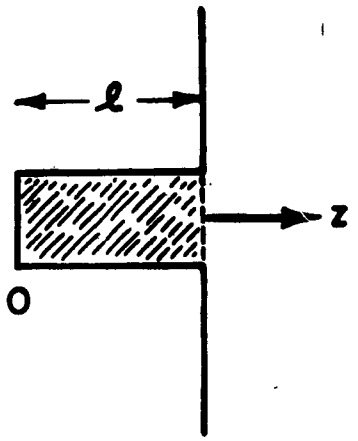

Fig. 39. Waveguide cavity.

The first thing to do is to set up the cavity eigenfunctions. The solenoidal functions may be constructed by observing that they consist of two sets, one TE, and one TM, to the z-axis. The cross-sectional variation will be just the waveguide modes, described in section II, and the z-dependence is such as to make $\overset{t}{E}$ zero at $z = 0$ and $z = \ell$. The TE modes may therefore be written as

$$\underline{E}_{\alpha\nu}^{TE}(xyz) = N_{\alpha\nu}\, \underline{e}_{\nu}^{TE}(xy) \sin\frac{\alpha\pi z}{\ell} \quad , \qquad \alpha = 1, 2, 3, \cdots . \tag{A.80}$$

Up to now there has been a single subscript, α, on the mode functions. This actually stood for three indices, because the cavity is a three-dimensional region. In eq. (A.80), α takes on integral values, and the subscript ν stands for two indices.

The normalization condition determines $N_{\alpha\nu}$:

$$1 = N_{\alpha\nu}^2 \int_0^{\ell} \sin^2\frac{\alpha\pi z}{\ell}\, dz \int_A \underline{e}_{\nu}^{TE}(xy) \cdot \underline{e}_{\nu}^{TE}(xy)\, ds. \tag{A.81}$$

With the result that

$$\underline{E}_{a\nu}^{TE}(xyz) = \sqrt{\frac{2}{\ell}} \sin \frac{a\pi z}{\ell} \underline{e}_{\nu}^{TE}(xy) , \qquad a = 1, 2, 3, \cdots \qquad (A.82)$$

$$\underline{E}_{o\nu}^{TE}(xyz) = 0. \qquad a = 0. \qquad (A.83)$$

Then, from eq. (A.33),

$$\underline{H}_{a\nu}^{TE} = \frac{1}{k_{a\nu}} \nabla \times \underline{E}_{a\nu}^{TE} \qquad (A.84)$$

$$= \frac{1}{k_{a\nu}} \sqrt{\frac{2}{\ell}} \frac{a\pi}{\ell} \cos \frac{a\pi z}{\ell} (-\underline{x}\, e_{\nu y} + \underline{y}\, e_{\nu x}) + \underline{z} \text{ component.} \qquad (A.85)$$

The main interest here will be on the transverse fields, so the $\underline{z}$-component is merely indicated. The quantity in brackets is equal to $\underline{z} \times \underline{e}_{\nu}$, and, from eq. (2.46), the TE magnetic modes become

$$\underline{H}_{a\nu}^{TE}(xyz) = \sqrt{\frac{2}{\ell}} \frac{\frac{a\pi}{\ell}}{k_{a\nu}} \cos \frac{a\pi z}{\ell} \underline{h}_{\nu}^{TE}(xy) + \underline{z}\, cpt., \qquad a = 1, 2, 3, \cdots \qquad (A.86)$$

$$\underline{H}_{o\nu}^{TE}(xyz) = 0, \qquad a = 0. \qquad (A.87)$$

Similarly,

$$\underline{H}_{a\nu}^{TM}(xyz) = \sqrt{\frac{2}{\ell}} \cos \frac{a\pi z}{\ell} \underline{h}_{\nu}^{TM}(xy), \qquad a = 1, 2, 3, \qquad (A.88)$$

$$\underline{H}_{o\nu}^{TM}(xyz) = \sqrt{\frac{1}{\ell}}\, \underline{h}_{\nu}^{TM}(xy), \qquad a = 0 \qquad (A.89)$$

and

$$\underline{E}_{\alpha\nu}^{TM}(xyz) = \sqrt{\frac{2}{\ell}}\,\frac{\frac{\alpha\pi}{\ell}}{k_{\alpha\nu}}\,\sin\frac{\alpha\pi z}{\ell}\,\underline{e}_\nu^{TM}(xy) + \underline{z}\ \text{cpt}, \qquad \alpha = 1,2,3,\cdots \tag{A.90}$$

$$\underline{E}_{0\nu}^{TM}(xyz) = \underline{z}\ \text{cpt}, \qquad \alpha = 0. \tag{A.91}$$

The above functions are all the solenoidal functions for the cavity. The irrotational functions $\underline{H}_\rho$ are also needed. They are defined by eqs. (A.51) through (A.54).

In view of the boundary condition on ψ, the z-variation must be $\cos\frac{\rho\pi z}{\ell}$, where ρ is an integer. Let

$$\psi_{\rho\nu}(xyz) = T_\nu(xy)\cos\frac{\rho\pi z}{\ell}, \qquad \rho = 0,1,2,\cdots \tag{A.92}$$

then

$$\nabla_2^2 T_\nu + \kappa_\nu^2 T_\nu = 0 \qquad \text{on cross section} \tag{A.93}$$

$$\frac{\partial T_\nu}{\partial n} = 0 \qquad \text{on contour}, \tag{A.94}$$

where

$$\nabla_2^2 = \frac{\partial^2}{\partial x^2} + \frac{\partial^2}{\partial y^2} \tag{A.95}$$

and

$$\kappa_\nu^2 = \lambda_{\rho\nu}^2 - \left[\frac{\rho\pi}{\ell}\right]^2 . \tag{A.96}$$

Now (A. 93) and (A. 94) are just the equations satisfied by the potential functions which generate the TE waveguide modes.[36] Hence the eigenvalues κ_ν must be the cutoff wavenumbers for the TE modes, and the functions $T_\nu(xy)$ are equal to the potential functions, apart from a constant. This furnishes an opportunity to express the functions $\underline{H}_\rho$ in terms of $\underline{h}_\nu^{TE}$.

The potential functions $\underline{F}_\nu$ are defined by

$$\underline{e}_\nu^{TE}(xy) = \nabla_2 \times \underline{F}_\nu(xy), \tag{A.97}$$

and they have a z-component only. If the curl is expanded it is seen that

$$\underline{e}_\nu^{TE}(xy) = -\underline{z} \times \nabla_2 F_\nu(xy), \tag{A.98}$$

where F_ν is the z-component of $\underline{F}_\nu$. If we substitute for $\underline{e}_\nu^{TE}$ from eq. (2.46), we have

$$\underline{h}_\nu^{TE}(xy) = \nabla_2 F_\nu(xy). \tag{A.99}$$

To find T_ν in terms of F_ν, set

$$T_\nu(xy) = N_\nu F_\nu(xy). \tag{A.100}$$

Then

$$1 = \int_V \psi_{\rho\nu}^2 \, dv = \int_0^{\ell} \cos^2 \frac{\rho\pi z}{\ell} \, dz \int_A T_\nu^2(xy) \, ds$$

$$= -\frac{\ell}{2} \frac{N_\nu^2}{\kappa_\nu^2} \int_A F_\nu \nabla_2^2 F_\nu \, ds$$

$$= \frac{\ell}{2} N_\nu^2 \frac{1}{\kappa_\nu^2} \int_A \underline{h}_\nu^{TE} \cdot \underline{h}_\nu^{TE} \, ds. \qquad \text{(A.101)}$$

Therefore,

$$N_\nu = \sqrt{\frac{2}{\ell}} \, \kappa_\nu \qquad \rho = 1, 2, 3, \cdots \qquad \text{(A.102)}$$

and

$$N_\nu = \sqrt{\frac{1}{\ell}} \, \kappa_\nu \qquad \rho = 0. \qquad \text{(A.103)}$$

Then

$$\underline{H}_{\rho\nu} = \frac{1}{\lambda_{\rho\nu}} \nabla\psi_{\rho\nu} = \frac{1}{\lambda_{\rho\nu}} \nabla \left[N_\nu F_\nu (xy) \cos \frac{\rho\pi z}{\ell} \right] \qquad \text{(A.104)}$$

$$\underline{H}_{\rho\nu}(xyz) = \sqrt{\frac{2}{\ell}} \frac{\kappa_\nu}{\lambda_{\rho\nu}} \cos \frac{\rho\pi z}{\ell} \underline{h}_\nu^{TE}(xy) + \underline{z} \text{ cpt.}, \qquad \rho = 1, 2, 3, \cdots \qquad \text{(A.105)}$$

$$\underline{H}_{o\nu}(xyz) = \sqrt{\frac{1}{\ell}} \, \underline{h}_\nu^{TE}(xy) \qquad \rho = 0. \qquad \text{(A.106)}$$

The functions in eqs. (A.105) and (A.106) are the irrotational functions needed.

b. EXPANSION OF MAGNETIC FIELD

In section III, in connection with the normal modes of the radiating waveguide-cavity, it was stated that the transverse magnetic field obtained from the eigenfunction expansion agrees with that computed from transmission line theory. This will now be shown.

The expansion is given in eq. (A.65), and now replace ω by the complex frequency p. The integrands are zero except in the aperture, so

$$\underline{H} = \sum_{\alpha}\sum_{\nu} \underline{H}_{\alpha\nu} \frac{jp\epsilon}{k^2 - k_{\alpha\nu}^2} \int_A (\underline{z} \times \underline{E}) \cdot \underline{H}_{\alpha\nu}\, ds + \sum_{\rho}\sum_{\nu} \underline{H}_{\rho\nu} \frac{j}{p\mu} \int_A (\underline{z} \times \underline{E}) \cdot \underline{H}_{\rho\nu}\, ds. \tag{A.107}$$

Consider first the TM modes of the first sum. Substitute for $\underline{H}_{\alpha\nu}^{TM}$ from eqs. (A.88) and (A.89), retaining only the transverse fields.

$$\underline{H}^{t}(xyz) = \sum_{\alpha=1}^{\infty} \sum_{\nu} \underline{h}_{\nu}^{TM}(xy) \frac{2}{\ell} \cos\frac{\alpha\pi z}{\ell} \frac{jp\epsilon}{k^2 - k_{\alpha\nu}^2} (-1)^{\alpha} \int_A (\underline{z} \times \underline{E}) \cdot \underline{h}_{\nu}^{TM}\, ds$$

$$+ \sum_{\nu} \underline{h}_{\nu}^{TM}(xy) \frac{1}{\ell} \frac{jp\epsilon}{k^2 - k_{0\nu}^2} \int_A (\underline{z} \times \underline{E}) \cdot \underline{h}_{\nu}^{TM}\, ds. \tag{A.108}$$

The $(-1)^{\alpha}$ comes from the $\cos\frac{\alpha\pi z}{\ell}$ in the integrand, evaluated at $z = \ell$. The notation is rather cumbersome, so the following list of symbols is included for clarification:

α = number of $\frac{\lambda_g}{2}$ in the waveguide (for the eigenfunctions $\underline{E}_{\alpha}$, etc.)

ν = waveguide mode number (stands for two indices)

κ_ν = $2\pi \times$ cut-off wavenumber of νth waveguide mode

$k = p\sqrt{\mu\epsilon} = 2\pi\sqrt{\mu\epsilon} \times$ complex oscillation frequency of the normal mode of the radiation problem.

$k_{a\nu} = 2\pi\sqrt{\mu\epsilon} \times$ oscillation frequency of the $a\nu$th cavity mode.

$k_{a\nu}^2 = \left(\frac{a\pi}{\ell}\right)^2 + \kappa_\nu^2$ mode.

$$\gamma_\nu^2 = \kappa_\nu^2 - k^2. \tag{A.109}$$

Hence,

$$k^2 - k_{a\nu}^2 = -\gamma_\nu^2 - \left(\frac{a\pi}{\ell}\right)^2 \tag{A.110}$$

Rearrange eq. (A.108) to give

$$\underline{H}^t(xyz) = \sum_\nu -\frac{jp\epsilon}{\gamma_\nu}\,\underline{h}_\nu^{TM}(xy)\int_A \underline{E}\cdot\underline{e}^{TM}\,ds\left\{\frac{1}{\gamma_\nu \ell} + \sum_{a=1}^{\infty}\frac{2}{\ell}(-1)^a\frac{\gamma_\nu}{\gamma_\nu^2+\left(\frac{a\pi}{\ell}\right)^2}\cos\frac{a\pi z}{\ell}\right\}. \tag{A.111}$$

But, as may be verified, the quantity in the brackets is the cosine expansion of $\left(\frac{\cosh\gamma_\nu z}{\sinh\gamma_\nu \ell}\right)$, over the range $0 \leq z \leq \ell$. Also, for TM modes, the quantity $\frac{jp\epsilon}{\gamma_\nu}$ is the waveguide characteristic admittance, y_ν^{TM} (see section II). Hence the contribution of the TM modes to the transverse magnetic field reduces to

$$\underline{H}^t(xyz) = \sum_\nu -y_\nu^{TM}\,\underline{h}_\nu^{TM}(xy)\,\frac{\cosh\gamma_\nu z}{\sinh\gamma_\nu \ell}\int_A \underline{E}\cdot\underline{e}_\nu^{TM}\,ds. \tag{A.112}$$

Now consider the TE modes. We will consider the irrotational modes together with these because their transverse dependence is of

the TE type. Substitute for $\underline{H}_{a\nu}^{TE}$ and $\underline{H}_{\rho\nu}$ in (A.107) to obtain

$$\underline{\overset{t}{H}}(xyz) = \sum_{\alpha=1}^{\infty} \sum_{\nu} \underline{h}_{\nu}^{TE}(xy) \frac{2}{\ell}\left[\frac{\frac{\alpha\pi}{\ell}}{k_{a\nu}}\right]^2 \cos\frac{\alpha\pi z}{\ell}(-1)^{\alpha} \frac{jp\epsilon}{k^2 - k_{a\nu}^2} \int_A (\underline{z}\times\underline{E})\cdot\underline{h}_{\nu}^{TE} ds$$

$$+\sum_{\rho=1}^{\infty} \sum_{\nu} \underline{h}_{\nu}^{TE}(xy) \frac{2}{\ell}\left[\frac{\kappa_{\nu}}{\lambda_{\rho\nu}}\right]^2 \cos\frac{\rho\pi z}{\ell}(-1)^{\rho} \frac{j}{p\mu} \int_A (\underline{z}\times\underline{E})\cdot\underline{h}_{\nu}^{TE} ds$$

$$+ \sum_{\nu} \underline{h}_{\nu}^{TE}(xy) \frac{1}{\ell}\frac{j}{p\mu} \int_A (\underline{z}\times\underline{E})\cdot\underline{h}_{\nu}^{TE} ds. \qquad (A.113)$$

After using eqs. (A.96), (A.109) and (A.110), the equation becomes

$$\underline{\overset{t}{H}}(xyz) = \sum_{\nu} \underline{h}_{\nu}^{TE}(xy) \int_A \underline{E}\cdot\underline{e}_{\nu}^{TE} \left\{\frac{1}{\ell}\frac{j}{p\mu} + \sum_{\rho=1}^{\infty}\frac{2}{\ell}\frac{j}{p\mu}(-1)^{\rho}\frac{\kappa_{\nu}^2}{\kappa_{\nu}^2+\left(\frac{\rho\pi}{\ell}\right)^2}\cos\frac{\rho\pi z}{\ell}\right.$$

$$\left. + \sum_{\alpha=1}^{\infty}\left(\frac{2}{\ell}\right) jp\epsilon(-1)^{\alpha}\frac{\left(\frac{\alpha\pi}{\ell}\right)^2}{\left[\kappa_{\nu}^2+\left(\frac{\alpha\pi}{\ell}\right)^2\right]}\frac{(-1)}{\left[\gamma_{\nu}^2+\left(\frac{\alpha\pi}{\ell}\right)^2\right]}\cos\frac{\alpha\pi z}{\ell}\right\}. \qquad (A.114)$$

The last two sums may be combined (change the dummy index ρ to α) and, after a little manipulation, one obtains

$$\underline{\overset{t}{H}}(xyz) = \sum_{\nu} \frac{-\gamma_{\nu}}{jp\mu}\underline{h}_{\nu}^{TE}(xy) \int_A \underline{E}\cdot\underline{e}_{\nu}^{TE} ds\left\{\frac{1}{\gamma_{\nu}\ell}\right.$$

$$\left. + \sum_{\alpha=1}^{\infty}\frac{2}{\ell}(-1)^{\alpha}\frac{\gamma_{\nu}}{\gamma_{\nu}^2+\left(\frac{\alpha\pi}{\ell}\right)^2}\cos\frac{\alpha\pi z}{\ell}\right\}. \qquad (A.115)$$

The bracketed quantity is again $\left(\frac{\cosh\gamma_\nu z}{\sinh\gamma_\nu \ell}\right)$; and $\left(\frac{\gamma_\nu}{jp\mu}\right)$ is the characteristic admittance for the νth TE mode. Therefore, the contribution of the TE and irrotational eigenfunctions has the same form as that of the TM eigenfunctions. Let the subscript ν denote all the waveguide modes, and as a final result, write

$$\underline{\overset{t}{H}}(xyz) = \sum_\nu -y_\nu \, \underline{h}_\nu(xy) \, \frac{\cosh\gamma_\nu z}{\sinh\gamma_\nu \ell} \int_A \underline{E} \cdot \underline{e}_\nu \, ds. \qquad (A.116)$$

Now consider the cavity from waveguide theory. We have a section of waveguide, shorted at $z = 0$, and with $\underline{z} \times \underline{E}$ prescribed at $z = \ell$. From section II,

$$\underline{\overset{t}{H}}(xyz) = \sum_\nu I_\nu(z) \, \underline{h}_\nu(xy) \qquad (A.117)$$

$$\underline{\overset{t}{E}}(xyz) = \sum_\nu V_\nu(z) \, \underline{e}_\nu(xy) . \qquad (A.118)$$

At any point z, I_ν is the sum of two waves:

$$I_\nu(z) = A_\nu (e^{\gamma_\nu z} + e^{-\gamma_\nu z}). \qquad (A.119)$$

Let $z = \ell$, then

$$A_\nu = \frac{I_\nu(\ell)}{2\cosh\gamma_\nu \ell} \qquad (A.120)$$

But, from eq. (3.27),

$$I_\nu(\ell) = -V_\nu(\ell) \, y_\nu \coth\gamma_\nu \ell = -y_\nu \coth\gamma_\nu \ell \int_A \underline{E} \cdot \underline{e}_\nu \, ds. \qquad (A.121)$$

It follows then that

$$I_\nu(z) = -y_\nu \frac{\cosh \gamma_\nu z}{\sinh \gamma_\nu \ell} \int_A \underline{E} \cdot \underline{e}_\nu \, ds \qquad (A.122)$$

and

$$\underline{\overset{t}{H}}(xyz) = \sum_\nu -y_\nu \underline{h}_\nu(xy) \frac{\cosh \gamma_\nu z}{\sinh \gamma_\nu \ell} \int_A \underline{E} \cdot \underline{e}_\nu \, ds. \qquad (A.123)$$

It has therefore been shown that the transverse magnetic field of a waveguide cavity calculated from the expansion in cavity eigenfunctions agrees with the much simpler calculation based on waveguide theory.

APPENDIX III. THE STATIONARY PRINCIPLE

It is desired to show that the propagation constant k, as calculated from eq. (3.17) of the text, is stationary with respect to first-order variations of tangential $\underline{E}$ about the true value. This stationary principle follows from Schwinger's work. This particular proof is due to Professor Rumsey (Final Engineering Report 400-11, ARDC).

The equation under investigation is

$$\int_{A_Q} \int_{A_P} \tilde{\mathbb{K}}(Q)\, \Gamma(Q,P,k)\, \mathbb{K}(P)\, ds_P\, ds_Q = 0, \tag{A.124}$$

where

$$\Gamma = \overset{1}{\Gamma} - \overset{2}{\Gamma}. \tag{A.125}$$

Take the first variation:

$$\int_{A_Q} \int_{A_P} \delta\, \tilde{\mathbb{K}}(Q)\, \Gamma(Q,P,k)\, \mathbb{K}(P)\, ds_P\, ds_Q$$

$$+ \int_{A_Q} \int_{A_P} \tilde{\mathbb{K}}(Q)\, \delta\, \Gamma(Q,P,k)\, \mathbb{K}(P)\, ds_P\, ds_Q$$

$$+ \int_{A_Q} \int_{A_P} \tilde{\mathbb{K}}(Q)\, \Gamma(Q,P,k)\, \delta\, \mathbb{K}(P)\, ds_P\, ds_Q = 0. \tag{A.126}$$

Now $\overset{1}{\Gamma}$ and $\overset{2}{\Gamma}$ are symmetric, and therefore Γ is symmetric (with interchange of Q and P). The last term therefore becomes (c. f. eq. (3.14) of the text)

$$\int_{A_Q} \int_{A_P} \tilde{\mathbb{K}}(Q)\, \Gamma(Q,P,k)\, \delta\, \mathbb{K}(P)\, ds_P\, ds_Q$$

$$= \int_{A_Q} \int_{A_P} \delta\, \tilde{\mathbb{K}}(P)\, \Gamma(P,Q,k)\, \mathbb{K}(Q)\, ds_P\, ds_Q. \tag{A.127}$$

If the order of integration is interchanged this is just equal to the first term of (A.126). But the first term is zero when evaluated at the correct $\mathbb{K}$, because

$$\underline{z} \times \int_A \Gamma(Q,P,k)\,\mathbb{K}(P)\,ds_P = \underline{z} \times \left[\underline{\overset{1}{H}}(Q) - \underline{\overset{2}{H}}(Q)\right] = 0. \qquad (A.134)$$

Tangential $\underline{H}$ is continuous across the aperture.

Thus the first variation is

$$\int_{A_Q} \int_{A_P} \tilde{\mathbb{K}}(Q)\,\delta\Gamma(Q,P,k)\,\mathbb{K}(P)\,ds_P\,ds_Q = 0, \qquad (A.135)$$

or

$$\delta k \int_{A_Q} \int_{A_P} \tilde{\mathbb{K}}(Q)\,\frac{\partial\Gamma}{\partial k}\,\mathbb{K}(P)\,ds_P\,ds_Q = 0. \qquad (A.136)$$

The integral is presumably not zero, so

$$\delta k = 0. \qquad (A.137)$$

REFERENCES

1. Notes on Lectures by Julian Schwinger: Discontinuities in Waveguides, prepared by D. S. Saxon, MIT Radiation Laboratory Report, February 1945. pp. xviii to xxiv.

2. Chu, L. J. Physical Limitations of Omni-directional Antennas. J. Appl. Phys., Vol. 19, December 1948. pp. 1163 to 1175.

3. Counter, V. A. Miniature Cavity Antennas. Quarterly Report No. 2, Microwave Laboratory, Stanford University; prepared under Contract W 28-099 ac382. June 1948.

4. Stratton, J. A. Electromagnetic Theory. McGraw-Hill Book Company, Inc., New York, 1941. p. 554.

5. Schelkunoff, S. A. Advanced Antenna Theory. Wiley and Sons, New York, 1952. chap. 6.

6. Notes on Lectures by Julian Schwinger: Discontinuities in Waveguides, prepared by D. S. Saxon, MIT Radiation Laboratory Report, February 1945.

7. Levine, H. and Schwinger, J. On the Theory of Diffraction by an Aperture in an Infinite Plane Screen, Part I, Phys. Rev.,Vol. 74, October 1948. pp. 958 to 974; Part II, Phys. Rev., Vol. 75, May 1949. pp. 1423 to 1432.

8. Crowley, T. H., Variational Impedance Calculations, Project Report 478-5, Antenna Laboratory, The Ohio State University Research Foundation; prepared under Contract AF 18(600)-88, Wright Air

Development Center, Wright-Patterson Air Force Base, Ohio, July 1952.

9. Harrington, R. F., Propagation Along a Slotted Cylinder, Field Theory Project 289, Antenna Laboratory, The Ohio State University, Columbus, Ohio, March 1952.

10. Schelkunoff, S. A. Electromagnetic Waves. D. Van Nostrand Company, New York, 1943. p. 158.

11. Stratton, J. A. Op. cit. pp . 464 to 470.

12. Ibid. pp. 486 to 488.

13. Baker, B. B. and Copson, E. T. The Mathematical Theory of Huygens' Principle. Oxford University, 1939. chap. 3.

14. Schelkunoff, S. A. Electromagnetic Waves. Op. cit. p. 31.

15. Marcuvitz, N. Waveguide Handbook. MIT Radiation Laboratory Series, Vol. 10, McGraw-Hill Book Company, Inc., New York, 1951. chap. 1.

16. Schelkunoff, S. A. Electromagnetic Waves. Op. cit., pp. 126 to 128.

17. Cohen, M. H., Crowley, T. H., and Levis, C. A. The Aperture Admittance of a Rectangular Waveguide Radiating into Half-Space, Project Report 339-22, Antenna Laboratory, The Ohio State University Research Foundation; prepared under Contract W 33-038 ac21114, Wright Air Development Center, Wright-Patterson Air Force Base, Ohio, November 1951.

18. Montgomery, C. G., Dicke, R. H., and Purcell, E. M. Principles

of Microwave Circuits, MIT Radiation Laboratory Series, Vol. 8, McGraw-Hill Book Company, Inc., New York, 1948. p. 230.

19. Guillemin, E. A. Communications Networks, Vol. 2, Wiley and Sons, New York, 1935. chap. 5.

20. Schelkunoff, S. A. Representation of Impedance Functions in Terms of Resonant Frequencies. Proc. I.R.E., Vol. 32, January 1944. p. 83.

21. Montgomery, C. G., Dicke, R. H., and Purcell, E. M. Op. cit. chap. 7.

22. Montgomery, C. G. Techniques of Microwave Measurements. MIT Radiation Laboratory Series, Vol. 11, McGraw-Hill Book Company, Inc., New York, 1947. chap. 5.

23. Slater, J. C. Microwave Electronics. Revs. Modern Phys., Vol. 18, October 1946. chaps. 3 and 4.

24. Slater, J. C. Microwave Electronics, D. Van Nostrand Co., New York, 1950. chaps. 4 to 7.

25. Von Hipple, A. Tables of Dielectric Materials. Laboratory for Insulation Research, MIT, Cambridge, Mass.; prepared under ONR Contract N5 ori-78, T.O.I.; June 1948.

26. Slater, J. C. Microwave Electronics. Revs. Modern Phys., Vol. 18, October 1946. p. 482

27. Interim Engineering Report 478-1, Antenna Laboratory, The Ohio State University Research Foundation; prepared under Contract

AF 18(600)-88, Wright Air Development Center, Wright-Patterson Air Force Base, Ohio, January 1952.

28. Gardner, M. F. and Barnes, J. L. Transients in Linear Systems. Wiley and Sons, New York, 1942. p. 256.

29. Stratton, J. A. Op cit. p. 428.

30. Sommerfeld, A. Partial Differential Equations. Academic Press, New York, 1949. chap. 5.

31. Schwinger, J. The Theory of Obstacles in Resonant Cavities and Waveguides. MIT Radiation Laboratory, Report 205, May 1943.

32. Teichmann, T. Completeness Relations for Loss-Free Microwave Junctions. J. Appl. Phys., Vol. 23, July 1952. pp. 701 to 710.

33. Teichmann, T. and Wigner, E. P. Electromagnetic Field Expansions in Loss-Free Cavities Excited Through Holes. (Unpublished).

34. Weyl, H. Uber die Randwertaufgabe der Strahlungstheorie und asymptotische Spektralgesetze. J. für Mathematik, bd. 143, August 1913. pp. 177 to 202.

35. Stratton, J. A. Op. cit. p. 250.

36. Marcuvitz, N. Op cit. p. 4.

ACKNOWLEDGMENTS

The author is indebted to Professor V.H. Rumsey for the stimulation of this work and for his many helpful suggestions and criticisms. Credit is also due many members of the Antenna Laboratory for various clarifying discussions; in particular, credit is due Professor A. Calderon for some illuminating discussions concerning the material in Appendix II.

The work described in this dissertation was done, in part, under a contract between The Ohio State University Research Foundation and Air Research and Development Command, Wright-Patterson Air Force Base, Ohio

PROJECT REPORT 486-7

CONTRACT AF 18(600)85

1 DECEMBER 1952

NOTE: In submitting this report it is understood that all provisions of the contract between The Foundation and the Cooperator and pertaining to publicity of subject matter will be rigidly observed.

Investigator Marshall H. Cohen **Date** 20 November 1952

Supervisor W. A. Ramsey **Date** 20 Nov 52

For The Ohio State University Research Foundation

Executive Director Oran C. Wolfert **Date** 21 Nov. 1952

W. L. H.

GOVERNMENT NOTICES

When Government drawings, specifications, or other data are used for any purpose other than in connection with a definitely related Government procurement operation, the United States Government thereby incurs no responsibility nor any obligation whatsoever; and the fact that the Government may have formulated, furnished, or in any way supplied the said drawings, specifications, or other data, is not to be regarded by implication or otherwise as in any manner licensing the holder or any other person or corporation, or conveying any rights or permission to manufacture, use, or sell any patented invention that may in any way be related thereto.

The information furnished herewith is made available for study upon the understanding that the Government's proprietary interests in and relating thereto shall not be impaired. It is desired that the Office of the Judge Advocate, Wright Air Development Center, Wright-Patterson AFB, Ohio, be promptly notified of any apparent conflict between the Government's proprietary interests and those of others.